



中國醫藥大學
臨床醫學研究所
博士學位論文

耳蝸缺血性病變的細胞機制及治療的蘊涵

The cellular mechanisms and therapeutic implications of
cochlear ischemia

指導教授：蔡銘修 教授

共同指導教授：高銘欽 教授

研究生：林嘉德

中華民國一百年四月

中國醫藥大學 臨床醫學研究所

博士班 學位考試

論文題目

中文：耳蝸缺血性病變的細胞機制及治療的蘊涵

英文：The cellular mechanisms and therapeutic implications of cochlear ischemia

本論文係林嘉德於中國醫藥大學臨床醫學研究所完成之博士論文，經考試委員審查及口試合格，特此證明。

考試委員

蔡銘修

高銘欽

林清淵

許權振

張文正

蔡銘修

高銘欽

林清淵

許權振

張文正

所長：藍安文

中華民國一〇〇年四月二十六日

中文摘要

聽力損傷是常見的感覺系統障礙之一，耳蝸缺血則是導致聽力損傷的重要因素。因為耳蝸代謝旺盛，需要許多能量來維持正常功能；但其血液供應只來自迷路動脈，易受到影響而造成缺血性病變。已知許多聽力疾患與耳蝸缺血有關，如老化、噪音性聽損等。本論文在於建立一個可逆式耳蝸缺血動物模式，並配合開發耳蝸缺血的體外模式以完整地探討耳蝸缺血時內耳細胞變化，有助於了解耳蝸缺血相關聽力病變之可能機轉，藉此平臺探尋耳蝸缺血與常見耳毒性的交互作用，並進而探尋對缺血性耳蝸病變可能有效的治療方式。

首先完成對天竺鼠迷路動脈解剖構造的探索，並建立耳蝸可逆性缺血的動物模式(第二章)，以及確認天竺鼠迷路動脈暫時性缺血時間與劑量的反應(第三章)。在瞭解動物耳蝸缺氧的組織形態變化後，進而探討動物耳蝸在高壓純氧下的變化(第四章)，以作為未來進一步研究的基礎。在與耳毒性與生物能量的交互作用研究上，首先建立一個動物耳蝸粒線體功能障礙的動物模式，在此模式下顯示耳蝸對醣胺類抗生素的耳毒性會增加(第五章)；最後經由上述建立的動物耳蝸缺血模式，顯示暫時性耳蝸缺血也會明顯增加對醣胺類抗生素的耳毒性，接下來利用HEI-OC1耳蝸細胞株進一步探討缺血與醣胺類抗生素時耳蝸細胞死亡的分子機制(第六章)。最後總結本系列缺血性耳蝸病變的研究，並檢討如何應用本模式下探尋可能有助於治療這類疾病的方式，以作為未來臨床應用的基礎(第七章)。

關鍵詞：耳蝸缺血、動物模式、體外模式、耳毒性、治療策略

Abstract

The cochlea is a highly metabolic organ and requires much energy to maintain the normal physiologic function. However, it is an end-artery organ and mainly supplied by the labyrinthine artery, which is a branch of anterior inferior cerebellar artery (AICA). Therefore, the cochlea is sensitive to disturbance of blood flow. Cochlear ischemia has been implicated to be the causative factor in various hearing disorders such as noise induced hearing loss, presbycusis, or sudden deafness. The first aim of this thesis is to establish an animal model of reversible cochlear ischemia after the detailed exploration of the inner ear circulation. The interaction of aminoglycoside ototoxicity and bioenergetic deficiency of cochlea is then explored. In addition, the *in vivo* model in coordination with *in vitro* cochlear ischemia model will provide a new approach to the investigation of the cellular and molecular mechanisms in cochlear ischemia.

In this thesis, the detailed exploration of the inner ear circulation in guinea pigs was completed, followed by the establishment of a reversible cochlear ischemia model in guinea pigs (chapter 2). The time courses and dose responses of cochlear ischemia in guinea pigs were shown in chapter 3. The effects of hyperbaric oxygen on guinea pig cochlea were investigated and demonstrated in chapter 4, which could provide the basis for future researches in therapeutic applications. This thesis also established an animal model of acute cochlear mitochondrial dysfunction to elucidate the interaction of aminoglycoside ototoxicity with bioenergetic deficiency (chapter 5). Increased aminoglycoside ototoxic susceptibility was depicted in the impaired bioenergetic deficiency of acute cochlear mitochondrial dysfunction and ischemia-reperfusion injuries. The molecular mechanisms after the interaction of aminoglycoside and hypoxia/ischemia was investigated via the *in vitro* model using HEI-OC1 cochlear cell line and described in chapter 6. Finally, previous researches on the therapeutic purposes for cochlear ischemic damage were reviewed in chapter 7. The potential therapeutic opportunities for the ischemia-related hearing losses were raised. By virtue of the *in vitro* and *in vivo* model, some evidence-based therapeutic strategies may be identified, which may be useful in clinical applications.

Keywords: cochlear ischemia, animal model, *in vitro* model, ototoxicity, therapeutic strategy

致謝

回首五年前正要由而立跨入不惑之際帶著期待與興奮的心情進入臨醫所，繼續追求對科學的不惑；時間匆匆飛逝，在電腦鍵盤上終於要敲下致謝的同時，臨醫所博士班的學業即將劃下一個句點。這幾年來，在工作、生活和學業的多重交會下，構成一個令人難忘的淬煉修行的經驗。從對於基礎研究朦朧的憧憬，研究計畫的請教與研擬，進行實驗時的挫折與寂寞，獲得結果的喜悅與滿足，到最後論文的修飾與漫漫等待，這一連串的過程中，感謝許多貴人的相助，才能達到最後的目標。就如巴西著名作家鮑羅科爾賀(Paulo Coelho)在他的名著『牧羊少年的奇幻之旅』曾藉著引領猶太人祖先亞伯拉罕的撒冷王麥基洗德一再地描述一個”Maktub”的天命觀念：「每個人在他們年輕的時候，都知道自己的天命，那時候每件事都清晰不昧，每件事都有可能...這一股神秘力量會說服人們，讓人們相信...引導你去完成你的天命。它能淬煉你的精神、砥礪你的願力，因為這是這個星球最偉大的真理；不管你是誰...只要你真心渴望一樣東西，就『放手去做』，因為渴望是源自天地之心；那就是你來到這世間的任務」在這五年中這個”Maktub”的信念也不斷地催促著我去完成屬於自己的”Maktub”。

最要感謝的是我的指導老師蔡銘修教授，從12年前來到中國附醫後，就從蔡老師翩翩君子的身教與言教中，得到莫大的啟發；甚至蔡老師親自帶領我三次遠赴日本拜山求藝，自古以來，常吟詠的是劉備三顧茅廬拜請軍師出山，卻少聽到三次帶著晚輩拜門入山；終於讓我得以進入日本東北大學研修，接受一個完整日式內耳研究的基本訓練，並進而作為我在臨醫所延續研究的基礎。也要感謝高銘欽教授與林清淵教授，高老師與林老師淵博的學識、嚴謹的治學態度及敏銳的洞察力，在向這兩位老師的請益中，對研究計畫精確中肯的批評，就如武林明師，一點就找出可能的破綻，進而修正研究方向。更要感謝解剖學科蔡孟宏老師、魏一華老師及吳慶祥教授在實驗技術上的指導與支持，林振文教授在蛋白質體學和生物資訊學上的啟發，微生物學科賴志河老師對於實驗的全力幫忙、論文寫作的指導以及投稿經驗的分享，能夠與這樣聰明、熱心與誠實的學者一起學習研究，實在是一個莫大的幸福。最後要感謝麻醉部動物實驗空間的分享及黃久珍博士在動物實驗的指導，林慧娟小姐在組織切片上的協助，以及摯友鄭元凱醫師這些年來的同行與鼓勵，更要感謝中國附醫醫研部支持研究案(DMR96-121, DMR99-046)及中國醫大與臺大醫學院研究合作案(CMU97-069, CMU98-NTU-13)，除了經費的支援外，更是對於研究理念的認可、贊同與鼓勵。

論文底定，心中如釋重負，在臨醫所的求學過程，此刻更覺歷歷在目，然而，最令人難忘的是同學間的切磋勉勵，更因此締結成了生活上的好友。最後，感謝所有家人的支持，由於他們的體諒與辛勞，吾人方能得以在此求學過程中無後顧之憂，順利完成學業，謹此獻上我最高的敬意與感謝。

Contents

中文摘要	i
Abstract.....	ii
致謝.....	iii
Contents	iv
Original papers.....	vii
Abbreviations	viii
Chapter 1 Introduction	1
1.1 Background	1
1.1.1 Epidemiology of hearing loss.....	1
1.1.2 Peculiar anatomy of cochlea.....	1
1.1.3 Ischemia-related hearing loss.....	2
1.2 Clinical relevance and specific aims	2
Chapter 2 Animal models of selective cochlear ischemia	4
2.1 Animals.....	4
2.2 Methods.....	4
2.2.1 Animal model of cochlear ischemia.....	4
2.2.1.1 Previous animals models of cochlear ischemia.....	4
2.2.1.2 Anatomical exploration to labyrinthine artery via ventral approach.....	5
2.2.1.3 Using microclamp to produce cochlear ischemia via ventral approach.....	6
2.2.2 Verification of the effect of labyrinthine artery occlusion.....	6
2.2.2.1 Cochlear blood flow (CBF) monitoring with laser Doppler equipment	6
2.2.2.2 Auditory testing.....	7
2.2.2.3 Cardiac perfusion with trypan blue	7
2.3 Results	8
2.3.1 Cochlear blood flow during temporary occlusion of labyrinthine artery.....	8
2.3.2 Gait and hearing disturbance after disrupting labyrinthine artery.....	8
2.3.3 Effect of microclamps to occlude labyrinthine artery.....	8
2.4 Conclusion.....	9
2.5 Figures.....	10
Chapter 3 Chronic cochlear changes after transient cochlear ischemia	19
3.1 Background	19
3.2 Materials and methods	20
3.2.1 Surgical procedures.....	20
3.2.2 Hearing test.....	21
3.2.3 Surface preparation of the cochlea and the hair cell-counting procedure.....	22
3.2.4 Histopathological examination.....	23
3.2.5 Experimental groups	23
3.2.6 Statistical analysis.....	23
3.3 Results	24
3.3.1 Time/dose responses in ABR threshold shifts caused by cochlear ischemia.....	24
3.3.2 Hair cell loss.....	24
3.3.3 Histopathological analysis.....	25
3.4 Comments and conclusion	25
Conclusion.....	29

3.5 Figures.....	30
Chapter 4 Effect of hyperbaric oxygen on guinea pig’s cochlea.....	35
4.1 Background	35
4.1.1 Therapeutic implications of cochlear ischemia.....	35
4.1.2 Role of hyperbaric oxygen therapy in inner ear diseases.....	37
4.2 Materials and Methods.....	38
4.2.1 Animals.....	38
4.2.2 HBOT Model.....	38
4.2.3 Otosopic Evaluation.....	39
4.2.4 Auditory Test.....	40
4.2.5 Immunohistochemistry.....	40
4.2.5.1 Preparation of Specimens.....	40
4.2.5.2 Immunohistochemistry.....	41
4.2.5.3 Semi-quantitative morphometric analysis.....	41
4.2.5.4 Immunofluorescence labeling.....	42
4.2.5.5 <i>In Situ</i> Detection of Nuclear DNA Fragmentation.....	42
4.2.6 Statistical Analysis	43
4.3 Results	43
4.3.1 Animal behavior during HBOT and otoscopic findings after HBOT.....	43
4.3.2 ABR measurements before and after HBOT.....	44
4.3.3 Immunohistochemical analysis of NOS in cochleae.....	44
4.3.4 TUNEL assay of cochleae after HBOT.....	45
4.4 Comments and conclusion	45
Conclusion.....	49
4.5 Figures.....	50
Chapter 5 Increased aminoglycoside ototoxicity in acute cochlear mitochondrial dysfunction—interaction of kanamycin to 3-nitropropionic acid	57
5.1 Background	57
5.2 Materials and Methods.....	59
5.2.1 Animals.....	59
5.2.2 Animal treatment.....	60
5.2.3 Auditory brainstem response (ABR)	60
5.2.4 Hair cell counting.....	61
5.2.5 Statistical analysis.....	61
5.3 Results	62
5.3.1 ABR measurements.....	62
5.3.2 Histological analysis.....	62
5.4 Comments and conclusion	63
Conclusion.....	67
5.5 Figures and table	68
Chapter 6 Transient ischemia/hypoxia may enhance aminoglycoside ototoxicity	73
6.1 Background	74
6.2 Materials and methods	77
6.2.1 Animals, medications, reagents and antibodies.....	77
6.2.2 <i>In vivo</i> study.....	78
6.2.2.1 Surgical procedures	78

6.2.2.2 Hearing test.....	79
6.2.2.3 Surface preparation of cochlea and hair cell counting.....	80
6.2.2.4 Histopathological examination.....	80
6.2.2.5 Grouping.....	81
6.2.3 Tracking gentamicin uptake using fluorescence gentamicin.....	81
6.2.4 <i>In situ</i> detection of nuclear DNA fragmentation <i>in vivo</i>	82
6.2.5 <i>In vitro</i> study.....	83
6.2.5.1 Cell culture.....	83
6.2.5.2 Hypoxia of cultured HEI-OC1 cells.....	83
6.2.5.3 MTT assay.....	84
6.2.5.4 Quantification of apoptosis by flow cytometry.....	84
6.2.5.5 Determination of the mitochondrial membrane potential.....	85
6.2.5.6 Measurements of ROS.....	85
6.2.5.7 Detection of Ca ²⁺ concentrations.....	86
6.2.5.8 Western blot analysis.....	86
6.2.5.9 Determination of caspase activity.....	86
6.2.6 Statistics analysis.....	87
6.3 Results.....	87
6.3.1 Transient ischemia increases the gentamicin-induced ABR threshold shifts.....	87
6.3.2 Increased hair cell loss after interaction of gentamicin and ischemia.....	88
6.3.3 Histological analysis after combination of gentamicin and transient ischemia.....	88
6.3.4 Enhanced gentamicin uptake after transient cochlear ischemia.....	88
6.3.5 TUNEL stain <i>in vivo</i>	89
6.3.6 Gentamicin-induced cell apoptosis in HEI-OC1 cells.....	89
6.3.7 Gentamicin caused mitochondrial dysfunction in HEI-OC1 cells.....	90
6.3.8 Gentamicin caused ER stress, Ca ²⁺ release and calpain activity.....	90
6.4 Comments and conclusion.....	91
Conclusion.....	97
6.5 Figures.....	99
Chapter 7 Further clinical implications and conclusion.....	113
References.....	116
Appendix.....	130

Original papers

This dissertation is mostly based on the following papers, which will be properly referred in the subsequent chapters 2 to 7.

1. **Lin CD**, Oshima T, Oda K, Yamauchi D, Tsai MH, Kobayashi T*. Ototoxic interaction of kanamycin and 3-nitropropionic acid. Acta Oto-Laryngologica (SCI, 2009 IF:0.984) 2008; 128:1280-5 (In chapter 5)

2. **Lin CD**, Wei IH, Tsai MH, Kao MC, Lai CH, Hsu CJ, Oshima T, Tsai MH*. Changes in guinea pig cochlea after transient cochlear ischemia. NeuroReport (SCI, 2009 IF: 1.805) 2010; 21:968-75 (In chapters 2, 3). **This paper was selected as the cover story for the print in NeuroReport 2010, Volume 21, Issue 15.**



3. **Lin CD**, Wei IH, Lai CH, Hsia TC, Kao MC, Tsai MH, Wu CH, Tsai MH*. Hyperbaric oxygen upregulates cochlear constitutive nitric oxide synthase. BMC Neuroscience (SCI, 2009 IF: 2.744) 2011; 12:21 e1-e10. (In chapter 4). **This paper was selected as the image highlight as featured image for BMC Neuroscience homepage in February 2011.**



4. **Lin CD**, Kao MC, Tsai MH, Lai CH, Wei IH, Tsai MH, Tang CH, Lin CW, Hsu CJ, Lin CY*. Transient ischemia/hypoxia enhances gentamicin ototoxicity via caspase-dependent cell death pathway. Laboratory Investigation (SCI, 2009 IF: 4.602, ranking 7/71) 2011, accepted. (In chapter 6)

Abbreviations:

3-NP: 3-nitropropionic acid; ABR: auditory brainstem response; AG: aminoglycoside; AICA: anterior inferior cerebellar artery; ATA: atmosphere absolute, atm abs.; BBB: blood-brain barrier; BLB: blood-labyrinthine barrier; CAP: common action potential; CBF: cochlear blood flow; cNOS: constitutive form of NOS; CTM: Chinese traditional medicine; DAB: 3,3'-diaminobenzidine; dB: decibel; DFX: Desferrioxamine; DPOAE: distortion product of otoacoustic emission; EDTA: ethylenediamine tetra-acetic acid; EGCG: Epigallocatechin gallate; EGF: epidermal growth factor; eNOS: endothelial NOS; FHC: ferritin heavy chain; GDNF: glial-cell-derived neurotrophic factor; GM: gentamicin; HBO: hyperbaric oxygen; HBOT: hyperbaric oxygen therapy; HC: hair cell; HEI-OC1: House Ear Institute-organ of Corti 1; i.m.: intramuscular; i.p.: intraperitoneal; IGF: insulin-like growth factor; IHC: inner hair cell; iNOS: inducible form of NOS; IR: ischemia/reperfusion; KM: kanamycin; MMP: mitochondrial membrane potential; Mn-SOD: mitochondrial superoxide dismutase; MTT: 3-(4,5-dimethylthiazol-2-yl)-2,5-diphenyltetrazolium bromide; NBA: normobaric air; NGS: normal goat serum; NHS: normal horse serum; NMDA: N-methyl-D-aspartate; nNOS: neuronal NOS; NO: nitric oxide; NOS: nitric oxide synthase; OD: optical density; OC: organ of Corti; OHC: outer hair cell; PBS: phosphate-buffered saline; PFA: paraformaldehyde; PI: propidium iodide; POD: post-operative day; PS: phosphatidylserine; rhEPO: recombinant human erythropoietin; RNS: reactive nitrogen species; ROS: reactive oxygen species; RWM: round window membrane; RWN: round window niche; S.E.: standard error; SG: spiral ganglion; SGN: spiral ganglion neuron; SL: spiral ligament; SOD: sodium dismutase; SPL: sound pressure level; SSHL: sudden sensorineural hearing loss; SV: stria vascularis; TBS: Tris-buffered solution; TUNEL: terminal deoxynucleotidyl transferase (TdT)-mediated deoxyuridine triphosphate (dUTP)-biotin nick end labeling.

Chapter 1 Introduction

1.1 Background

1.1.1 Epidemiology of hearing loss

It is known that more than 70 million people suffer from severe hearing disturbances worldwide (Tekin et al., 2001). On the basis of this incidence, hearing loss can be regarded as one of the most frequent neurosensory diseases of the human being. Bilateral severe sensorineural hearing loss occurs in about every 752 births in Taiwan (Lin et al., 2002). The incidence of hearing loss increases significantly after 60 years of age. In the elderly, the progressive deterioration of auditory sensitivity associated with the aging process is known as “presbycusis”. Approximately 23% of the population between 65 and 75 years of age, and 40% of the population older than 75 years of age are affected by this condition (Seidman et al., 2004). It was estimated in 1993 that 7% of the population was 65 years or older and this number was 9.2% in 2003, 10.6% in 2000 and is expected to be nearly 20% in 2030 (Department of Household Registration, 2010). Multiple factors contribute to the hearing loss, including genetic factors, degeneration, trauma, inflammation, vascular insufficiency. Hypoxia and ischemia has been postulated to be essential pathogenic factors in the clinicopathogenesis of hearing loss (Mazurek et al., 2008; Mazurek et al., 2006).

1.1.2 Peculiar anatomy of cochlea

Normal hearing relies on the integrity of cochlear function which is dependent upon the maintenance of a delicate homeostatic environment. The cochlea plays a key role in converting the mechanical sound energy into electrical potential and sensory inputs. It comprised essentially of two components, the organ of Corti and the stria vascularis. The organ of Corti is an organ of high metabolic activity. The processes of high-energy consumption are involved in the activation of ion pump in the stria vascularis to the maintenance of electrochemical gradient between perilymph and endolymph and tuning of the basilar membrane by the outer hair cells (Brass and Kemp, 1993). However, it is an

end-artery organ and mainly supplied by the labyrinthine artery, which is a branch of anterior inferior cerebellar artery (AICA) (Nakashima et al., 2003). Therefore, the cochlea is sensitive to disturbance of blood flow.

1.1.3 Ischemia-related hearing loss

Perturbations in the inner ear microcirculation have been considered to be one of the factors implicated in the pathophysiology of various kinds of sensorineural hearing loss (Nakashima et al., 2003). Clinical and experimental studies have shown that hearing disorders, including presbycusis (Riva et al., 2005; Riva et al., 2007), noise-induced hearing loss (Lamm and Arnold, 1996; Scheibe et al., 1990), sudden deafness (Yamasoba et al., 1993; Kim et al., 1999), endolymphatic drops (Larsen et al., 1988; Yazawa et al., 1998; Yamamoto et al., 1991) are related to alterations in the blood flow of inner ear.

1.2 Clinical relevance and specific aims

Giving the complexity of cell death pathway in cochlea (Jiang et al., 2006), an intervention in the early stages of ischemia may be a promising approach to the prevention of ischemia-related hearing loss in clinical setting. Therefore, we propose to investigate the role of oxidative stress and its time response in the inner ear following ischemia change both *in vitro* and *in vivo*. The *in vitro* method is feasible to study the molecular changes and the *in vivo* method is more relevant to clinical situation. The further clarification of the change of oxidative stress in cochlear ischemia will increase our understanding of the complexity of ischemia-related hearing loss and may offer additional possibilities to protect against hearing loss related to ischemia such as noise induced hearing loss, sudden deafness or presbycusis.

Specific aims:

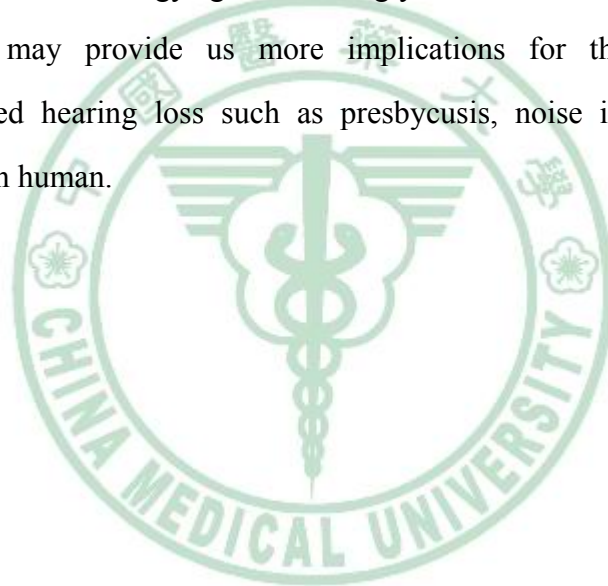
1. Establishment of an animal model of reversible cochlear ischemia, which is more relevant to clinical situations. Through this model, we can get more understanding to the complicated molecular mechanisms of cell death after cochlear ischemia, which may be applied to our understanding of other ischemia-associated hearing loss such as

presbycusis, noise induced hearing loss or sudden deafness.

2. Building-up an *in vitro* model of cochlear ischemia which is more feasible to cellular investigation. Such *in vitro* model could also provide an *in vitro* system for drug screening.

3. Investigation of the interaction of cochlear ischemia with common ototoxic agents such as aminoglycosides in order to elucidate the complicated interaction between ischemia and aminoglycoside, plus cytotoxic mechanisms they may induce within cochlea that potentiate ischemia or aminoglycoside ototoxicity into cytotoxic phenomenon. These results should aid the understanding of the interacting mechanism and potential preventive strategy against aminoglycoside ototoxicity.

These results may provide us more implications for the treatments of other ischemia-associated hearing loss such as presbycusis, noise induced hearing loss or sudden deafness in human.



Chapter 2 Animal models of selective cochlear ischemia

2.1 Animals

Adult albino guinea pigs were used for this study. Guinea pigs have been proved to be a reliable animal model for hearing loss, in which a robust pathological response to aminoglycoside induced cochlear damage could be elicited. In addition, the historic role of guinea pigs in cochlear research is based on the easy surgical access to its cochlea, and well characterized cochlear anatomy and physiology (Forge and Schacht, 2000).

2.2 Methods

2.2.1 Animal model of cochlear ischemia

2.2.1.1 Previous animals models of cochlear ischemia

There have been several methods to produce cochlear ischemia in animals: (1) ventral approach via the auditory bulla cavity (Kimura and Perlman, 1958; Perlman et al., 1959); (2) skull base approach (Tabuchi et al., 1998; Kusakari et al., 1981); (3) vertebral artery occlusion (Hata et al., 1993; Fujita et al., 2007) and (4) occipital craniotomy approach (Mom et al., 1997; Short et al., 1985). These methods are able to induce complete and reversible anoxia without any additional microvascular damage. In addition to these mechanical methods, other methods, e.g. the photochemical AICA occlusion method (Asai et al., 1996) or the ferromagnetic thrombosis method (Schweinfurth and Cacace, 2000; Scheibe et al., 1997) have been also reported. To induce reversible local anoxia, however, the mechanical occlusion is superior to these methods in which large interindividual differences are seen in the degree of ischemia. The inner ear is principally supplied by the labyrinthine artery, which is a branch of anterior inferior cerebellar approach (AICA). The labyrinthine artery is the target artery to be occluded, rather than the AICA because there are many anastomoses among the cerebellar arteries and occlusion of AICA alone cannot ensure complete ischemia in the cochlea (Ren et al., 1995).

2.2.1.2 Anatomical exploration to labyrinthine artery via ventral approach

In this study, we plan to use the ventral approach to occlude the labyrinthine artery because the esophagus and trachea will not be exposed in this method (which have to be exposed by the method of vertebral artery occlusion and skull base approach) and ventral approach also offers a easier way for long-term observation (which is difficult in the other approaches).

The surgical approach to the labyrinthine artery of anterior inferior cerebellar artery was ventral through the tympanic bulla cavity (Kimura & Perlman, 1958; Perlman et al., 1959). The animal was in supine position after anesthesia was setup by intramuscular injection of mixtures of zoletil (30 mg/kg) and xylazine (10 mg/kg). This allows non-ventilator dependent oxygenation and a maintenance dose, 25% of the initial dose, was injected i.m. every 60 min to maintain constant blood levels. The animal was placed in a supine position with head holder apparatus. The cervical hair was shaved and skin was disinfected with 75% alcohol. A submental incision about 2-3 centimeters of skin incision was made medial to mandibular edge. The submandibular gland was separated to expose the digastric muscle and the paracondylar process. After the digastric muscle was separated from the fractured paracondylar process, the tympanic bulla was exposed. The anterior wall of tympanic bulla was opened by Rongeur to expose the cochlear turns. The drilling was then started on the petrous bone, medial to the basal turn and anterior to the intracranial opening of the cochlear aqueduct and the inferior petrosal sinus (Fig 2.1) (Kimura & Perlman, 1958). The dura and the inferior petrosal sinus were protected from damage by a piece of thin silastic sheeting. The drill was stopped at about 2mm anterior to internal auditory meatus. Through the drill hole, the labyrinthine branch of AICA was visible under the dura. The dura was excised and opened wide so that the labyrinthine branch of AICA was fully exposed for further research purpose. The serial figures are summarized in Fig. 2.2.

2.2.1.3 Using microclamp to produce cochlear ischemia via ventral approach

In order to produce reversible cochlear ischemia, a microclamps (S&T Micro Clamps B-2, No. 00398-02) was used. According to the manufacturer's manual, the B-2 microclamps is recommended for vessel diameter at around 0.5mm to 1.5mm at which the clamp pressure is at about 5 to 15g/mm². The labyrinthine artery was further clamped by this microclamps. The morphology of labyrinthine artery was observed under microscopy. After releasing the microclamps, the labyrinthine artery was noted to reperfuse immediately after the release of the clamp (Fig. 2.3).

2.2.2 Verification of the effect of labyrinthine artery occlusion

2.2.2.1 Cochlear blood flow (CBF) monitoring with laser Doppler equipment

CBF was assessed from the velocity measurements of a Perimed PF 4001 laser Doppler equipment _HeNe, wave-length 632.8 nm, probe PF418rB500-0. The laser probe was applied to the second cochlear turns (Fig. 2.3). The CBF signal coming from the velocimeter system was continuously recorded before, during and after clamping using the series input of a PC computer. Two generical remarks about laser Doppler velocimetry must be kept in mind. First, this equipment only provides a relative evaluation of CBF in percentage of a reference flow. Second, the output of the laser Doppler velocimeter resulted from the combination of true CBF and spurious contributions from more superficial vessels in the bony wall of the cochlea or at its surface. These contributions were not expected to vary when the labyrinthine artery was clamped, so that 0% signal could never be reached even for a complete cochlear ischemia with 0% CBF. Nevertheless, the residual signal could be assessed at the end of the experiment after complete section of the eighth nerve bundle, including the arterial supply. The percentage of CBF corresponding to really complete ischemia was ascertained by this last measurement. Throughout flow measurements, a green Wratten filter was placed

on the microscope lighting in order to allow visual control without interference with the detection of red laser light.

2.2.2.2 Auditory testing

The hearing status of all animals is evaluated with tone burst ABR. The sound delivery tubes are inserted into the external ear canal during the ABR measurement. These tubes had custom adapters attached for curved insertion into the external ear canal. Different frequencies (1, 2, 4, 8 kHz) will be checked. For the ABR measurement, the guinea pigs are anesthetized with the mixture of xylazine and Zoletil intramuscularly injected before the steel needle electrodes are subdermally inserted in the ipsilateral and contralateral retro-auricular region as reference electrode and active electrode and in the neck as the ground electrode. The auditory stimuli are band-passed filtered (30-3000 Hz), amplified and averaged for 12.7 milliseconds after stimulus. An average of 512 responses is recorded and the visual detection threshold is determined by attenuating stimulus intensities by 20-dB increments from the maximal output level at each frequency until the waveform is lost, then raised by 10-dB increments until the waveform re-appeared, and then approached by 5-dB increments until the waveform is reestablished. At the threshold intensity, at least two sequences of recordings are made to verify the reproducibility of the ABR responses.

2.2.2.3 Cardiac perfusion with trypan blue

The animals were deeply anesthetized by the i.p. administration of an excessive dose of pentobarbital sodium (50 mg/kg). They were perfused intracardially with physiological saline containing 0.1% heparin followed by 0.3% trypan blue in 0.1M phosphate buffer (pH 7.4). The cochleae were removed and dissected to expose the organ of Corti and modiolus.

2.3 Results

2.3.1 Cochlear blood flow during temporary occlusion of labyrinthine artery

Laser dopplerometry was used to verify the blood flow in the cochlea. The laser probe was applied to the cochlear turn and external compression of the labyrinthine artery was done by microspatula. The baseline of the cochlear blood flow was significantly decreased after the external compression of the labyrinthine artery. Return of the blood flow was demonstrated after the release of the compression. The cochlear blood flow was slightly higher than the baseline after the release the compression. Reperfusion was shown in Fig. 2.4

2.3.2 Gait disturbance and elevated auditory threshold after disrupting labyrinthine artery

Permanent occlusion of the labyrinthine artery was performed by the suction cauterization method. After the suction cauterization of the labyrinthine artery, the animals exhibited significant gait deviation and spontaneous nystagmus (Fig. 2.5). The ABR threshold also was significantly elevated (Fig. 2.6). The sham surgery itself will not cause ABR threshold shifts (Fig. 2.7).

2.3.3 Effect of microclamps to occlude labyrinthine artery

The labyrinthine artery was further clamped by this microclamps. After the microclamps was applied to the labyrinthine artery, the cochlear function was monitored with click ABR at 120dB sound pressure level (SPL) at least every 3 minutes. Compared with the pre-operative apparent ABR waveform, persistent loss of ABR waveform could be depicted as the microclamps was successfully occluded the labyrinthine branch of AICA (Fig. 2.8). The occlusion effect of the labyrinthine artery by this microclamps was verified by intracardiac perfusion of 3% trypan blue. The cochlea of the control ear was stained by trypan blue while the cochlea of the operated ear was not (Fig. 2.9).

2.4 Conclusion

The surgical approach to the labyrinthine artery in guinea pigs is feasible by way of ventral approach as described by Kimura et al (Kimura & Perlman, 1958). Through this approach, the animal model of precise cochlear infarct or ischemia could be made. In this study, the effect of labyrinthine artery occlusion was verified by ABR threshold shifts, gait disturbance and morphological changes. ABR threshold shifts happened immediately after the application of the microclamps and restored after the release of the microclamp. However, the sham surgery itself will not cause ABR threshold shifts. This provides the basis for further reversible model of cochlear ischemia



2.5 Figures

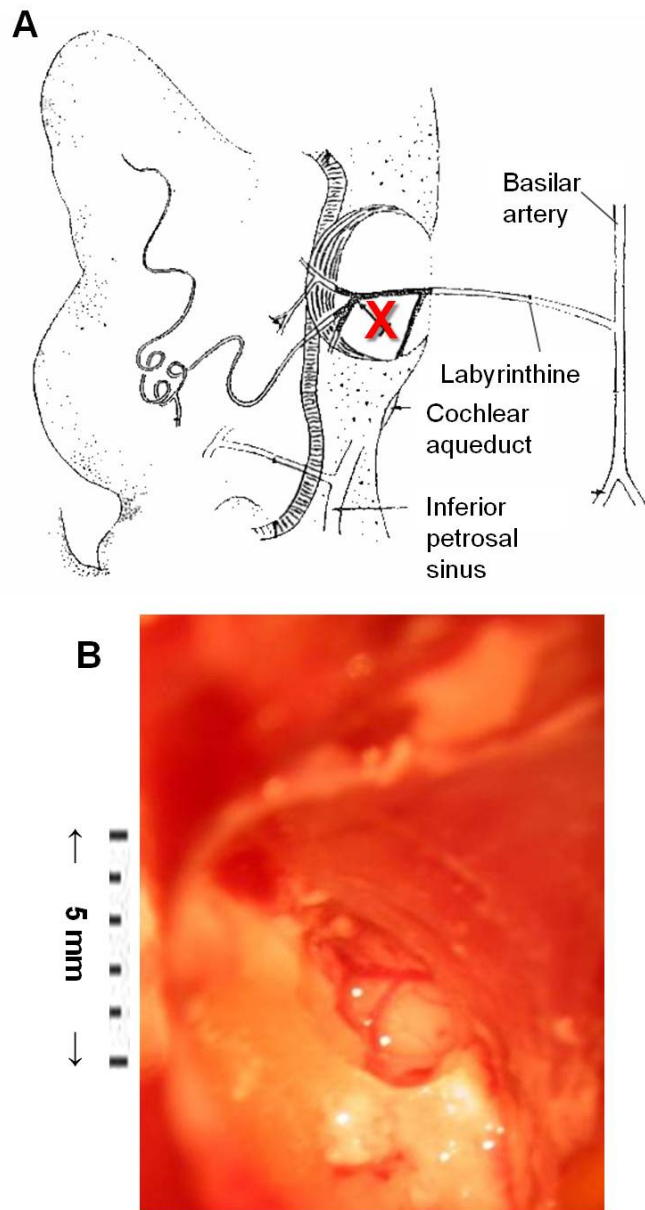


Figure 2.1 Diagrammatic sketch (A) of the surgical approach to left labyrinthine branch of anterior inferior cerebellar artery (AICA) modified from the Kimura et al (Kimura & Perlman, 1958). Red cross indicates the occlusion point by the microclamps. A 3x2mm fenestrum was made medial to the cochlear basal turn (B).

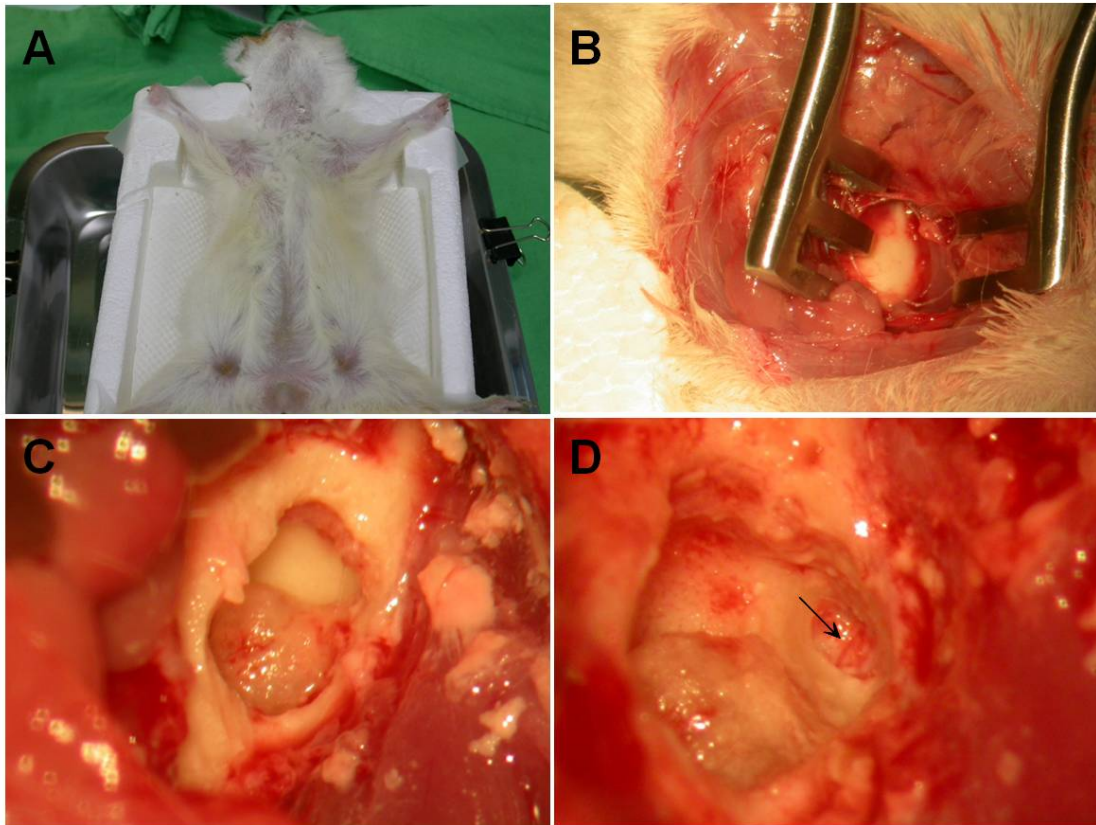


Figure 2.2 Surgical procedures of the ventral approach to the exploration of labyrinthine artery. A. supine position for op; B. exposure of tympanic bulla; C. opening the tympanic bulla to exposure the cochlea; D. drilling medial to basal turn of cochlea to expose the labyrinthine artery (arrow).

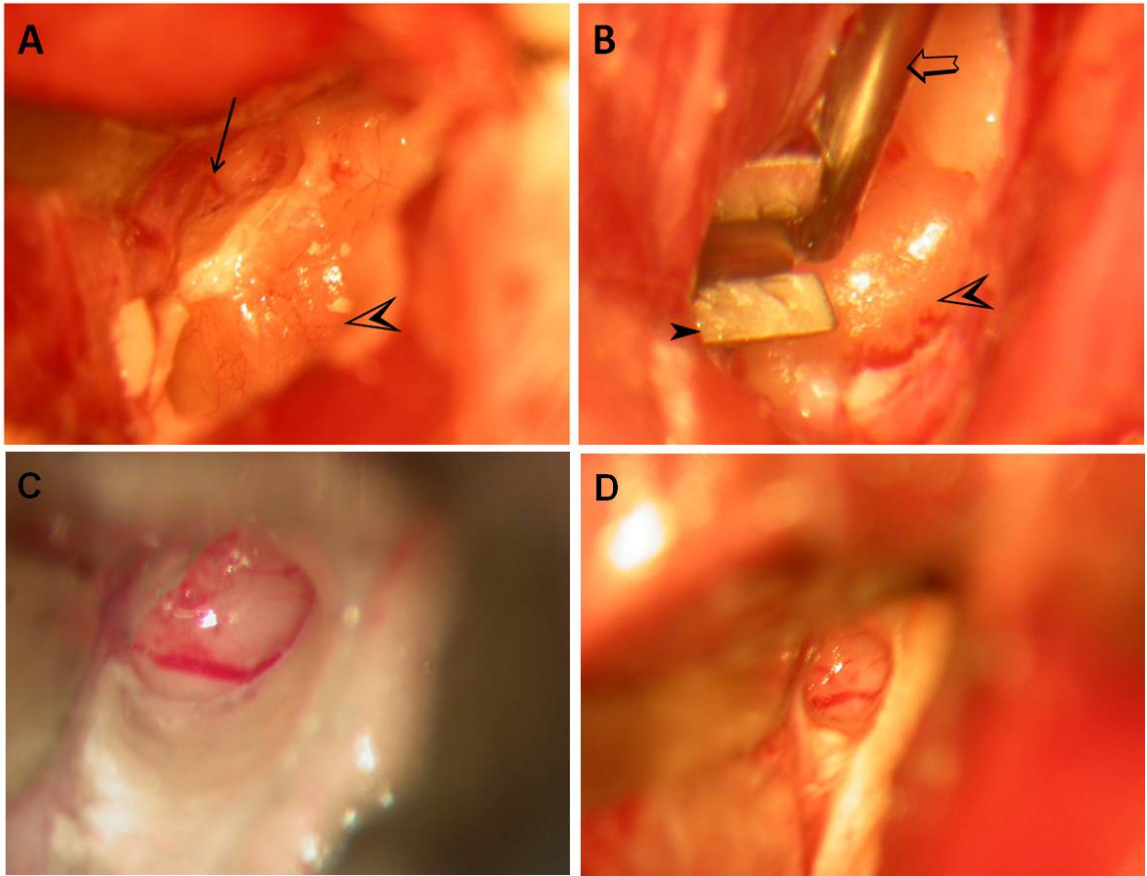


Figure 2.3 Application of laser probe for measurement of cochlear blood flow. A. Exposure of labyrinthine artery (arrow) and cochlear turns (empty arrowhead) via ventral approach. B. The microclamps (filled arrowhead) was applied to occlude the labyrinthine artery. The cochlear blood flow was monitored by laser Doppler with the probe (empty arrow) near the cochlear turn (empty arrowhead). Compared with the pre-clamped view (C), no significant morphologic change of labyrinthine artery was observed after the application of the microclamps (D).

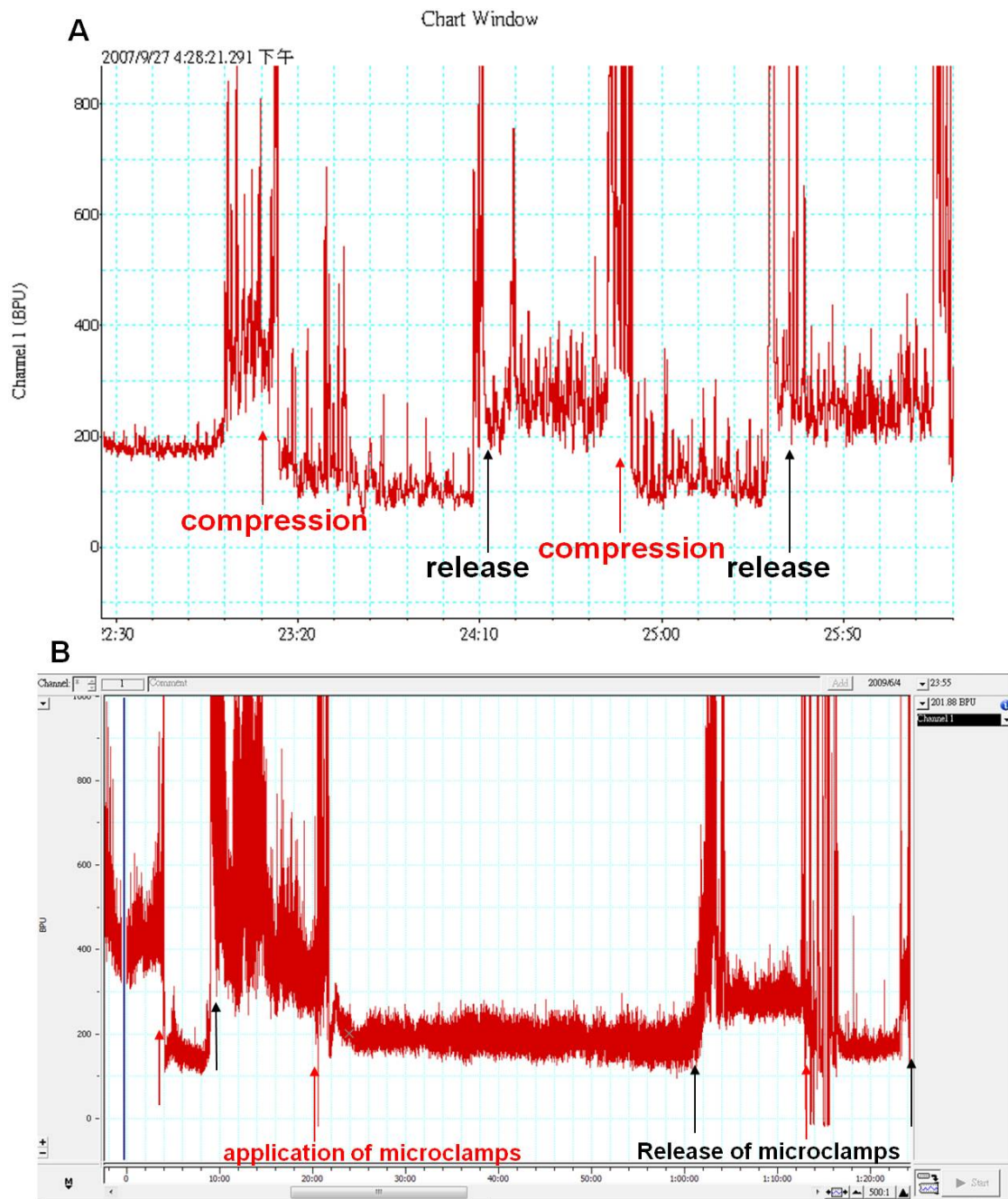


Figure 2.4 Measurement of the cochlear blood flow by laser dopplerometry. A. Reduction of cochlear blood flow was recorded immediately after compression of the labyrinthine artery (red arrow); however, return of cochlear blood flow was depicted immediately after release of the external compression (black arrow). Hyperperfusion of the cochlea was observed immediately after the release. B. Persistence reduction of cochlear blood flow was observation in the 40-min microclamped period. Similar hyperperfusion of the cochlea was observed after the release of the microclamps.

A: Pre-op

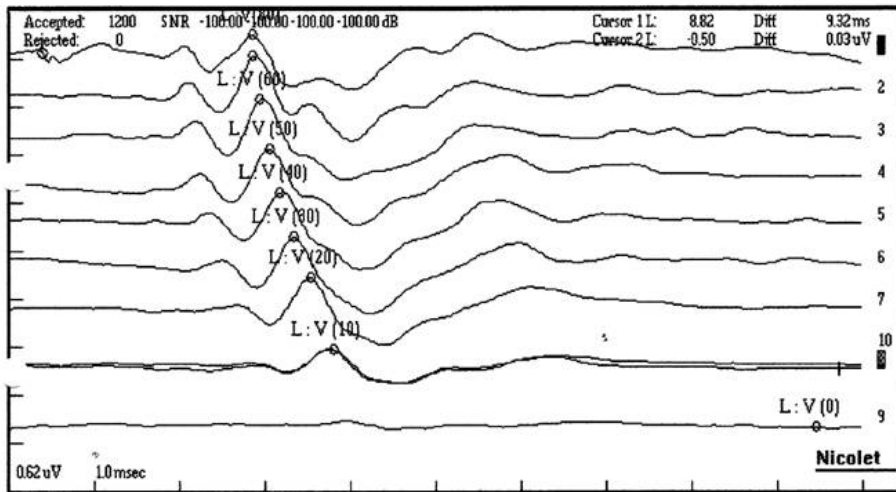


B: Post-op



Figure 2.5 Alterations of gait control before and after disruption of labyrinthine artery. A. Normal gait before op; B. Deviated gait to the left side was observed after cauterization of left labyrinthine artery.

A. Pre-op ABR



B. Post-op ABR

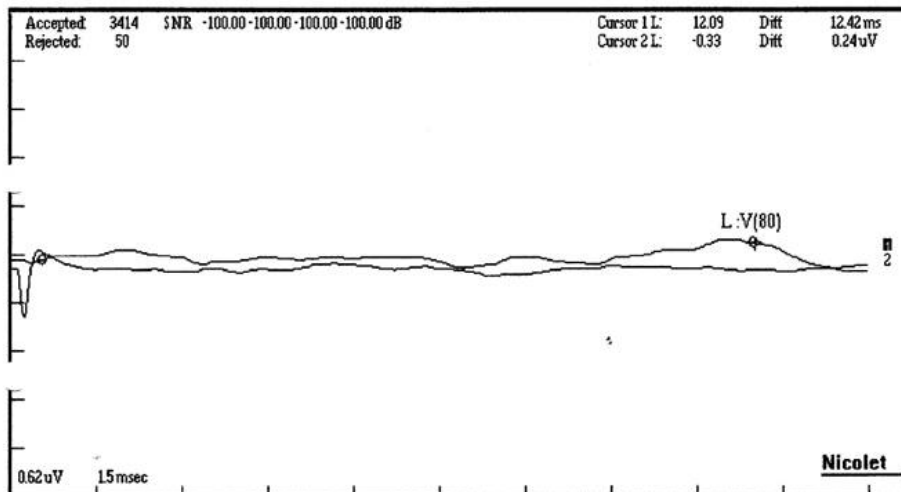
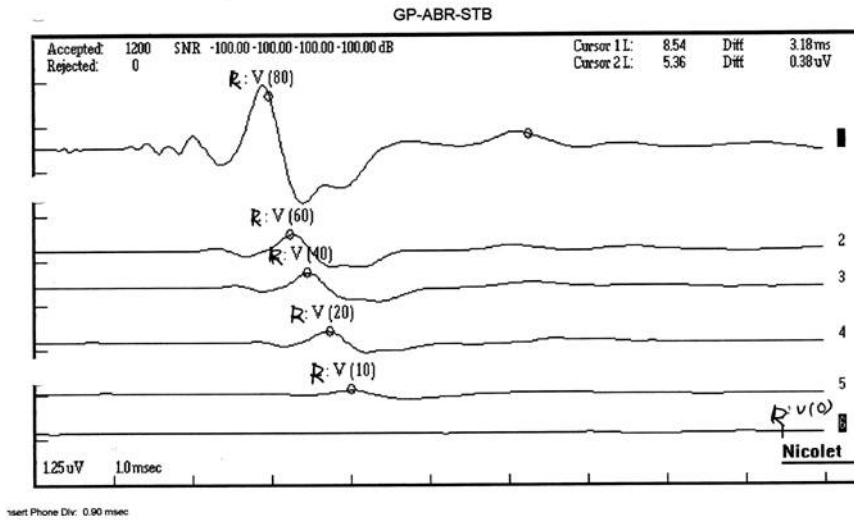


Figure 2.6 ABR threshold changes before and after the disruption of labyrinthine artery. A. Normal ABR before op. B. ABR threshold > 80dB SPL after suction cauterization of labyrinthine artery. Stimulation sound: short tone burst at 8k Hz.

A. Pre-op



B. Post-op 4 th days

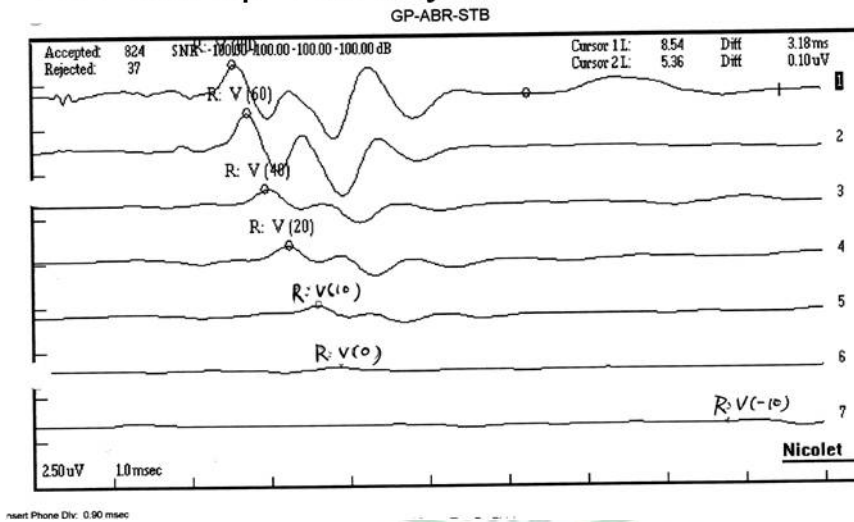


Figure 2.7 Hearing level in sham surgery. Compared with the ABR waveform and auditory level before the surgery (A), no obvious auditory threshold shifts was noted 4 days after the surgery (B). Stimulation sound: short tone burst at 8 kHz.

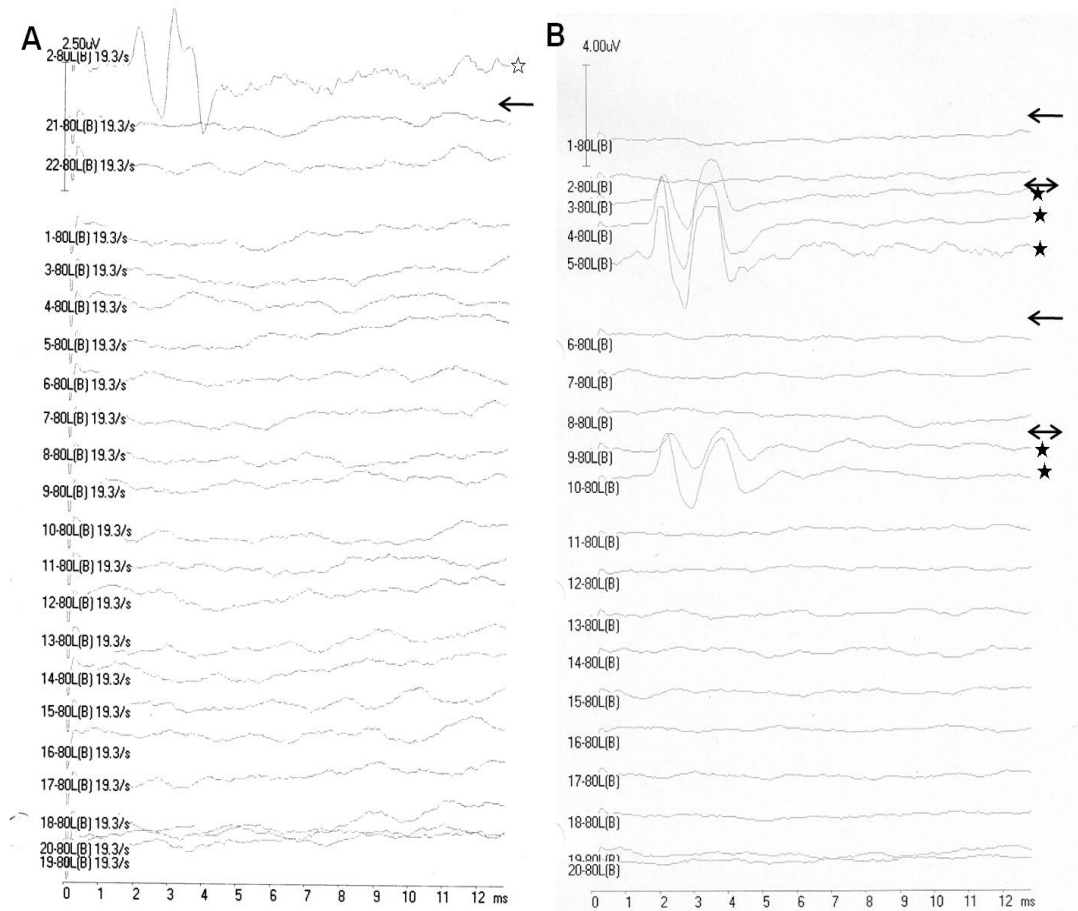


Figure 2.8 Serial changes of ABR waveform during the clamping procedure. A. Before surgery, an apparent ABR waveform was recorded (top) (☆). After the microclamps was applied (←), the ABR waveform disappeared. b. The ABR waveform reappeared (★) when the microclamps was released (↔). The ABR waveform did, however, disappear again when the microclamps was reapplied (←). Stimulating sound: click at 80 dB HL, which is comparable to 120 dB SPL.

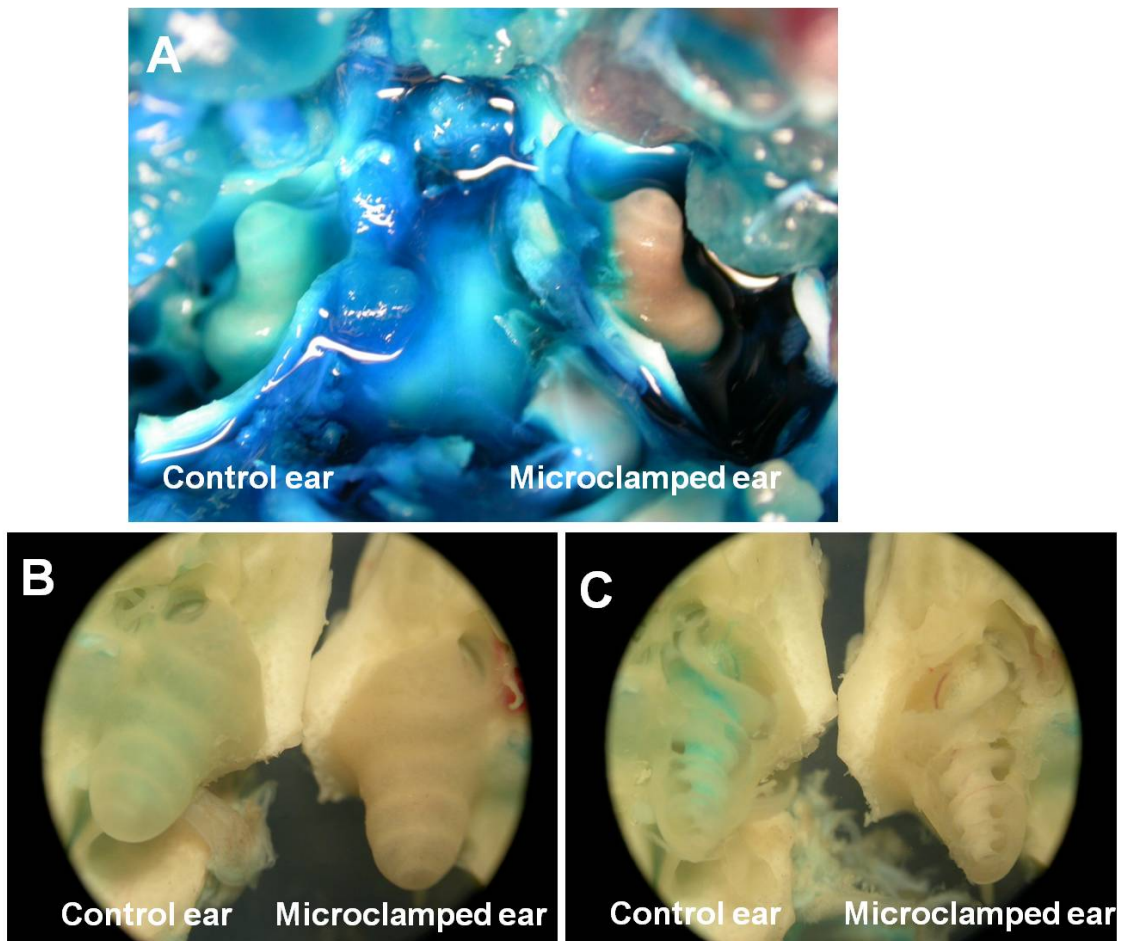


Figure 2.9 Verification of the occlusion effect by the microclamps. After trypan blue perfusion, blue stain over the cochlear bony wall was noted in the control ear, but not in the microclamped ear (A, B). In the control ear, the cochlea was stained in the cochlear wall, modiolus and stria vascularis. However, in the clamped ear, the cochlear wall, modiolus and stria vascularis was free of trypan blue (C).

Chapter 3 Chronic cochlear changes after transient cochlear ischemia

ABSTRACT

Perturbation of cochlear microcirculation is a major cause of hearing impairment. Previous studies examined the short-term (≤ 7 days) effect of cochlear ischemia. This study characterized the long-term (4 weeks) functional and morphological changes caused by transient ischemia that was induced in the adult guinea pig cochleae by clamping the labyrinthine artery for 0.25–3 h. Notably, treatments ≥ 1 h increased auditory brainstem response thresholds and caused loss of high-frequency hearing, basal-turn hair cells, and spiral ganglions. The time for functional recovery of the cochleae after ischemia may be up to 30 min. The extent of the functional and morphological changes depended on the ischemia period, and the changes progressed in intensity from the apical to the basal turn in an orderly fashion.

3.1 Background

The cochlea is a metabolically active organ that requires a substantial amount of energy to maintain its normal physiological function. Because it is an end-artery organ, mainly supplied by the labyrinthine artery (a branch of the anterior inferior cerebellar artery, AICA) (Nakashima et al., 2003), it is sensitive to blood flow disturbances. Disturbance of the cochlear microcirculation causes local hypoxia, which may result in common otologic disorders, such as noise-induced (Henderson et al., 2006), or sudden sensorineural hearing loss (SSHL) (Nagahara et al., 1983).

Although there have been many attempts to characterize how ischemia causes cochlear damage, no definitive animal model to induce ischemia exists. Previous attempts to induce cochlear ischemia included occluding the bilateral vertebral arteries (Maetani et al., 2003) and compressing the neurovascular bundles in the internal auditory canals via either an skull base approach (Kusakari et al., 1981) or occipital approach (Tsuji et al., 2002). Post-operation observation periods were, however, relatively short (1 week at most

(Tsuji et al., 2002). Because the post-operative observation times of the experimental animals used in these studies were limited, a full evaluation of the effects of the ischemia treatments was not possible. Changes in hearing caused by common cochlear ischemia-induced disorders, e.g., SSHL, may evolve over a relatively long period of time after the initial acute insult. Early intervention may aid the recovery process in SSHL patients (Byl, Jr., 1984). Yet for SSHL patients, their hearing may continue to improve for 1 month after treatment cessation (Wilkins, Jr. et al., 1987). Therefore, a study incorporating a long observation period is needed to better understand the functional and morphological cochlear changes caused by ischemia, which is the purpose of this study.

3.2 Materials and methods

Adult albino guinea pigs between the ages of 2 and 4 months (body weight, 350–550 g) were used. The use and care of animals in this study were approved by the Institutional Animal Care and Use Committee of the China Medical University (permission number: 97-60-N). Animals were anesthetized by intramuscular injection of a mixture of Zoletil (30 mg/kg) and xylazine (10 mg/kg), which allowed for non-ventilator dependent oxygenation. A maintenance dose, 50% of the initial dose, was injected intramuscularly every 60 min thereafter. After sedation, atropine (0.05 mg/kg) and chloramphenicol (400 mg/kg) were given intramuscularly. For surgical accessibility and convenience, only the left ear was treated, but to avoid acoustical crossover from the cochlea of the right ear during auditory brainstem response (ABR) measurements, the latter was surgically destroyed.

3.2.1 Surgical procedures

After an animal had been anesthetized, the cervical hair was shaved. It was placed in the prone position, and 1% xylocaine was injected into the posterior auricular area of the right ear. The skin and subcutaneous myofascial plane of the ear were dissected to expose the mastoid bulla, which was then opened so that the cochlea could be directly destroyed by needle penetration and disruption.

The ventral-approach procedure to the labyrinthine artery has been described (Perlman et al., 1959). Electrodes were inserted subcutaneously into the left mastoid (anode), right mastoid (cathode), and the back (ground), and an earphone was inserted into the left ear canal to monitor the ABR perioperatively. The animal was then placed in the supine position. The skin over the ventral neck was disinfected with 75% alcohol and draped with aseptic dressings. A submental incision ~2–3 centimeters in length was made medially to the mandibular edge. The submandibular gland was separated to expose the digastric muscle and the paracondylar process. Separation of the digastric muscle from the fractured paracondylar process exposed the tympanic bulla. The anterior wall of the tympanic bulla was opened using a rongeur so that the basal cochlear turns were visible. Drilling started at the petrous bone, continued medially to the basal turn and anteriorly to the inferior petrosal sinus. The dura and the inferior petrosal sinus were protected during drilling by placing a thin Silastic sheet over them. A fenestration $\sim 1.5 \times 3.0$ mm was made at the base of the skull, so that the labyrinthine artery was visible under the dura. The dura was excised, and the area opened so that the labyrinthine artery was fully exposed. The labyrinthine artery was closed with V1 microclamps] (#00396-01, S&T Microsurgical Instruments, USA), and cochlear function was thereafter monitored by click ABR at a 120-dB sound pressure level (SPL) at least every 3 min. Compared with the pre-operative apparent ABR waveform, persistent absence of the ABR waveform indicated that the microclamps had successfully occluded the labyrinthine artery (Fig. 2.8).

3.2.2 Hearing test

Tone burst ABR pre-operative and serial post-operative hearing tests were performed in a sound attenuated room. The pure tone bursts were generated with the amplitude specified by a real-time programmable attenuator (IHC Smart EP version 3.97, USA) with ER2 insert earphone, with stimulus frequency at 1, 2, 4, 8, 16 and 24 kHz (0.2ms rise/fall time and 1ms flat segment) with maximal output level 125, 123, 111, 117, 98 and 96dB SPL. The click/tone bursts were produced by IHS high frequency transducer in a

closed acoustic system through the sound delivery system. Responses for 1024 sweeps were averaged at each intensity level around the threshold in 5 dB SPL steps. Threshold was defined as the lowest intensity at which a clear waveform was visible upon inspection of an evoked trace. At least two sequences of recordings were made at the threshold intensity to verify the reproducibility of the ABR responses. Each ABR threshold was compared with the pre-operative threshold, which served as the baseline measurement.

For the sham operation (sham-op) and the treatment groups (described below), serial ABR measurements were performed pre-operatively, immediately after the operation (PODi), 1 and 3 days after the operation (POD1d, 3d,) and 1, 2, 3, and 4 weeks after the operation (POD1w, 2w, 3w, 4w).

3.2.3 Surface preparation of the cochlea and the hair cell–counting procedure

At the end of the study, the animals were deeply anesthetized and then sacrificed by decapitation. The left cochleae were fixed with 4% paraformaldehyde in 0.1 M phosphate-buffered saline (PBS) by perilymphatic perfusion and then immersed in 4% paraformaldehyde in 0.1 M PBS for 1 day. The bony modiolus with the organ of Corti was carefully detached at the base of the cochlea following removal of the bony capsule, lateral wall, and tectorial membrane. After permeabilization with 0.3% Triton X-100 in PBS for 10 min, the tissues were incubated at room temperature with rhodamine-coupled phalloidin (Molecular Probes, Eugene, OR, USA) diluted 1:200 with PBS for 30 min. After the tissues were rinsed with PBS, strips of the organ of Corti were divided into the four turns, which were mounted on glass slides and examined with a fluorescence microscope (Model Leitz DM RBE; Leica, Wetzlar, Germany) to count the number of hair cells (HCs) present at each cochlear turn, thereby determining the extent of HC loss. For each group of animals, the mean losses of inner HCs (IHCs) and at each row of outer HCs (OHCs) in each group were calculated.

3.2.4 Histopathological examination

Cochlear sectioning along the paramodiolar axis was done followed by hematoxylin/eosin staining. After fixation as described above, the cochleae were decalcified by immersion in 10% ethylenediamine tetra-acetic acid (EDTA) (in 0.1M PBS, pH 7.4) for 4 weeks, with gentle stirring at 4°C. The cochleae were then dehydrated, embedded in paraffin, and serially sectioned (4 µm thick) parallel to the modiolar axis. The sections were plated for hematoxylin/eosin staining and examined under a high-power light microscope.

3.2.5 Experimental groups

The animals were divided into the following groups. (1) Control (n = 6): No surgery. (2) Sham operation (n = 6): The animals received surgery as described above until the step at which the labyrinthine artery was exposed. Although the overlying dura was excised, the labyrinthine artery was fully exposed only momentarily, and then the wound was closed. (3) Treatment groups: The animals received surgery as described above until the step at which the labyrinthine artery was exposed. The labyrinthine artery was then temporarily occluded with microclamps for 15 or 30 min or for 1, 2, or 3 h (6 animals per subgroup). Then the microclamps was released, and the wounds were closed. During the time that the arteries were occluded, the effects that clamping had on hearing were monitored by serial click ABR at 120-dB SPL.

In each group of 6 sacrificed animals, 4 cochleae were prepared for cochlear surface preparation and HC counting. The cochleae of the other two animals were sectioned along paramodiolar axis and stained with hematoxylin/eosin.

3.2.6 Statistical analysis

The ABR threshold shifts and the percentages of HC loss between the control and the sham-op group, and between the control and each of the treatment groups were analyzed using the non-parametrical Mann-Whitney *U*-test contained in the SPSS program (version 13.0 for Windows, SPSS Inc., USA). A *p* value of <0.05 was considered statistically

significant.

3.3 Results

3.3.1 Time and dose responses in ABR threshold shifts caused by cochlear ischemia

The serial ABR threshold shifts found after transient cochlear ischemia of different durations are depicted in Fig. 2. No significant ABR threshold shifts were noted for the control group or the sham-op group. When the labyrinthine artery was clamped off for 15 or 30 min, marked ABR threshold shifts occurred but returned to pre-operative levels within 3 days. Persistent ABR threshold shifts were noted for the groups treated for ≥ 1 h. For the 1-h ischemia group, threshold shifts associated with higher frequencies (8–24 kHz) were larger than those associated with lower frequencies (1–4 kHz). More-severe threshold shifts were noted for the 2-h treatment group, and for this group, threshold changes were also larger for the high-frequency region than for the lower-frequency region. After a 3-h treatment period, the ABR threshold shift nearly approached the maximum stimulation level.

In Fig. 3, we summarize the mean ABR threshold shifts for each group taken from the ABR audiograms recorded 4 weeks after treatment. No significant differences were found for the control group, the sham-op group, and the 15- and 30-min ischemia groups. For the 1-h treatment group, marked ABR threshold shifts that decreased as the frequencies increased were found. Severe ABR threshold shifts were noted for the 2-h treatment group, and profound ABR threshold shifts were found for the 3-h treatment group.

3.3.2 Hair cell loss

The amount of OHCs lost increased as the ischemia duration increased, but OHC loss did not increase significantly until the ischemia period was ≥ 1 h. OHC loss was more severe in the basal turn than in the apical turn. The amount of IHCs lost did not increase significantly until the animals were treated for at least 1 h, and for these animals, the loss was more severe in the basal turn than in the apical turn. The loss of IHC in the upper

turns was not significant until ischemia was ≥ 2 h (Fig. 4). There was a loss of HCs, especially the OHCs, 4 weeks after the 2-h ischemia (Fig. 5). The OHCs of the basal turn were nearly completely absent 4 weeks after the 2-h ischemia, although residual HCs were still present in the upper turns (Fig. 5).

3.3.3 Histopathological analysis

The morphology of spiral ganglion neurons (SGNs) were grossly normal 4 weeks after a 30-min ischemia treatment (Fig. 6A, B). SGN loss was, however, apparent after 1 h of ischemia (Fig. 6C) and became more severe as the treatment period increased (Fig. 6D). The gross architecture of the organ of Corti remained intact 4 weeks after the 30-min treatment (Fig. 6B). When ischemia lasted ≥ 1 h, however, hair cells had flattened and there was progressive loss of SGNs (Fig. 6C, D).

3.4 Comments and conclusion

Several different approaches have been developed to study the effects of transient cochlear ischemia in different animals. The occipital approach, during which the neurovascular bundles in the internal auditory canal are exposed by occipital craniotomy before being temporarily occluded, has been used in guinea pig (Tsuji et al., 2002), gerbil (Mom et al., 1997), and rabbit (Morawski et al., 2006). The skull base approach involves transient compression of the neurovascular component in the internal auditory canal after surgically entering through the base of the skull. This method has been used in gerbils (Ren et al., 1995) and guinea pigs (Kusakari et al., 1981). The ventral approach, during which the labyrinthine artery just medial to the cochlear turns is accessed through the auditory bulla cavity (Perlman et al., 1959), has been used in guinea pigs. The hindbrain approach for which, because of the peculiar anatomy of posterior brain circulation in gerbils, transient cochlear ischemia is achieved by compressing the bilateral vertebral artery (Maetani et al., 2003). Although the guinea pig labyrinthine artery originates from the AICA, and only it supplies blood to the cochlea, marked variations exist in the anastomoses and the branching pattern of the AICA. Therefore, attempts to produce

cochlear ischemia by compressing the AICA is unreliable and should not be used in guinea pigs (Ren et al., 1993).

The various surgical approaches have different limitations and applications when used with different species. For example, the hindbrain approach to occlude the bilateral vertebral artery produces reversible and consistent cochlear ischemia in gerbils but can be used only with gerbils because of their peculiar posterior brain circulation. When bilateral vertebral artery occlusion was used in guinea pigs, the results were inconsistent (Randolf et al., 1990). Bilateral occlusion of the vertebral artery for ≥ 1 h may also damage the brainstem vital nuclei, thereby limiting the ischemia period. The esophagus and pharynx must be removed when the skull base approach is used. Therefore, longer observation periods of > 1 d may not be feasible. A relatively long observation period (1 week) after transient cochlear ischemia was possible when the occipital approach was used (Tsuji et al., 2002). In the study reported herein, we used the ventral approach to expose the labyrinthine artery. The surgical field was accessed through the auditory bulla, which limited brain damage. The pharynx and trachea were also preserved. The guinea pigs survived for a relatively long period of time (4 weeks) after their operations, so that observation over a period of weeks was possible.

A possible drawback to the ventral approach is that the operative field is very narrow. We could not continuously and directly monitor the ischemia induced by the microclamps using an instrument such as a laser dopplerometry. When we placed a probe of laser dopplerometry at the basal turn of the cochlea and attempted to continuously monitor the ischemia, decreased cochlear blood flow was observed (Fig. 2.4). However, cerebrospinal fluid that leaked from the fenestrum at the base of the skull interfered with the continuous measurement of cochlear blood flow and made the measurements variable and inconsistent. Therefore, we monitored the occlusions by serial ABR. The cochlea has a very low oxidative reserve and is very sensitive to interruption of the blood supply; the electrical activity of the cochlea disappears within seconds when the blood supply is interrupted (Perlman et al., 1959). Serial ABR monitoring has been widely used during skull base surgery and during operations on lesions in the cerebellopontine area, e.g.,

vestibular schwannoma surgery (Legatt, 2002). Once the cochlear blood flow is interrupted, the entire ABR waveform disappears (Legatt, 2002). In contrast, when the damage is localized to the auditory nerve or the central auditory pathways in the brainstem or mesencephalon, the classic ABR waveforms may instead be altered: late ABR waveforms (e.g., waveforms III–V) may disappear, whereas early ABR waveforms, (e.g., waveforms I and/or II) remain visible (Legatt, 2002). In this study, when the microclamps were successfully applied to the labyrinthine artery, the ABR waveforms completely disappeared but rapidly reappeared when the microclamps were removed (Fig. 2.8). These observations suggest that the ABR waveform disappeared when cochlear blood flow was interrupted. In our preliminary studies, we verified the occlusion effect produced by the microclamps using intracardiac perfusion with 3% trypan blue. Trypan blue did not perfuse into the microclamped cochlea but did perfuse into the control cochlea. Therefore, we believe that the microclamps successfully and reversibly occluded the arterial blood supply to the guinea pig cochlea.

The ABR threshold shifts returned to pre-operative levels when cochlear ischemia was induced for ≤ 30 min. Partial recovery of ABR threshold shifts occurred if cochlear ischemia was induced for ≥ 1 h, and poor ABR recovery occurred if cochlear ischemia was ≥ 3 h (Fig. 2, 3). As defined by Perlman and colleagues (Perlman et al., 1959), the revival time is the maximum duration of ischemia after which auditory responses can fully return. The revival time of the guinea pig cochlea after transient ischemia may therefore be up to 30 min. The recovery of ABR threshold shifts after shorter periods of cochlear ischemia (≤ 30 min) occurred within 3 days. ABR recovery from the 1-h ischemia did, however, seem to progress up to 2 weeks, which is a time period similar to the clinical course of SSHL. It has been proposed that ischemic damage possibly contributes to SSHL (Nagahara et al., 1983). Most patients with SSHL spontaneously recover, although some continue to suffer from variable degrees of hearing loss (Byl, Jr., 1984). The time between the initial insult and when treatment begins is a major prognostic indicator of hearing recovery from SSHL. Early intervention aids in recovery. The longer patients wait before beginning medical treatment after the onset of SSHL, the

poorer the recovery (Byl, Jr., 1984). The hearing status in a substantial number of SSHL patients does, however, improve long after the cessation of treatment (Wilkins, Jr. et al., 1987), possibly because of the long recuperation potential, as shown in this study.

Our results also showed that ABR threshold shifts were associated more with the high-frequency range than with the low-frequency range. These observations were confirmed by morphological examination of the cochlear surface preparation and the numbers of HCs that were stained with phalloidin. The basal turn HCs seemed to be more susceptible to ischemic damage than were the upper turn HCs. These observations had been found in previous cochlear ischemia studies that used guinea pigs (Perlman et al., 1959) and gerbils (Maetani et al., 2003). The basal portion of the cochlea has a greater rate of oxygen consumption than does the upper apical portion (Mizukoshi and Daly, 1967). Conversely, the energy reserve of the organ of Corti, especially glycogen, follows an inverse base-to-apex distribution—more glycogen is found in the apical turns than in the basal turns (Thalmann et al., 1972). A base-to-apex gradient of differential intrinsic susceptibility to free radicals has also been reported (Sha et al., 2001). Free radicals and reactive oxygen species are common products of ischemia-reperfusion injuries. The HCs in the basal turns are more vulnerable to free-radical damage than are those in the apical turns (Sha et al., 2001). These observations could explain why the apical turn tolerates ischemic damage better than the basal turn does.

In addition to the intrinsic base-to-apical differential susceptibility to ischemia, this study also showed that guinea pig OHCs were more vulnerable to ischemia than were the IHCs. After 4 weeks, minimal OHC loss occurred when ischemia lasted 15 min, but OHC loss in each cochlear turn was apparent after a 1-h ischemia treatment. Mild loss of IHCs was found after a 30-min ischemia treatment, and significant basal-turn IHC loss was found 4 weeks after a 1-h treatment (Fig. 3.3). In guinea pigs, OHCs may be more vulnerable to ischemia-reperfusion injury than are IHCs (Perlman et al., 1959; Tabuchi et al., 2002). In addition to ischemic damage, OHCs in guinea pigs are more vulnerable to other kinds of cochlear injuries, such as aminoglycoside ototoxicity (Suzuki et al., 2008). With the longer periods of ischemia, both IHCs and OHCs may be affected. Early IHC

loss rather than OHC loss after cochlear ischemia may occur in other species, as IHC loss occurs more readily in gerbils when their cochleae are subjected to ischemia-reperfusion by occlusion of the bilateral vertebral artery (Maetani et al., 2003). Comparatively, more OHC loss after ischemic injury was found for guinea pigs when a similar surgical approach was used to perturb the bilateral vertebral artery (Olszewski et al., 2003). Glucocorticoids possess protective effects against cochlear ischemic damage to guinea pig OHCs (Tabuchi et al., 2006) and gerbil IHCs (Maetani et al., 2009). Therefore, the susceptibility differences of IHCs and OHCs to ischemia may reflect a species difference.

We also found that SGNs were damaged 4 weeks after induced transient ischemia. In addition to direct injury produced by ischemia, secondary SGN loss occurs after HC loss, especially IHC loss (Bae et al., 2008). External insults such as noise trauma, aminoglycoside ototoxicity, or cochlear ischemia could induce excessive glutamate release from IHCs into synaptic clefts. A large glutamate concentration causes SGN cell death (Steinbach and Lutz, 2007). In this study, hair cell loss was not apparent unless the animals were treated for 1 h or longer. In the 30-min ischemia group, mild OHC loss was found, whereas IHCs remained relatively unaffected. Additionally, SGN loss was not apparent unless the animals were treated for 1 h, and the morphology of the SGNs remained relatively intact in the 30-min ischemia group. The loss of the SGNs paralleled the loss of IHCs.

Conclusion

Orderly functional and cellular changes in the cochlea were found depending on the duration of ischemia. A base-to-apex gradient of ischemia susceptibility seemed to exist. HCs and SGNs were most vulnerable to ischemia. The loss of SGNs paralleled the loss of IHCs. The revival time for guinea pig cochlea after transient ischemia may be up to 30 min.

3.5 Figures

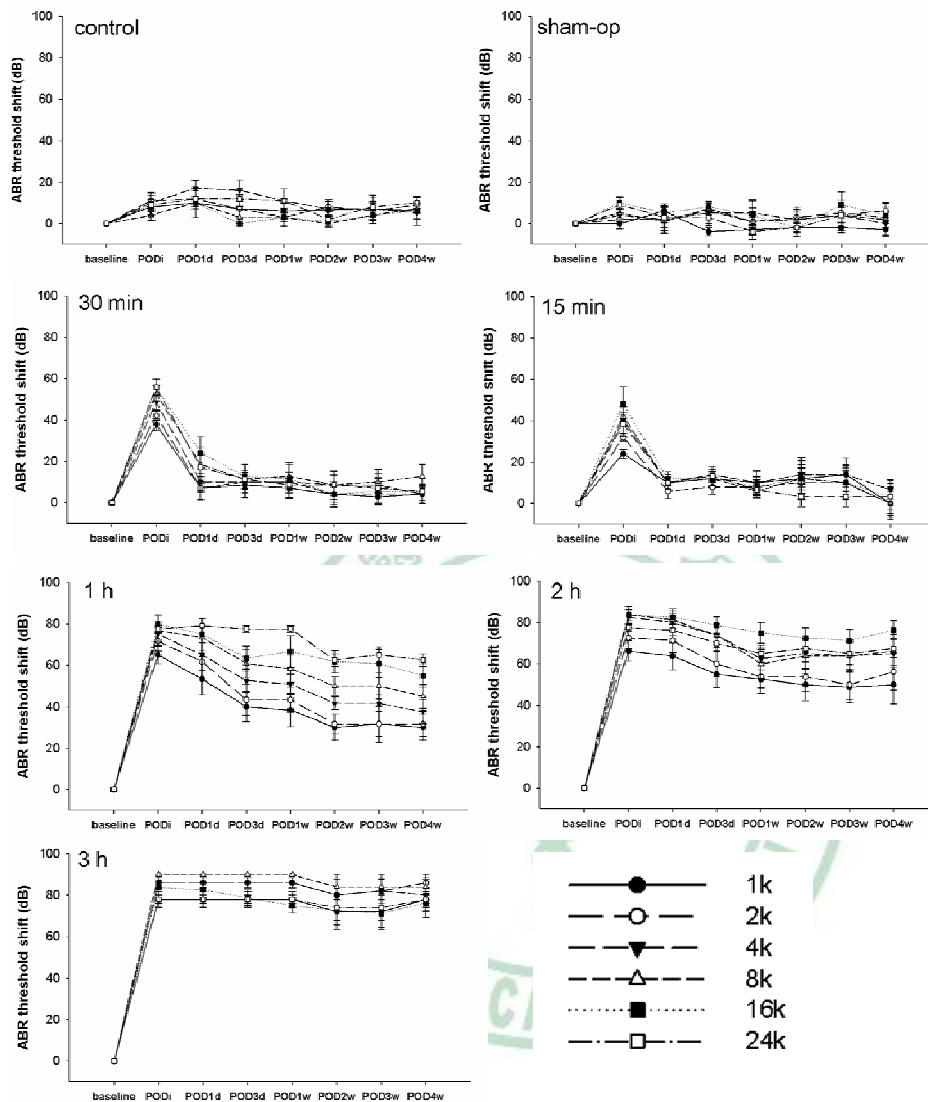


Figure 3.1 Serial ABR threshold shifts after different periods of transient cochlear ischemia induced by microclamps. No significant ABR threshold shifts were noted in the control and sham-op groups. Transient ABR threshold shifts were found for the 15- and 30-min ischemia groups. Progressive partial recovery of the ABR threshold shifts was found for the 1-h ischemia group. X-axis indicates the timing for serial ABR measurement, from baseline, PODi, POD1d, 3d, 1w, 2w, 3w, and 4w. The abbreviations PODi, POD1d, 3d, 1w, 2w, 3w, and 4w are defined in Materials and Methods. The value with error bar in each point indicates mean \pm standard error (S.E.)

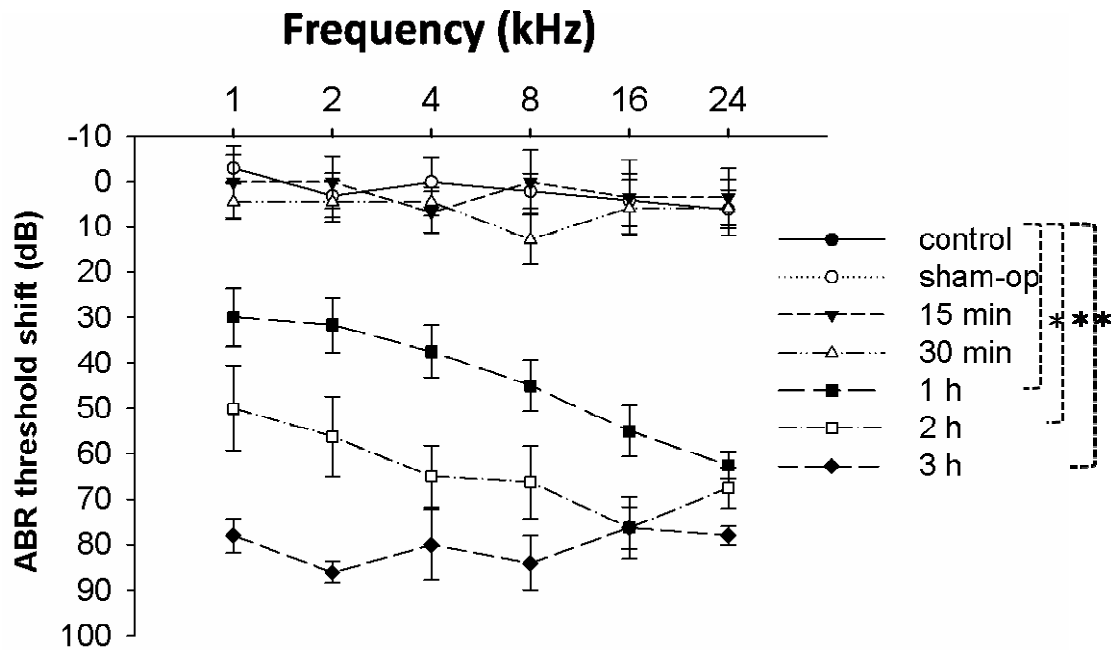


Figure 3.2 ABR threshold shifts 4 weeks after cochlear ischemia treatments of different durations. Compared with the control group, no significant threshold shifts were noted for the sham-op group or when ischemia lasted ≤ 30 min ($p > 0.05$) but significant ABR threshold shifts were found when ischemia lasted ≥ 1 h (*, $p < 0.001$). A decline-type audiogram was found for the 1 h treatment. The ABR threshold shifts were more severe for the 2 h treatment. The value with error bar in each point indicates mean \pm standard error (S.E.).

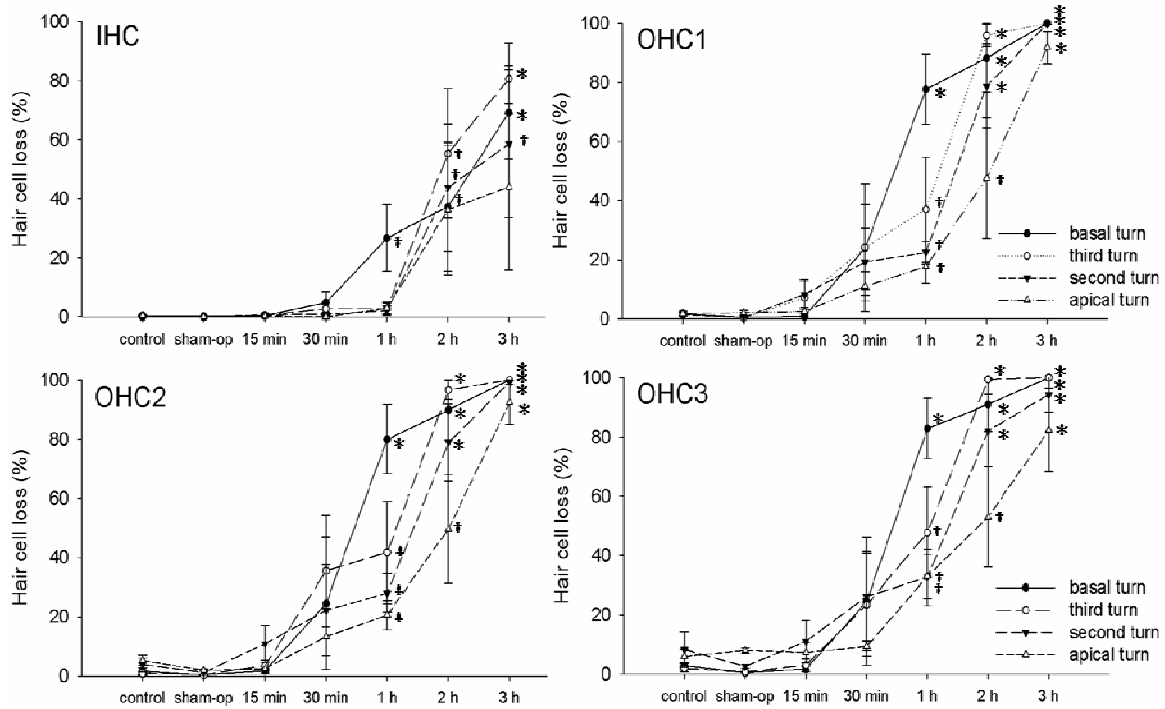


Figure 3.3 Hair cell loss induced by ischemia. Compared with the control group, OHC loss and IHC loss at the basal turn were significant when ischemia was ≥ 1 h. However, loss of IHCs in the upper turns was not significant unless ischemia was ≥ 2 h. The value with error bar in each point indicates mean \pm standard error (S.E.). (†, $p < 0.05$; *, $p < 0.001$).

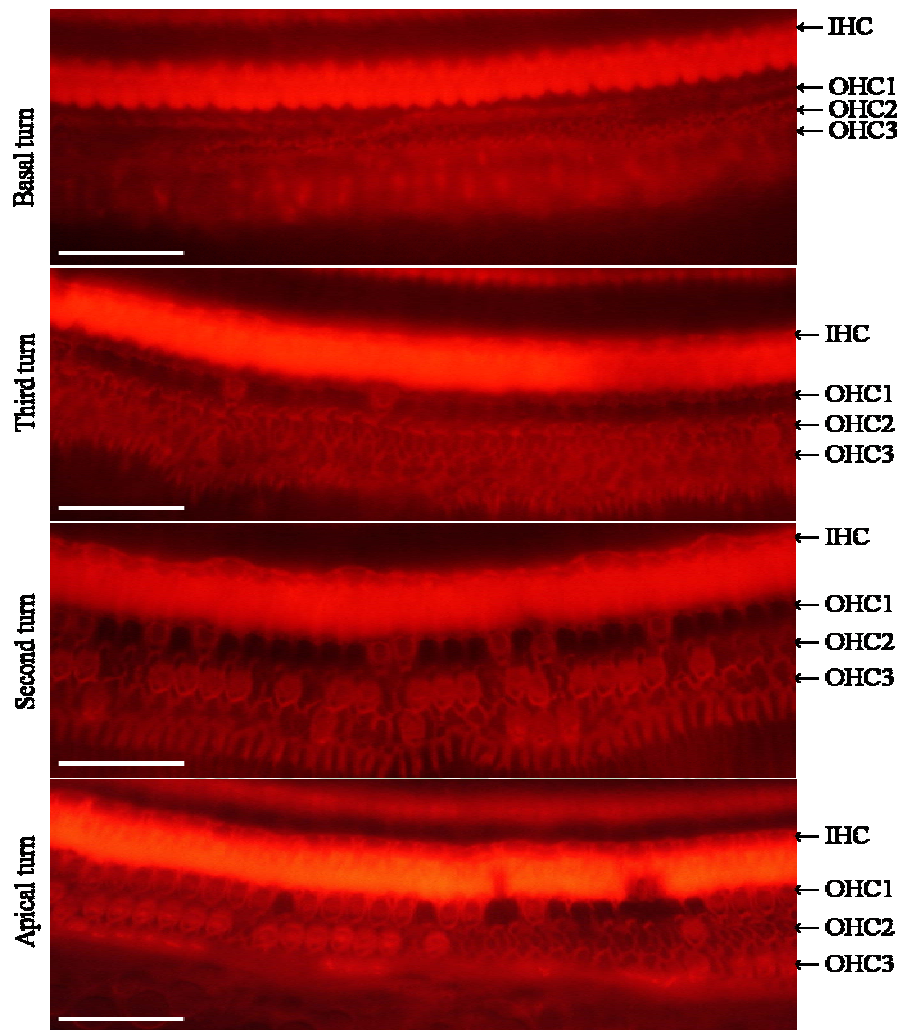


Figure 3.4 Hair cell (HC) labeling with rhodamine-conjugated phalloidin in animals 4 weeks after 2 h ischemia. Complete loss of Inner HCs (IHC) and the three rows of outer HCs (OHC1, OHC2, OHC3) were depicted in the basal turn. Significant loss of HCs was present in the third turn. Some IHCs and OHCs were identifiable in the second and apical turns. Bar=20 μ m

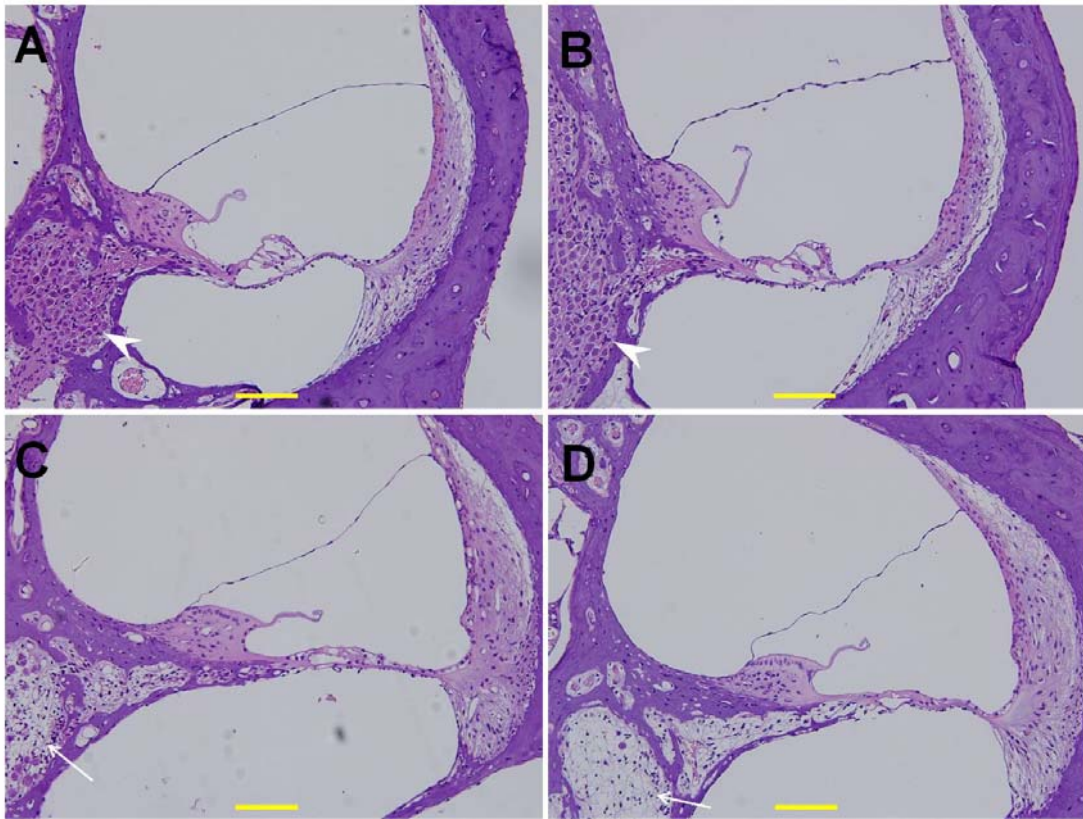


Figure 3.5 Hematoxylin/eosin-stained cochlear sections. A. Normal cochlear section. B. A cochlear section taken 4 weeks after 30 min of ischemia. The architecture of the organ of Corti was intact, contained abundant spiral ganglion neurons (SGNs), and did not show significant spiral neuron loss (arrow head). C. Cochlear section taken 4 weeks after 1 h of ischemia. Apparent loss of SGN (arrow) and flattening of the organ of Corti were observed. D. Cochlear section taken 4 weeks after 2 h of ischemia. Severe loss of SGNs was accompanied by additional flattening of the organ of Corti. Bar=50 μ m

Chapter 4 Effect of hyperbaric oxygen on guinea pig's cochlea

ABSTRACT

Hyperbaric oxygen therapy (HBOT) is a known adjuvant for treating ischemia-related inner ear diseases. Few studies have yet to investigate the cellular changes that occur in inner ears after HBOT. Nitric oxide, which is synthesized by nitric oxide synthase (NOS), is an important signaling molecule in cochlear physiology and pathology. This study investigated the effects of hyperbaric oxygen on eardrum morphology, cochlear function and expression of NOS isoforms in cochlear substructures after repetitive HBOT in guinea pigs. Minor changes in the eardrum were observed after repetitive HBOT, which did not result in a significant hearing threshold shift by tone burst auditory brainstem responses (ABR). A differential effect of HBOT on the expression of NOS isoforms was identified. Upregulation of constitutive NOS (nNOS and eNOS) was found in the substructures of the cochlea after HBOT, but inducible NOS was not found in normal and HBOT animals, as shown by immunohistochemistry. There was no obvious DNA fragmentation present in this HBOT animal model. The present evidences indicated that the customary HBOT protocol may increase constitutive NOS expression but such upregulation did not cause cell death in the treated cochlea. The auditory morphology and function are consequently not changed through the protocol.

4.1 Background

4.1.1 Therapeutic implications of cochlear ischemia

Since 1998, there were several trials of chemical agents in the hope to prevent or alleviate cochlear damage from ischemia. These trials could be classified into two major groups:

- (1) pre-condition or protective effect, i.e., the treatment was given before the episode of ischemia. The aim is to prevent, ameliorate or protect cochlear damage from ischemia.

(2) Therapeutic trial, i.e., the treatment was given after the ischemic episode.

Therefore, the aim is to treat the cochlear sequale from the ischemia.

There are many studies to discuss the protective agents used for the cochlear ischemia. Allopurinol (blocker of free radical formation) and sodium dismutase (SOD) (Seidman et al., 1991) as well as tirilated mesylate (U74006F, a potent inhibitor of lipid peroxidation) (Seidman and Quirk, 1991) has been shown to protect cochlear damage from ischemia/reperfusion (IR). These demonstrated the reactive oxygen species (ROS) play an important role in the IR damage of cochlea. Nitric oxide synthase (NOS) inhibitor, N-nitro-L-arginine administered 1 h before the onset of anoxia alleviated the cochlear dysfunction when the anoxic period was 15 or 30 min but not in the 60-min anoxia (Tabuchi et al., 1999). Mepacrine (phospholipase A2 inhibitor) could also decrease ischemic damage to the cochlea of less than 30 minutes but not in the 60-min anoxia (Tabuchi et al., 2000). Administration of deferoxamine (an iron chelator) or N-nitro-l-arginine (a nitric oxide synthase inhibitor) ameliorated the cochlea damage from IR injury 60 min after the onset of reperfusion (Tabuchi et al., 2001). Aminoguanidine, an inducible NO synthase (iNOS) inhibitor, significantly ameliorated the postischemic cochlear dysfunction induced by 60 min ischemia (Tsuji et al., 2002). Preventive magnesium supplement reduces ischemia-induced hearing loss and blood viscosity in the guinea pig (Scheibe et al., 2000). Ginsenoside Rb1 protects against damage to the spiral ganglion cells after cochlear ischemia (Fujita et al., 2007). AMPA/ kainate-type glutamate receptor antagonist reduces progressive inner hair cell loss after transient cochlear ischemia (Hakuba et al., 2003a). Gene therapy with an adenoviral vector expressing glial-cell-derived neurotrophic factor (GDNF) could prevent ischemia–reperfusion injury of the gerbil cochlea (Hakuba et al., 2003b). Recombinant human erythropoietin prevents ischemia-induced apoptosis and necrosis in explant cultures of the rat organ of Corti (Andreeva et al., 2006).

There were still very few studies to investigate the therapeutic agents after cochlear ischemia. Mannitol as a selective hydroxyl radical scavenger as well as a rheological agent has been shown to improve transient cochlear ischemia of less than 30 minutes in

rats, but of no beneficial effect after 60-minute ischemia (Tabuchi et al., 1998). Glucocorticoids and dehydroepiandrosterone sulfate prevent and treat ischemia-induced injury of the cochlea (Tabuchi et al., 2003; Tabuchi et al., 2006). Neural stem cells suppress the hearing threshold shift caused by cochlear ischemia (Hakuba et al., 2005). Such therapeutic module may be caused by paracrine effects (Yoshida et al., 2007).

4.1.2 Role of hyperbaric oxygen therapy in inner ear diseases

Hyperbaric oxygen therapy (HBOT) is an effective treatment method for decompression sickness and arterial gas embolism. In addition, HBOT is also a famous adjunct in treating ischemia-reperfusion injury of major organs such as brain and inner ear (Lamm et al., 1998; Aslan et al., 2002; Fujimura et al., 2007). After HBOT, the partial pressure of oxygen in cochlear perilymph increases up to 5-fold of its pre-treatment value (Lamm et al., 1998). HBOT has been proposed as an alternative treatment for sudden deafness (Nakashima et al., 1998; Aslan et al., 2002), endolymphatic hydrops, perilymphatic fistula (Lindberg et al., 2003), and acute noise trauma (Hu et al., 1991b; Lamm et al., 1998; Kuokkanen et al., 1997). The efficacy of HBOT in treating these inner ear diseases are variable and the mechanism of the HBOT in inner ears is still not fully understood. For example, HBOT has been proposed to be an effective rescue strategy for noise trauma (Kuokkanen et al., 1997; Ylikoski et al., 2008); however, one study found that HBOT had an adverse effect on the inner ear after noise trauma (Cakir et al., 2006). Consequently, a high degree of medical skepticism still exists regarding the role of HBOT in treating inner ear diseases. More studies on the functional and cellular changes that occur after HBOT may help to elucidate these conflicting results.

Nitric oxide (NO) has important roles in cochlear physiology, including neurotransmission (Zdanski et al., 1994), regulation of cochlear blood flow (Brechtelsbauer et al., 1994; Fessenden and Schacht, 1997), homeostasis of cochlear endolymph (Fessenden & Schacht, 1997) and induction of cytotoxicity under pathological conditions (Morizane et al., 2005; Takumida et al., 2000). NO is synthesized by nitric

oxide synthase (NOS) from the conversion of L-arginine to L-citrulline. Three isoforms of homologous NOS have been identified, including two constitutive isoforms (neuronal NOS [nNOS or NOS I] and endothelial NOS [eNOS or NOS III]) and one inducible isoform (iNOS or NOS II) (Fessenden & Schacht, 1997; Franz et al., 1996; Ruan, 2002). Constitutive NOS is calcium/calmodulin dependent and is continuously expressed, whereas iNOS is calcium independent and is expressed in response to specific stimulants such as cytokines or endotoxins (Takumida et al., 2000). Constitutive isoforms of NOS, both nNOS and eNOS, are expressed in the normal cochlea (Gosepath et al., 1997), but iNOS is expressed in the cochlea only after exposure to some pathologic condition such as endotoxins (Takumida et al., 2000), ischemia (Morizane et al., 2005) or acoustic trauma (Shi and Nuttall, 2003). The aim of this study was to investigate the effects of repetitive HBOT on cochlear function and the expression of NOS isoforms by means of immunohistochemical staining.

4.2 Materials and Methods

4.2.1 Animals

Adult male albino guinea pigs (400–600 g, 10–14 weeks of age) with intact Preyer reflexes and normal eardrums were used in this study. Animals were housed in groups under diurnal lighting conditions, and regular guinea pig diet and water were provided *ad libitum*. Animal use protocols were approved by the China Medical University Committee on Use and Care of Animals (permission number: 96-75-N). The experimental HBOT group included five animals that received regular repetitive HBOT (see below). The control, normobaric air (NBA) group included five animals that did not receive HBOT and were maintained in normobaric room air.

4.2.2 HBOT Model

Hyperbaric oxygen experiments were conducted in a balloon-bag acrylic chamber inside a large pressure chamber (Hyperbaric Oxygen Center in the China Medical University Hospital).(Fig. 4.1) The HBOT protocol used in the study was similar to the

HBOT protocol used in clinical practice for acute cerebral ischemia (Rusyniak et al., 2003). The temperature inside was maintained between 22 and 26 °C with relative humidity at ~60%. Animals were placed inside a small balloon-bag acrylic chamber (120 l) that received 100% oxygen with a ventilation rate at ~20–25 l/min, which is sufficient to allow complete gas exchange at least every 6 min to maintain the nearly pure oxygen and keep the CO₂ level below that in room air (~0.5%). The chamber pressure was steadily increased to a pressure of 2.5 atmosphere absolute (atm abs. or ATA). Compression and decompression were carried out at a rate of 0.2 ATA/min. Each treatment consisted of 17 min of compression time, 60 min of stable compression time at 2.5 ATA and 13 min of decompression time. The animals were continuously observed during the course of HBOT to manually adjust the oxygen ventilation rate and observe the behavior of the animals, particularly for signs of irritability or discomfort. A balloon that indicates the pressure balance between the inside and outside of the small chamber was mounted on the side wall of the small acrylic chamber. The animals in the experimental group received 20 HBOT treatments over a 4-week period (once per weekday, five times per week).

4.2.3 Otoscopic Evaluation

To minimize the frequency of anesthesia, visual assessment of the tympanic membrane was performed associated with the procedure for auditory brainstem response (ABR) measurements (described below). After guinea pigs were anesthetized with intramuscular injection of zoletil (30 mg/kg) and xylazine (10 mg/kg), photographs of the tympanic membrane were obtained using a Storz tele-otoscope. The severity of barotrauma on the tympanic membrane was graded using a modified Teed classification scheme (Teed, 1944): 0, normal; 1, slight vascular injection or retraction of the eardrum; 2, mild hemorrhage in the eardrum; 3, gross hemorrhage in the eardrum; 4, hemotympanum; 5, tympanic membrane perforation.

4.2.4 Auditory Test

Hearing tests were performed by tone burst ABR in a sound-attenuated room, before and after completion of the 20 HBOTs. The pure tone bursts were generated with the amplitude specified by a real-time programmable attenuator (Intelligent Hearing Systems, IHC Smart EP version 3.97, Miami, FL, USA) with ER2 insert earphone, with stimulus frequencies of 1, 2, 4 and 8 kHz (0.2-ms rise/fall time and 1-ms flat segment) with maximal output levels of 125, 123, 111 and 117 dB sound pressure level (SPL). The tone bursts were produced by an IHS transducer (IHS Inc., Miami, FL, USA) in a closed acoustic system through the sound delivery system. Responses for 1024 sweeps were averaged at each intensity level around the threshold in 5-dB SPL steps. Threshold was defined as the lowest intensity level at which a clear waveform was visible in the evoked trace and was determined by visual inspection of the responses. At least two sequences of recordings were made at the threshold intensity to verify the reproducibility of the ABR responses. ABR threshold at each time and at each frequency was compared with the pre-surgical threshold as a baseline. Threshold shift values were estimated.

4.2.5 Immunohistochemistry

4.2.5.1 Preparation of Specimens

Animals were sacrificed after the 20 HBOT treatments. They were first anesthetized by intramuscular injection of zoletil (30 mg/kg) and xylazine (10 mg/kg) and then perfused intracardially with 4% paraformaldehyde in 0.1 M phosphate-buffered solution (PBS) at pH 7.4. The temporal bones and spleen tissues of the animals were removed. The cochleae were opened at the apex and round window and oval window membranes for better penetration of the paraformaldehyde. The temporal bones were immersed in the same fixative overnight at 4 °C. Decalcification was performed with 0.1 M EDTA solution, buffered with PBS to pH 7.4, for 4 weeks at 4 °C. Serial sections (7 µm thick) were cut using a microtome in a plane parallel to the long axis of the cochlea and mounted on silane-coated slides for further immunohistochemical analysis. At least six sections obtained from the modiolus in each animal were immunostained. Serial sections

(7 μm thick) of spleen tissue were also cut using a microtome and mounted on silane-coated slides for further immunohistochemical analysis to act as positive control for the expression of iNOS.

4.2.5.2 Immunohistochemistry

A standard avidin-biotin-peroxidase (ABC) method was used to locate NOS immunoreactive regions (Wei et al., 2005). In brief, the sections were rinsed with 0.05 M Tris-buffered solution (TBS) at pH 7.4 and then incubated in 3% H_2O_2 for 1 h, followed by 0.1% Triton X-100 in 10% serum (normal goat serum [NGS] for eNOS/iNOS and normal horse serum [NHS] for nNOS) for 1 h. Subsequently, samples were incubated overnight at 4 °C with the primary antibodies to nNOS (mouse monoclonal, 1:100, Santa Cruz Biotechnology, Santa Cruz, CA, USA), eNOS (rabbit polyclonal, 1:1000, Santa Cruz Biotechnology) or iNOS (rabbit polyclonal, 1:2000, Santa Cruz Biotechnology). The sections were then incubated with the secondary antibodies, either biotin-conjugated goat anti-rabbit IgG for eNOS and iNOS or anti-mouse IgG for nNOS (Sigma, St. Louis, MO, USA), diluted 1:200 in 2% serum (NGS for eNOS and iNOS and NHS for nNOS). The reaction was developed with a horseradish peroxidase–streptavidin complex (Dako A/S, Denmark) at a 1:300 dilution for 1 h, followed by 0.06% 3,3'-diaminobenzidine (DAB, Sigma) with 0.066% H_2O_2 substrate medium in 0.05 M TBS. All specimens were then dehydrated in a graded series of ethanol and embedded in a Clearmount mounting solution (Zymed, USA). Sections from each of the experimental animals were immunostained during the same run to allow comparisons across the groups. The spleen from each animal was subjected to the same fixation process, sectioned and immunostained to serve as the iNOS-positive control. Sections were photographed and analyzed using a Zeiss Axioskopz light microscope (Axioskop 2, Zeiss, Germany).

4.2.5.3 Semi-quantitative morphometric analysis

The intensities of nNOS and eNOS immunoreactivity were measured in the cochlea by comparing the optical densities (ODs) of the immunoreactivity in the control (normal

room air, NBA) and experimental (hyperbaric oxygen treatment, HBOT) groups using the image analyzer (Image Pro Plus III, Media Cybernetics, USA) (Tsai et al., 2008). Two comparative paramodiolar sections were sampled and analyzed from the apical to the basal turn of the cochleae from both ears of each animal. Twenty different cochlear sections were analyzed in each group, including 80 different regions of each Corti's organ. The total areas of the selected immunoreactive regions were calculated and compared between the control and experimental groups. The packing ODs of the target regions in each cochlea were calculated and compared based on the summation of ODs relative to the selected areas in each cochlear turn, from the apical to basal region.

4.2.5.4 Immunofluorescence labeling

To study the co-expression of nNOS and eNOS in the cochlear sections, immunofluorescence labeling of eNOS and nNOS was performed. The sections were rinsed with 0.05 M TBS at pH 7.4 and then incubated in 3% H₂O₂ for 1 h, followed by 0.1% Triton X-100/10% NGS in PBS for 1 h. Subsequently, they were incubated overnight at 4 °C with the primary antibodies to nNOS (1:100 dilution, Santa Cruz Biotechnology) and eNOS (1:1000 dilution, Santa Cruz Biotechnology). The sections were then incubated with the secondary antibodies, FITC-conjugated goat anti-mouse IgG for nNOS and rhodamine-conjugated goat anti-rabbit IgG for eNOS (Sigma), diluted 1:200 by 2% NGS in PBS. Finally, the section slides were examined in a confocal laser scanning microscope (LSM510, Zeiss).

4.2.5.5 *In Situ* Detection of Nuclear DNA Fragmentation

We used the terminal deoxynucleotidyl transferase (TdT)-mediated deoxyuridine triphosphate (dUTP)-biotin nick end labeling (TUNEL) method to detect DNA fragmentation. The TUNEL assay was performed using an in situ cell death detection kit with a fluorescein label (Roche Diagnostics GmbH, USA). The kit contains TdT, which catalyzes the polymerization of fluorescein dUTP to free 3'-OH DNA ends in a template-independent manner. TUNEL-positive cells were identified by incorporation of

fluorescein-conjugated dUTP. According to the manufacturer's instructions, the sections were pre-treated with permeabilization solution (0.1% Triton X-100 in 0.1% sodium citrate) for 2 min on ice (4 °C) and then incubated for 60 min at 37 °C with the TUNEL reaction mixture. After washing in PBS, sections were photographed in a laser scanning confocal microscope (Zeiss). Brain tissue from guinea pigs that suffered penetrating trauma (under anesthesia) 3 days prior to sacrifice was used as a positive control (Lindh et al., 2008).

4.2.6 Statistical Analysis

All values from groups of animals were expressed as the mean \pm standard error (SE). ABR threshold levels were compared with baseline values before and after HBOT by paired *t*-tests. The statistical analysis for significance of OD values of DAB density, which reflects NOS immunoreactivity, with and without HBOT was performed by an unpaired *t*-test. A value of $p < 0.05$ was accepted as significant.

4.3 Results

4.3.1 Animal behavior during HBOT and otoscopic findings after HBOT

All the animals in the experimental group tolerated the entire course of HBOT without signs of irritability or discomfort. All eardrums were checked and were found to be normal before the study. After 20 HBOT sessions, one ear still remained clean and normal without evidence of hemorrhage (Teed's grade 0), one ear showed slight vascular injection (Teed's grade 1), seven ears developed minor hemorrhage (Teed's grade 2) and one ear developed moderate hemorrhage in the eardrum (Teed's grade 3; Fig. 4.2). No hemotympanum or eardrum perforation was observed in the experimental group. The eardrum condition in the control group remained normal throughout the duration of this study.

4.3.2 ABR measurements before and after HBOT

ABR was used to assess hearing before and after HBOT (Fig. 4.3). In the NBA and HBOT groups, the intragroup hearing level prior to the study and four weeks after commencing the study did not significantly differ. Although slight elevated hearing level at 1 kHz was recorded in the NBA group, the intergroup hearing level between the control NBA and experimental HBOT groups did not significantly differ (Fig. 4.3).

4.3.3 Immunohistochemical analysis of NOS in cochleae

The immunohistochemical results for NOS expression in cochleae from the control group and the experimental group are illustrated in Figs. 4.4–6. In the control NBA group, nNOS exhibited moderate immunoreactivity in the spiral ganglion and stria vascularis and faint immunoreactivity in the modiolar nerve fibers, afferent nerve fibers, limbus and organ of Corti (Fig. 4.4A). In the experimental HBOT group, enhanced immunoreactivity of nNOS was present in the spiral ganglion, modiolar nerve fibers, afferent nerve fibers and stria vascularis (Fig. 4.4B). Using semi-quantitative morphometric analysis, significant enhanced immunoreactivity of nNOS was noted in the limbus and in the nerve fiber bundles (Fig. 4.5A).

Immunohistochemistry using an antibody against eNOS in the control NBA group revealed moderate immunoreactivity in the stria vascularis, organ of Corti, limbus, spiral ganglion and modiolar blood vessels (Fig. 4.4C). In the experimental HBOT group, enhanced immunoreactivity of eNOS was present in the spiral ganglion, modiolar blood vessels, limbus and stria vascularis (Fig. 4.4B). Significantly enhanced eNOS immunoreactivity was noted in the spiral ganglion, modiolar blood vessels, nerve fibers and the limbus (Fig. 4.5B).

Immunohistochemistry using an antibody against iNOS did not reveal immunoreactivity in the NBA and HBOT groups, as compared with the iNOS expression in the positive control spleen tissue (Fig. 4.4E–G).

To assess the co-expression of nNOS and eNOS in the cochlea after HBOT, we used confocal microscopy (Fig. 4.6). Co-expression of nNOS and eNOS was noted in the spiral

ganglion and stria vascularis. Single expression of eNOS immunoreactivity was also present in the capillaries of the spiral ganglion (Fig. 4.6). In the cochlear modiolus, nNOS was expressed in the modiolar nerve fibers, whereas eNOS was expressed along the modiolar blood vessels.

4.3.4 TUNEL assay of cochleae after HBOT

To determine if there was any DNA fragmentation or apoptotic cell death after HBOT, we used the TUNEL assay to evaluate the cellular changes after HBOT. DNA fragmentation and possible apoptotic cell death were observed in the positive control obtained from brain tissue with penetrating damage (Fig. 4.7A–C); however, no DNA fragmentation was found in the cochlear tissue after HBOT (Fig. 4.7D–F).

4.4 Comments and conclusion

Our present study, which was designed according to the HBOT protocol used in clinical practice for acute cerebral ischemia (Rusyniak et al., 2003), provides a functional measurement and immunohistochemical evidence of cochlear NOS changes as well as morphological evaluation of the eardrum after HBOT. HBOT effects on hearing may be caused by decompression illnesses or barotraumas to the middle or inner ear (Klingmann et al., 2007). A slight increase in hearing sensitivity is evident in animals receiving extreme acute hyperbaric conditions (Miller, 1971). The increased hearing sensitivity may be caused by changes in the tympanic membrane and middle impedance, which may be altered under hyperbaric conditions (Miller, 1971). In this study, the tympanic membrane and mesotympanum were observed by otoscopy after repetitive HBOT. No significant changes in tympanic membrane or mesotympanic injury were observed, with the exception of one ear with moderate hemotympanum (Fig. 4.2). This result is similar to previous observations that barotraumas that are due to repetitive HBOT might gradually improve without significant sequels (Beuerlein et al., 1997). In this study, guinea pigs may have been able to tolerate chronic hyperbaric treatment possibly because of their normal Eustachian tube function. Therefore, the hearing threshold was not significantly

affected by the minor changes in the eardrum and middle ear (Fig. 4.3).

Another potential harmful effect of HBOT on hearing is possible damage to the inner ear. Transient deterioration of cochlear function during the initial exposure to HBOT has also been observed in guinea pigs and rabbits, which might be attribute to the vasoconstriction of cochlear blood vessels during the initial exposure to hyperbaric oxygen (Murata et al., 1974). Hyperbaric oxygen causes a slight morphologic alteration in the outer hair cells of newborn rats (Picciotti et al., 2005). After repetitive HBOT, minor changes in cochlear function were observed including cochlear degeneration, inner hair cell damage and hemorrhage in the perilymphatic space and scala media (Zheng and Gong, 1992). The cochlear hemorrhage phenomenon after hyperbaric treatment was also reported in rats (Levendag et al., 1981). The cochlear changes observed in these studies (Levendag et al., 1981; Zheng & Gong, 1992) might be caused by higher-pressure conditions and a more-rapid compression-decompression process, since cochlear degeneration and hemorrhage were more pronounced under higher-pressure conditions (up to 5 ATA) (Zheng & Gong, 1992). In that study, the rate of inflation was >0.3 ATA/min, and the deflation rate was about 0.5 ATA/min. These conditions exceed the standard HBOT protocols used in clinical practice. With a slower compression-decompression process and lower air pressure, no significant changes in hearing levels were observed after repetitive HBOT (Beuerlein et al., 1997; Mendel et al., 2000). In this study, a slower compression-decompression protocol (≤ 0.2 ATA/min) and lower maximum peak pressure (2.5 ATA) more closely mimic the current HBOT protocol used in clinical practice. It is of note that no significant shifts in the hearing level before and after HBOT and no obvious cell death by TUNEL assay were observed using this animal model. The results of this study may thus indicate more accurately the effects of HBOT treatment on the cochlea, which include a reduced effect of compression-decompression or of excessive hyperbaric exposure effects.

In theory, elevating the hydrostatic pressure, as occurs during HBOT, increases partial oxygen in target tissues. After hyperbaric treatment at 2.5 ATA with pure oxygen, partial oxygen pressure in the cochlear perilymph may increase by up to 5-fold (Lamm et al.,

1998). It is plausible that HBOT should be effective for some ischemia-related hearing impairment, such as sudden sensorineural hearing loss (Aslan et al., 2002; Nakashima et al., 1998) or noise-induced hearing loss (Kuokkanen et al., 1997; Ylikoski et al., 2008). In addition to elevation of partial oxygen pressure, oxidative stress is believed to be fundamental to the therapeutic mechanisms for HBOT (Thom, 2009). NO, as one of the basic signaling molecules of reactive nitrogen species that contribute to oxidative stress (Thom, 2009), is synthesized by different NOS isoforms. After HBOT, the expression of individual NOS isoforms varies among different target organs, which results in different responses. The cerebrovascular responses to hyperoxia may be modulated by eNOS and nNOS-derived NO (Atochin et al., 2003). Repetitive HBO exposure may upregulate eNOS and nNOS in the brain, which may enhance the sensitivity of the brain to convulsion and lead to seizures during subsequent oxygen exposure (Liu et al., 2008). Such hyperoxia-induced seizures may result from cerebral vasoconstriction by eNOS-derived NO (Atochin et al., 2003; Demchenko et al., 2003) and lead to superoxide generation mediated by nNOS-derived NO (Demchenko et al., 2003). In contrast, preconditioned HBOT may exert myocardial protection by way of eNOS (Cabigas et al., 2006). Therefore, the effect of HBO on the tissue can be beneficial or harmful depending on the type of tissue.

Different NOS isoforms are expressed in discrete regions of the cochlea. The constitutive NOS, nNOS and eNOS, are distributed in the substructures of the cochlea under normal physiologic conditions (Gosepath et al., 1997). nNOS immunoreactivity is found in the hair cells, spiral ganglion, stria vascularis, spiral ligaments, limbus and nerve fibers and spiral ganglion, whereas eNOS immunoreactivity is present in the endothelium of the cochlear microvascular trees, stria vascularis, limbus and the spiral ganglion (Gosepath et al., 1997; Franz et al., 1996). iNOS was not found in the structures of the normal cochlea (Ruan, 2002). iNOS is expressed in the cochlea only after exposure to some pathologic condition such as endotoxin (Takumida et al., 2000), ischemia (Morizane et al., 2005) or acoustic trauma (Shi & Nuttall, 2003; Gosepath et al., 1997). In this study, the distribution of nNOS and eNOS was similar to that of previous studies

(Franz et al., 1996; Gosepath et al., 1997). nNOS was distributed in the spiral ganglion, nerve fiber bundles, stria vascularis, limbus and hair cells. eNOS was distributed along the microvascular structures in the cochlea such as the endothelium of blood vessels in the modiolus, stria vascularis, spiral ganglion and limbus. Expression of iNOS was not, however, evident in this study. The HBOT protocol used in this study mimicked that being used in human beings; thus, this protocol might not induce significant pathologic changes for iNOS expression.

To our knowledge, this is the first report of the upregulation of constitutive NOS in some substructures of the cochlea after HBOT treatment. Constitutive NOS may act as a protective enzyme. In cerebrovascular tissue, hyperbaric oxygen can elicit a vasorelaxing effect from constitutively active NO by eNOS and nNOS (Atochin et al., 2003), although nNOS may have some vasoconstrictive effect during the early exposure to HBO (Demchenko et al., 2003). NOS produces NO, which induces relaxation of the smooth musculature and regulation of the vasotonia as a microbotic messenger (Atochin et al., 2003). Thus, the important role of NO in cardioprotection (Cabigas et al., 2006) and cerebroprotection (Helms et al., 2005) against ischemic damage is established. NO released from constitutive NOS such as eNOS also protects cochlear venules from excessive venular leakage (Shi and Nuttall, 2002). In contrast, iNOS usually has a devastation role in biological processes. Induction of iNOS has also been demonstrated in some cochlear pathologies like ischemia (Morizane et al., 2005) or noise trauma (Shi & Nuttall, 2003). When the cochlea is exposed to hypoxic or ischemic conditions, the expressed iNOS may lead to an overexpression of peroxides (Demchenko et al., 2003), which consecutively induce a direct toxic effect on neurons and may affect the endocochlear potential. The synaptic complex between the hair cells and the nerve fibers is another region that the NO may exert its role (Mazurek et al., 2006). NO could inhibit the glutamate receptors by positive feedback under normoxic conditions. Conditions causing cochlear hypoxia such as acoustic overstimulation may induce glutamate release and calcium influx at the synaptic complex between the hair cells and the nerve fibers (Mazurek et al., 2006) and increase iNOS expression with excessive formation of NO

(Shi & Nuttall, 2003). Upon glutamate release, overproduction of iNOS-derived NO can further increase the cochlear oxidative stress and cochlear dysfunction. In this study, only constitutive NOS, especially eNOS, was upregulated after HBOT, whereas iNOS was not immunoreactive. Thus, HBOT may play a therapeutic role rather than an adverse affect on cochlear pathology.

Conclusion

To clarify the mechanism of therapeutic effect by HBOT, we investigated the effect of HBO on immunoreactivity to eNOS, nNOS and iNOS in the cochlear of guinea pigs. In the experimental group, the animals received 20 sessions of HBO treatments. Significant increased expression of eNOS in the stria vascularis, spiral ganglion and blood vessels and nNOS in the modiolar nerve bundles in the experimental group than in the control group. No significant iNOS expression was shown in both groups. Confocal microscopy showed that the up-expression of nNOS in the modiolar blood vessels may be related to the expression of eNOS. Morphologic changes of the eardrums after HBOT were only minor changes. Functional evaluation with ABR did not exhibit significant threshold shifts after HBOT in both groups. TUNEL assay of the cochlea also did not show cell death after HBOT. These results suggest that the therapeutic effect of HBO may be through the up-regulation of eNOS.

4.5 Figures

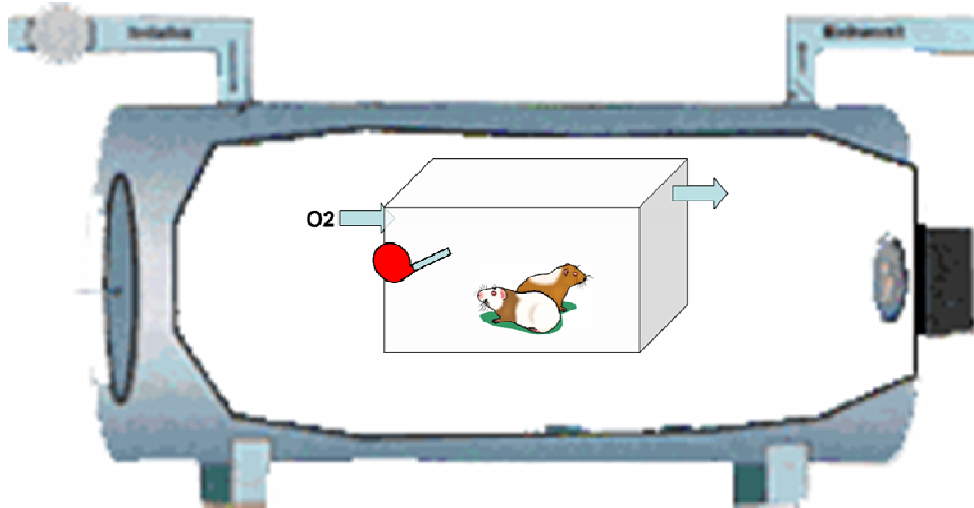


Figure 4.1 Design of HBO chamber for this study. Animals were placed inside a small balloon-bag acrylic chamber (120 l) that received 100% oxygen with a ventilation rate at ~20–25 l/min, which is sufficient to allow complete gas exchange at least every 6 min to maintain the nearly pure oxygen and keep the CO₂ level below that in room air (~0.5%). The chamber pressure was steadily increased to a pressure of 2.5 atmosphere absolute (atm abs. or ATA). Compression and decompression were carried out at a rate of 0.2 ATA/min. Each treatment consisted of 17 min of compression time, 60 min of stable compression time at 2.5 ATA and 13 min of decompression time. A balloon that indicates the pressure balance between the inside and outside of the small chamber was mounted on the side wall of the small acrylic chamber.

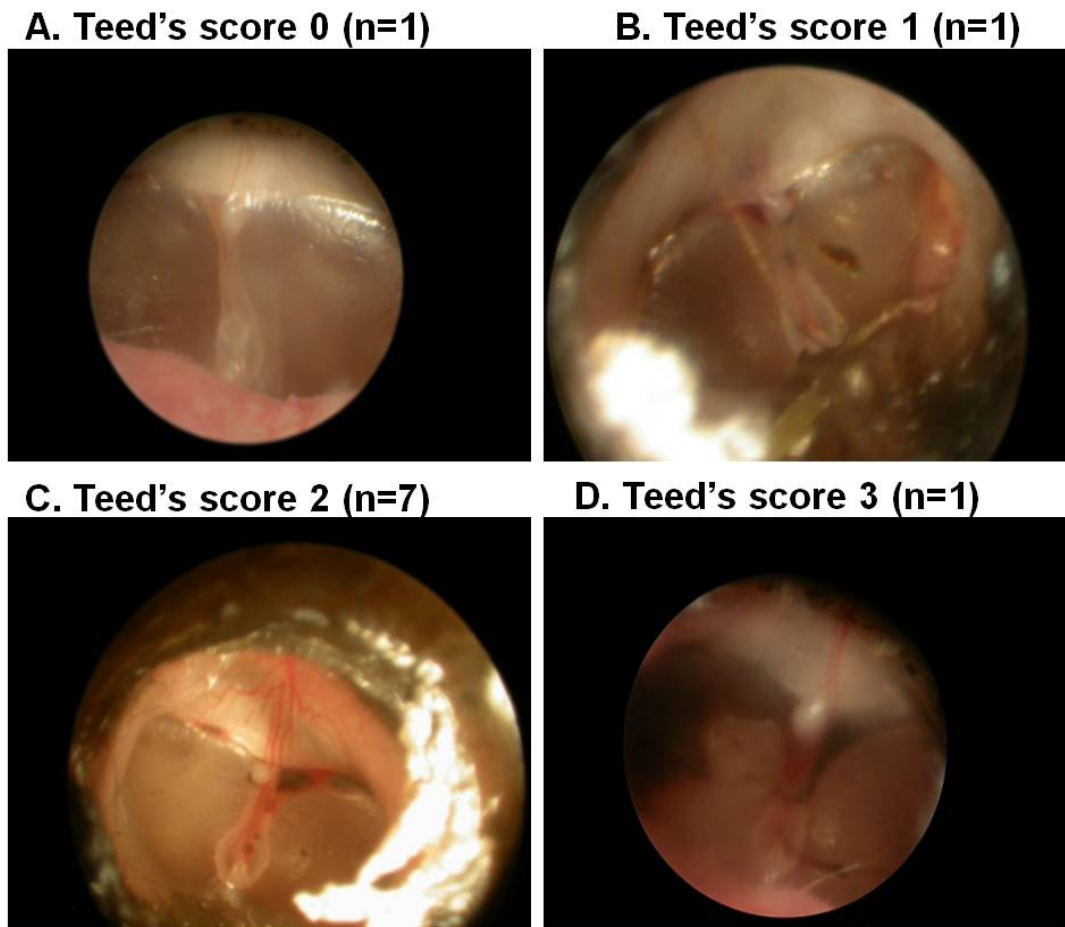


Figure 4.2 Otoscopic view of the eardrum in guinea pigs after 20 sessions of repetitive hyperbaric oxygen treatment. A. normal eardrum (Teed's score 0), n=1; B. Mild retraction of eardrum with minimal hemorrhage (Teed's score 1), n=1; C. mild hemorrhage over the eardrum, (Teed's score 2), n=7; D. Eardrum with moderate hemorrhage (Teed's score 3), n=1.

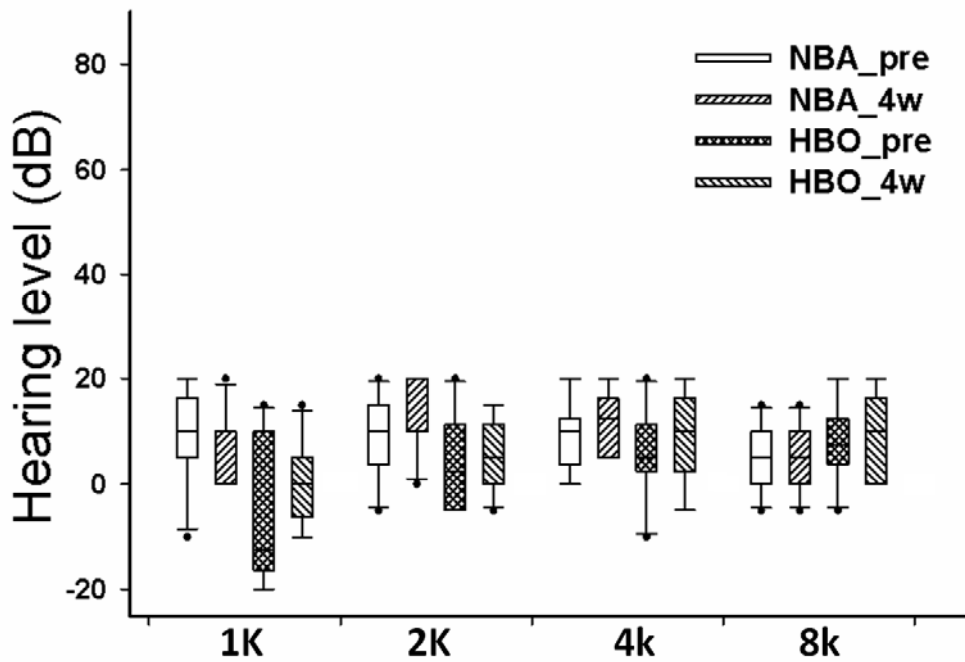


Figure 4.3 Box plot of the hearing level in the control, normobaric air (NBA) group and the experimental, hyperbaric oxygen (HBO) treatment group before (_pre) and 4 weeks after (_4w) the treatment sessions. There were no significant intra-group changes or inter-group differences in the hearing levels before and 4 weeks after the start of the treatment. The dots represent the outliers.

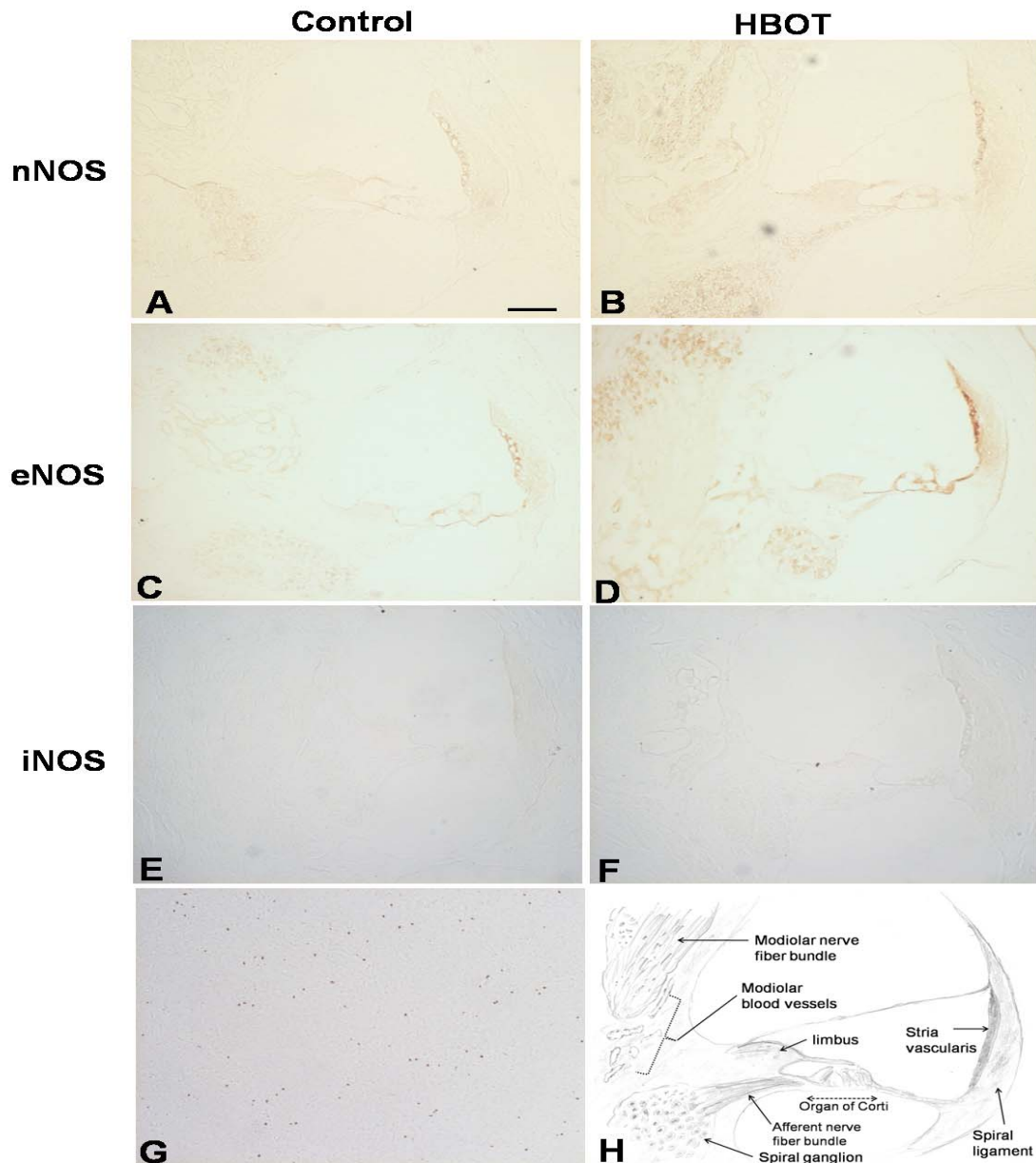


Figure 4.4 Immunohistochemistry of cochlear nNOS (A,B), eNOS (C,D) and iNOS (E,F) expression in the control and HBOT groups. (G) Spleen tissue was used as a positive control for iNOS. (H) Schematic drawing depicting a cross-section through cochlear canals and its related sub-structures. (A,B) nNOS immunoreactivity was present in the spiral ganglion, stria vascularis, organ of Corti and modiolar nerve bundles in both groups but enhanced immunoreactivity was present in the HBOT group. (C,D) eNOS immunoreactivity was found in the modiolar blood vessels, stria vascularis, organ of Corti and spiral ganglion in both groups with more enhanced immunoreactivity in the HBOT group. iNOS did not exhibit immunoreactivity in the control NBA (E) and HBOT (F) groups, as compared with the positive control of iNOS expression in the spleen tissue (G). Bar=50 μ m.

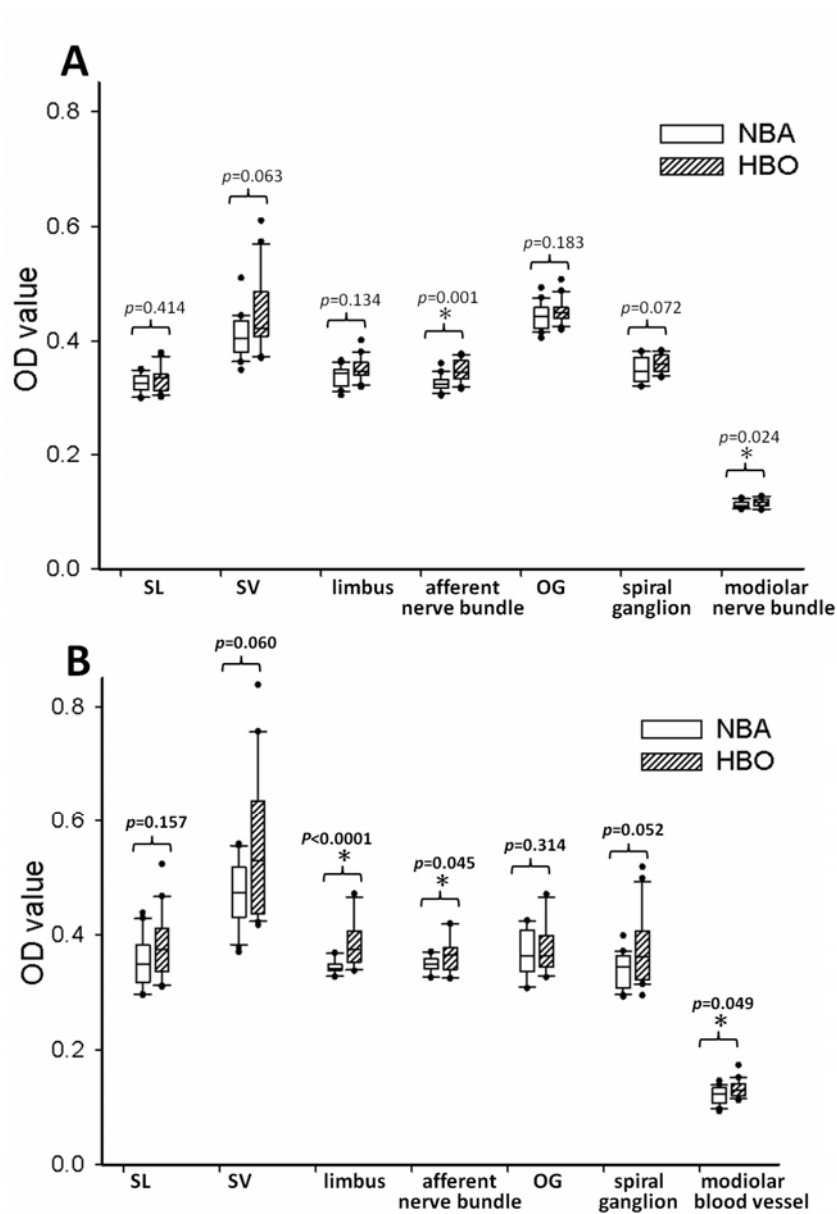


Figure 4.5 Box plot of the morphometric measurements as the changes in the ODs of nNOS (A) and eNOS (B) in the control NBA (in white box) and experimental HBO treatment group (in dash box). The expression of nNOS was significantly enhanced in nerve fiber bundles after HBOT. The expression of eNOS was significantly enhanced in the limbus, nerve fiber bundles and modiolar blood vessels after HBOT. The dots represent the outliers. OD, optical densities; SL, spiral ligament; SV, stria vascularis; OG, organ of Corti.

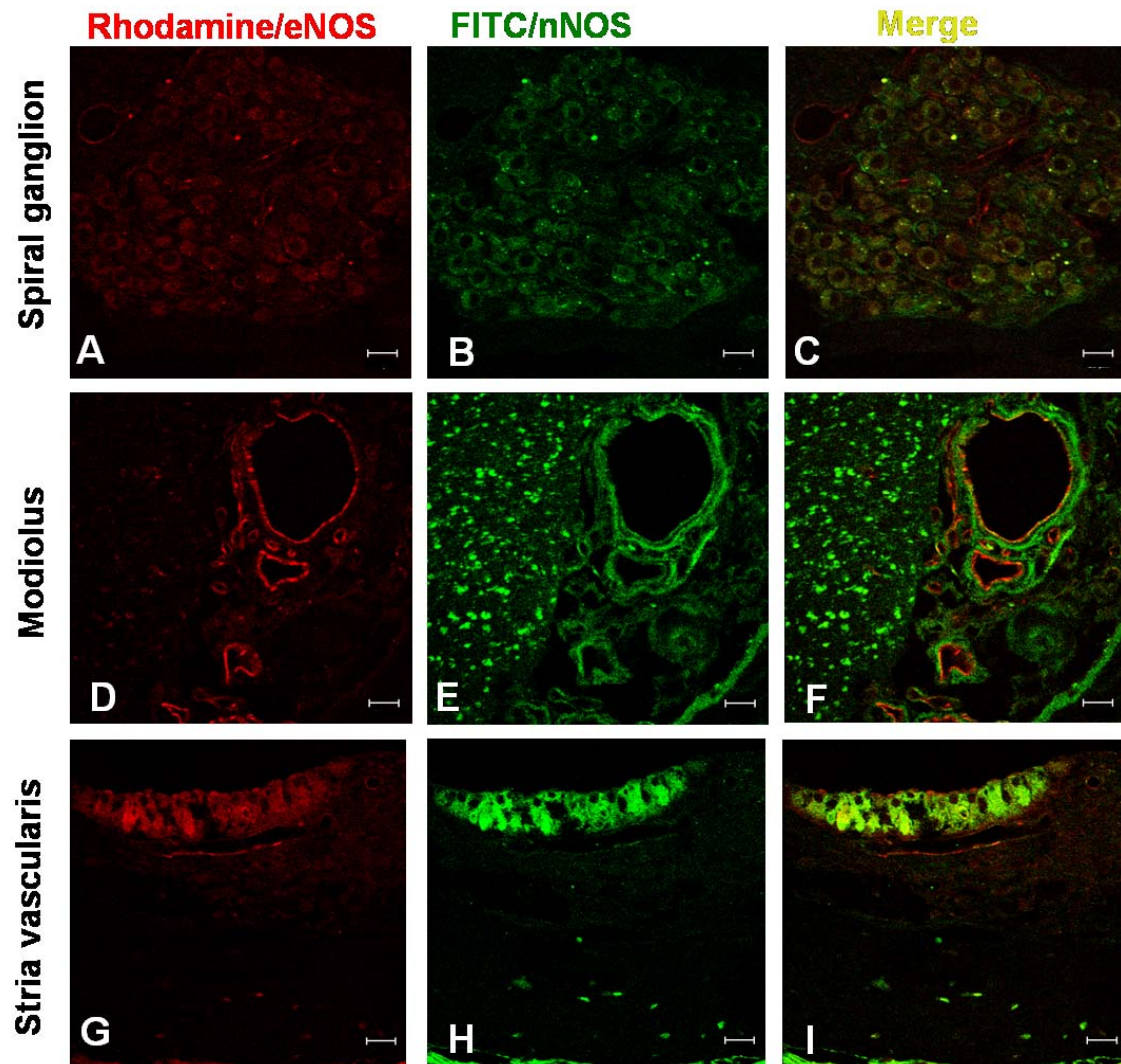


Figure 4.6 Immunofluorescence labeling of eNOS (red) and nNOS (green) in the spiral ganglion (A–C), cochlear modiolus (D–F) and stria vascularis (G–I) of the cochlea after repetitive HBOT. Co-expression of eNOS and nNOS occurred in the spiral ganglion (C) and stria vascularis (I). In the cochlear modiolus, nNOS was expressed in the modiolar nerve fibers, and eNOS was expressed along the modiolar blood vessel. Bar=20 μ m.

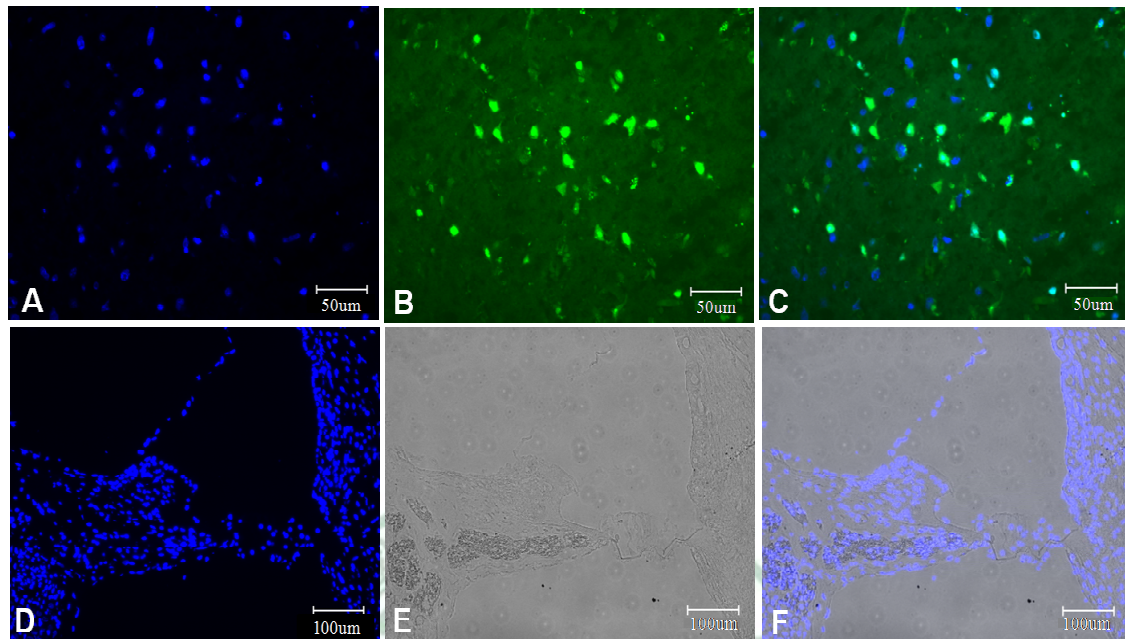


Figure 4.7 TUNEL assay of cochleae after HBOT. Significant DNA fragmentation was shown in the brain tissue with penetrating injury (A–C); however, no evidence of DNA damage was identified in the cochlear tissue after HBOT (D–F).

Chapter 5 Increased aminoglycoside ototoxicity in acute cochlear mitochondrial dysfunction—interaction of kanamycin to 3-nitropropionic acid

ABSTRACT

Ototoxicity of aminoglycoside has ever been well-researched. One of the risk factors for aminoglycoside ototoxicity was discovered as the mutation of mitochondrial DNA. The direct interaction of aminoglycoside in cochlear mitochondrial dysfunction is still lacking. We mimicked cochlear mitochondrial dysfunction by administering a mitochondrial toxin, 3-nitropropionic acid (3-NP), into the cochlea via the round window membrane. Guinea pigs treated with 150mM of 3-NP exhibited significant temporary threshold shifts in auditory brainstem response (ABR). The animals with normal thresholds of ABR were administered with 150mM of 3-NP and/or 400 mg/kg kanamycin (KM), followed by consecutive ABR measurements and their cochlear hair cell counting at sacrifice. Significant ABR threshold shifts were observed in the animals treated with 3-NP group and 3-NP+KM group at 14 days after administration. The threshold shifts were greater in 3-NP+KM group than those with 3-NP group. The recovery of ABR threshold shifts was observed in the animals treated with 3-NP group but not in the 3-NP+KM group. Significant loss of outer hair cells in the cochlear basal and second turns was observed in the 3-NP+KM group but not in the other groups (3-NP alone, KM alone and control group). In conclusion, this study demonstrated straightforwardly an increased susceptibility for aminoglycoside ototoxicity in cochlear mitochondrial dysfunction.

5.1 Background

Aminoglycoside antibiotics have been an important and integral part of our antibacterial drug armamentarium since their discovery in the 1940s (Schatz et al., 2005). On the other hand, their use is constrained by their well-known toxic effects on the inner

ear and kidney. The damage to the inner ear can be permanent, while renal dysfunction is usually reversible. Mechanisms for aminoglycoside ototoxicity have been well researched since then and revealed to the point that irrevocable loss of outer hair cells (OHCs) and, to some degree, inner ear cells (IHCs) as well result in a permanent auditory threshold shift (Forge & Schacht, 2000). The aminoglycoside ototoxicity initially damage the outer hair cells in the basal turn of the cochlea and gradually progress to the inner hair cells and supporting cells, from the base toward the cochlear apex (Leake and Hradek, 1988).

The aminoglycoside-induced hearing impairment occurs in a dose-dependent manner and idiosyncratic pattern (Fischel-Ghodsian, 1999a). There are 2~25% of patients who experience sensorineural hearing loss even when aminoglycosides are administered at the recommended or subtherapeutic levels or for a short time only (Meyers, 1970). Genetic predispositions are presumed to play a significant role in the idiosyncratic pathway of the susceptibility to aminoglycoside ototoxicity (Fischel-Ghodsian, 1999a). Genetic studies of the maternal transmission pattern in familial aminoglycoside ototoxicity suggest that mitochondrial DNA (mtDNA) mutations are involved in the susceptibility of aminoglycoside ototoxicity (Fischel-Ghodsian, 1999a; Prezant et al., 1993; Hu et al., 1991a; Higashi, 1989). An A-to-G substitution in location 1555 (A1555G) of the mitochondrial rRNA gene is one of the most common genetic causes of aminoglycoside-induced hearing loss (Fischel-Ghodsian, 1999a; Prezant et al., 1993; Hutchin et al., 1993). More than half of these patients with idiosyncratic aminoglycoside-induced hearing loss have the maternally inherited A1555G mutation (Usami et al., 2000). The deletion of thymine at position 961 combined with a heteroplasmic and variable increase of cytosine surrounding position 961 (Δ T961Cn) (Casano et al., 1999) and C-to-T transition at position 1494 (C1494T) (Zhao et al., 2004) in the 12S rRNA have also been found to predispose these patients to aminoglycoside-induced hearing loss. The mtDNA mutation in 12S rRNA is the hot spot for idiosyncratic aminoglycoside ototoxicity.

In addition to the mutation in 12S rRNA genes, non syndromic sensory neural hearing losses are also caused by mutation in mitochondrial tRNA^{Ser} gene (Willems, 2000; Guan,

2004a). In the absence of aminoglycoside, the severity and onset of hearing loss in these patients are extremely variable and a significant portion of them has normal hearing for their life long (Schrijver, 2004). Mitochondrial dysfunction itself has been well known to induce sensory neural hearing impairment. Progressive sensorineural hearing loss occurs in many patients with typical mitochondrial diseases, such as MELAS syndrome (mitochondrial encephalopathy with lactic acidosis and stroke-like episodes) and MERRF syndrome (myoclonic epilepsy and ragged red fibers) (Fischel-Ghodsian, 2003). These indicate that mitochondrial mutation alone may not be sufficient to produce hearing loss and some environmental factors may further induce the presentation of hearing loss. The actual effect of aminoglycoside in mitochondrial dysfunction needs to be clarified.

Recently the mitochondrial toxin, 3-nitropropionic acid (3-NP), which is an irreversible inhibitor of succinate dehydrogenase in the mitochondrial electron transport chain (Coles et al., 1979; Alston et al., 1977), were used by infiltrating through the round window of rat cochlea and induced hearing loss (Hoya et al., 2004). It was found by them that 3-NP affected to the rat cochlear by marked degeneration of the lateral wall of the cochlea (Okamoto et al., 2005; Hoya et al., 2004).

In the present study, we investigated the interaction of aminoglycoside in the model of cochlear mitochondrial dysfunction by administering 3-NP and kanamycin to the guinea pigs. The purpose is to demonstrate the direct boost effects of aminoglycoside ototoxicity in cochlear mitochondrial dysfunction.

5.2 Materials and Methods

5.2.1 Animals

Male albino guinea pigs aging weighing 140-250 g at the onset of the experiment were used. The use and care of animals reported in this study was approved by Tohoku University's Animal Care and Use Committee.

Before the beginning of the experiments, normal hearing was confirmed with auditory brainstem response (ABR) audiometry. All surgeries and ABR examinations were performed following anesthesia with xylazine (10 mg/kg) and ketamine (40 mg/kg).

Additionally, 1% lidocaine (Xylocaine) was infiltrated into the surgical area as local anesthesia prior to the surgery.

5.2.2 Animal treatment

3-NP (Sigma, St. Louise, MO, USA) was dissolved with normal saline (NS) and was adjusted to pH 7.4 with sodium hydroxide. Nineteen guinea pigs were divided into four groups (Fig. 1). All animals were performed a surgery. The surgical procedure was modified from that of Hoya et al (Hoya et al., 2004; Sha et al., 2001). After the postauricular incision, the mastoid bulla was opened. A tiny piece (about 1mm³) of Gelfoam (Pharmacia & Upjohn Company, Kalamazoo, MI) soaked with 3ul of NS (Groups A and B) or 3-NP (Groups C and D) was put on the cochlear round window niche (RWN) gently with a fine needle. The mastoid defect was then closed with carboxylate dental cement (ESPE, Durelon, Norristown, PA), followed by the suture of the skin incision. The cochlea of the other side was surgically destroyed to prevent the cross-hearing phenomenon during ABR measurement. Chloramphenicol (30 mg/kg) was administered intramuscularly as prophylaxis of infection after the surgery. The animals in both Group C (n=5) and Group D (n=5) were administrated 3-NP, in addition to which kanamycin (KM, 400 mg/kg; Sigma) was injected subcutaneously to the animals in Group D (3-NP+KM group) 2 hours later after the surgery. The animals in both Group B (n=5) and Group A (n=4) were administrated NS soaked gelfoam to the RWN instead of 3-NP. Subcutaneous injection of KM (400 mg/kg) was performed to Group B (KM group), not to Group A (control group). The experimental time course is summarized in Fig. 5.1.

5.2.3 Auditory brainstem response (ABR)

The course of hearing was evaluated with ABR at 1, 3 and 6 hours after the surgery and 1, 3, 7, 10 and 14 days after the surgery. ABR examination was performed in a double-walled sound booth. Pure tone bursts of 4, 8, 12, 16 and 20 kHz (0.2 ms rise/fall time and 1ms flat segment) were generated and the amplitude specified by a real-time

processor and programmable attenuator (RP2.1 and PA5, Tucker-Davis Technologies, FL, USA). The maximum output level was 94, 95, 106, 87 and 80 dB SPL at 4, 8, 12, 16 and 20 kHz, respectively. The tone bursts were produced by a coupler type speaker (ES1spc, Bio Research Center, Nagoya, Japan) and delivered to the external ear canal in a closed acoustic system through the sound delivery system. Responses for 1024 sweeps were averaged at each intensity level around threshold in 5 dB sound pressure level (SPL) steps. Threshold was defined as the lowest intensity level at which a clear waveform was visible in the evoked trace and was determined by visual inspection of the responses. At the threshold intensity, at least two sequences of recordings were made to verify the reproducibility of the ABR responses.

5.2.4 Hair cell counting

The animals were sacrificed at 14 days after the surgery by decapitation under deep anesthesia. Their temporal bones were immediately removed from the skull and fixed with 4% paraformaldehyde in 0.1M phosphate buffer saline (PBS) solution by perilymphatic perfusion and immersion. The bony modiolus with the organ of Corti was carefully detached at the base of the cochlea following removal of the bony capsule, lateral wall and tectorial membrane. After permeabilization with 0.3% Triton X-100 in PBS for 10 min, the tissues were incubated with rhodamine-coupled phalloidin (Molecular Probes, Eugene, OR, USA) diluted 1:100 in PBS at room temperature for 30 min. After rinsing with PBS, strips of the organ of Corti were detached from the modiolus, mounted on glass slides, and examined using a fluorescence microscope (Model Leitz DM RBE; Leica, Wetzlar, Germany) to observe the hair cells (HCs) and determine the extent of HC loss, as previously described (Raphael and Altschuler, 1991).

5.2.5 Statistical analysis

ABR threshold shifts and HC loss were calculated for each animal group. Comparisons of the inter-group differences were performed by the unpaired, two-tailed Student *t* test. A *p* value of less than 0.05 was considered statistically significant.

5.3 Results

5.3.1 ABR measurements

In the animal groups (Groups A and B) applied with NS instead of 3-NP, there were no significant threshold shifts in the study period of 14 days. A brief but significant threshold shift was observed at 20 kHz in Group B at 6 hours after surgery; however, the threshold shift was soon recovered to the pre-insult level. The application of a small piece of Gelfoam soaked with 150 mM of 3-NP (Groups C and D) onto RWN sparked off ABR threshold shift, which was significant but reversible (Fig. 5.2). In the animal groups treated with 3-NP (Groups C and D), the ABR thresholds shifts were significantly elevated at 16 k and 20 kHz at 1 hour after surgery, and at 4 k, 8 k and 12 kHz at 3 hours after surgery, compared with the ABR threshold shifts in Groups A and B.

In Group C, the elevated ABR thresholds were gradually recovered. At 4 and 8 kHz, ABR threshold shifts in Group C were not statistically significantly compared to the threshold shifts in Groups A and B at 3 days after surgery. The recovery at 12 kHz lagged a little behind ones at the lower frequencies, but the threshold shifts persisted at 16 and 20 kHz for at least 14 days. In Group D, more significant threshold shifts persisted for at least 14 days. Typical tracings of ABR measurements of Groups C and D are shown in the Fig. 5.3.

5.3.2 Histological analysis

To detect and count HCs, the organ of Corti stained with rhodamine-coupled phalloidin was whole-mounted followed by analysis with fluorescent microscopy. HC counting was performed in each turn of cochlea (Fig. 5.4). The loss of IHCs and each row of OHCs in each group was averaged (Table 1). Most IHCs were preserved in all the four animal groups (less than 0.5% of loss), except for the basal ($27.71 \pm 33.16\%$ of loss) and 2nd ($2.85 \pm 5.46\%$ of loss) turns in Group D. But the extent of the IHC loss was not significantly different from that of other three groups. Remarkable OHC loss was observed in Group D with predominance in the basal turn, where more than 90% of OHC loss was observed. OHC loss of the basal and 2nd turns was significantly different

between Group D and the other three groups. Mild OHC loss in the apical turn was found in all groups without significant inter-group difference.

5.4 Comments and conclusion

Aminoglycoside-induced deafness associated with mitochondrial ribosomal RNA mutation (Fischel-Ghodsian, 1999a; Higashi, 1989; Hu et al., 1991a; Prezant et al., 1993) suggests some relationship between mitochondrial dysfunction and aminoglycoside ototoxicity. The actual mechanism of the deafness has not yet been elucidated. There were different hypotheses to explain the increased aminoglycoside susceptibility in mitochondrial gene mutation. The A1555G or C1494T mutation in 12S rRNA genes of mtDNA is the common mutation known to be associated with the increased susceptibility of aminoglycoside ototoxicity. The A1555G or C1494T mutation may result in a conformational change in the A-site of mitochondrial 12S rRNA, which makes the mutated RNA more closely resemble the corresponding region of bacterial 16S rRNA and facilitates the binding of aminoglycoside with the mutated mitochondrial rRNA (Zhao et al., 2004; Guan, 2004a). However, biochemical evidences revealed that the mutated mitochondrial RNA genes, either A1555G (Guan et al., 1996) or C1494T (Zhao et al., 2004), could produce primary mitochondrial translation defects and result in variable reduction of protein synthesis. Such mild biochemical defects could not consistently produce a clinical phenotype of hearing loss, unless other modifier factors are added. Some nuclear modifying factors or genes have been proposed to modulate the phenotypic expression of mutated mitochondrial genes (Guan et al., 2006; Yan et al., 2006; Bykhovskaya et al., 2004). In this study, we demonstrated that mild mitochondrial dysfunction itself could increase the aminoglycoside ototoxicity.

We do not consider that the deafness associated with the mitochondrial genomic mutations causes by the same mechanism as the combination of 3-NP and KM, because patients with the mitochondrial genetic mutations sometimes suffer from sensorineural hearing loss in spite of no history of aminoglycoside exposure (Prezant et al., 1993; Matsunaga et al., 2004; Estivill et al., 1998). However, in a significant portion of patients,

the mitochondrial genetic mutation indeed increases the susceptibility of the patients to aminoglycoside ototoxicity (Casano et al., 1999; Fischel-Ghodsian, 1999a). Indirect biochemical evidence in the mutant cell lines derived from the patients with mitochondrial gene mutation also revealed that the severity of mitochondrial dysfunction was correlated with the presence or absence of hearing loss (Guan et al., 1996).

Why does acute mitochondrial dysfunction promote KM ototoxicity? It is well known that combination administration of aminoglycoside and the diuretics, ethacrynic acid, potentiates the aminoglycoside ototoxicity probably because ethacrynic acid facilitates penetration of aminoglycoside into the endolymph (Tran Ba Huy et al., 1983). Similar mechanism may be applied to the potentiation of KM ototoxicity by 3-NP. The injection of 3-NP into the central nervous system induces disruption of blood-brain barrier possibly because of 3-NP toxicity to endothelial cells (Nishino et al., 1997; Kim et al., 2003). 3-NP may destruct the blood-perilymph barrier, which is similar to blood-brain barrier, resulting in increase the concentration of KM in endolymph and perilymph.

Another explanation is that 3-NP might attack HCs without severe damage but might promote the vulnerability of HCs to KM through the cumulative oxidative stress. The mitochondrial dysfunction such as the 3-NP induced mitochondrial dysfunction model may increase the intracellular oxidative stress. Previous study demonstrated the generation of mitochondrial free radical in the striatal region after systemic administration of 3-nitropropionic acid in rats (Kim et al., 2002). The oxidative stress plays an important role in the induction of aminoglycoside ototoxicity and the following cell death (Forge & Schacht, 2000). The aminoglycoside can bind with iron to form a redox-active iron-aminoglycoside complex, which then react with unsaturated fatty acid to form superoxide ($O_2^{\cdot -}$) and lipid peroxide (Sha and Schacht, 1999). Meanwhile, gentamicin and ferrous iron was demonstrated to peroxidize L- α -phosphatidylinositol 4,5-bisphosphate, accompanied by the release of arachidonic acid. The arachidonic acid can form a ternary complex with $Fe^{2+/3+}$ -gentamicin, which can reacts with lipid peroxides and molecular oxygen, leading to propagation of arachidonic acid peroxidation (Lesniak et al., 2005). Aminoglycoside antibiotics, such as gentamicin, also were verified

to increase nitric oxide (Takumida and Anniko, 2001) by the induction of nitric oxide synthetase (Hong et al., 2006; Heinrich et al., 2006). The nitric oxide can act as a direct initiator for cell death cascades or react with the superoxide ion to form the highly destructive peroxynitrite. Therefore, the aminoglycoside susceptibility in this 3-NP induced mitochondrial dysfunction model may represent the sum of the destructive actions of free radicals as ensues from a variety of pathways. The resulting oxidative stress can invoke multiple forms of cell death, including apoptotic or necrotic pathways (Jiang et al., 2006).

At 14 days after administration of 3-NP soaked gelfoam to the RWN, the animals in Group C still had high frequency hearing loss without any HC loss. The toxicity of 3-NP to the cochlea lateral wall rather than to HCs can account for this (Hoya et al., 2004). In the acute cochlear mitochondrial dysfunction model by topical application of 3-nitropropionic acid to the RWN, the fibrocytes in the spiral ligament and limbus are the most vulnerable (Hoya et al., 2004). In the chronic cochlear mitochondrial dysfunction model by chronic administration of germanium dioxide, the stria vascularis and cochlear supportive cells are the most preferentially affected (Yamasoba et al., 2006). The hair cells remained nearly intact in either acute or chronic model of cochlear mitochondrial dysfunction (Hoya et al., 2004; Yamasoba et al., 2006). The temporal bone histopathological study in the patients with mtDNA also showed that the stria vascularis is the preferentially affected structure, followed by organ of Corti (Lindsay and Hinojosa, 1976; Takahashi et al., 2003; Yamasoba et al., 1999). In this study, the morphology of hair cells in cochlear mitochondrial dysfunction induced by topical application of 3-NP alone also showed no apparent morphologic alterations even when significant ABR threshold shifts happened. Likely 3-NP alone, the administration of KM only could not cause significant ABR threshold shift (except transient threshold shift for 20 kHz at 6h after surgery) or any HC loss. However, the combined administration of 3-NP and KM induced significant ABR threshold shifts at all frequencies examined. The hearing deterioration was considered to be permanent, because any recovery was not observed in ABR by 14 days after surgery, and HCs, which are exceptionally difficult to be

regenerated yet in mammals, were lost to a significant extent. The administration of 3-NP alone or KM alone under the condition in this study could not cause permanent hearing loss or significant HC loss.

Although significant ABR threshold shifts were noted after the administration of 3-NP with/without combination of KM, the IHCs still remained morphologically intact. The IHCs exhibited a higher tolerance to the toxic effects of kanamycin even in the 3-NP mitochondrial dysfunction model. The survival capability of IHCs to aminoglycoside is known to be associated with the nuclear translocation of NF- κ B (Jiang et al., 2005). The NF- κ B plays a pivotal role in promoting cell survival, which is associated with the suppression of ROS by the induction of mitochondrial superoxide dismutase (Mn-SOD) and upregulation of ferritin heavy chain (FHC)--a component of ferritin (Bubici et al., 2006). In a mouse model of aminoglycoside-induced chronic ototoxicity (Jiang et al., 2005), the oxidative status is elevated after the administration of kanamycin. The activation and nuclear translocation of NF- κ B, which increases the intrinsic antioxidant and antiapoptotic capability, is shown in the IHCs but not in the OHCs.

In this study, we delivered drug to the perilymph not by injecting drug directly to the round window membrane but by applying drug-soaked gelfoam to the RWN, which is adjacent to the round window membrane (RWM), in order to avoid damage to the cochlea such as perilymph fistula. The RWM is a thin membrane barrier which borders the perilymph of the cochlea, and is a reliable route of drug delivery to the cochlea (Salt and Ma, 2001). Using a piece of Gelfoam as a local delivery vesicle allows an effective drug delivery to the cochlea with reproducibility (Sheppard et al., 2004). Prior to the present study, we tried different concentrations of 3-NP. Topical application of 150 mM of 3-NP soaked Gelfoam sparked off the transient threshold shift of hearing, and the permanent threshold shift of hearing was observed in higher concentration (300 mM) of 3-NP. The lower concentration (100 mM) of 3-NP could not cause significant hearing loss (data not shown). Assuming that 3-NP-induced mitochondrial dysfunction promotes aminoglycoside ototoxicity, we decided, in the present study, to apply 150 mM of 3-NP, which occurs transient threshold shift, indicative of apparent but reversible cochlear

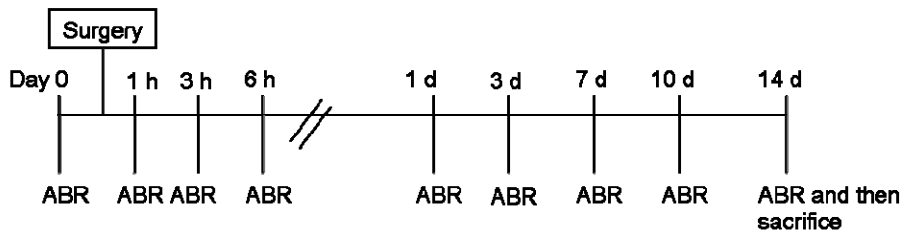
dysfunction. The transfer of the small molecule, like 3-NP, through the RWM is presumed to be primarily a passive diffusion(Hoya et al., 2004), so 3-NP topically applied to the RWM was not considered to be equally distributed throughout the cochlear duct, that is, the farther from the RWM, the lower might be the concentration of 3-NP. Actually, the ABR threshold shift in Group C (3-NP only) revealed the damage dependent on the frequency, indicative of the basal to apical predominance. We cannot deny the possibility of higher susceptibility to the ototoxicity in the basal (higher frequency) side than the apical (lower frequency) side, because the hair cells in the apical turns hold more endogenous antioxidant capacity than those in the basal turns, which creates a differential vulnerability to reactive oxidative stress from base-to-apex (Sha et al., 2001; Usami et al., 1996).

Conclusion

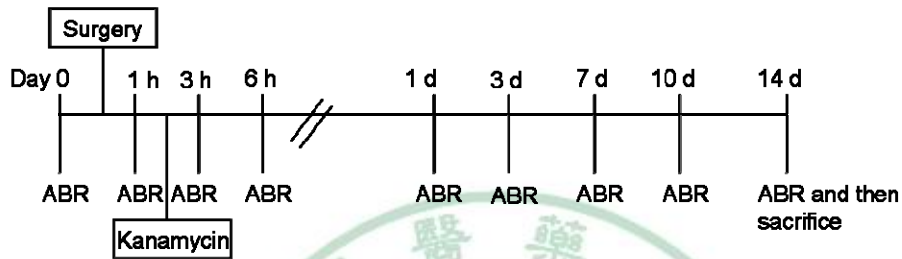
The present study revealed severe damages of hair cells and cochlear function when kanamycin was added in a guinea pig model of cochlear mitochondrial dysfunction by the administration of 3-NP soaked gelfoam in the RWN. This exhibits a direct demonstration of increased aminoglycoside susceptibility in acute cochlear mitochondrial dysfunction and is likely to contribute to the further understanding of the idiosyncrasy of aminoglycoside ototoxicity.

5.5 Figures and table

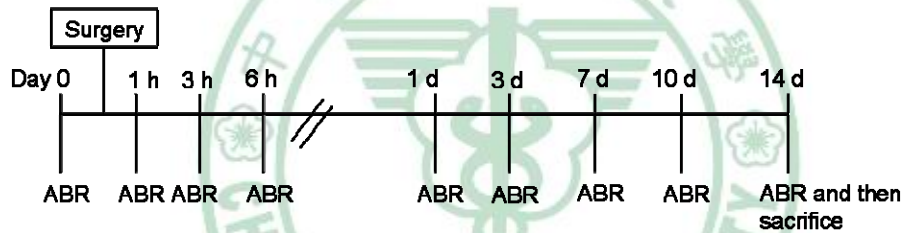
Group A (n=4): NS, control



Group B (n=5): KM



Group C (n=5): 3-NP



Group D (n=5): 3-NP+KM

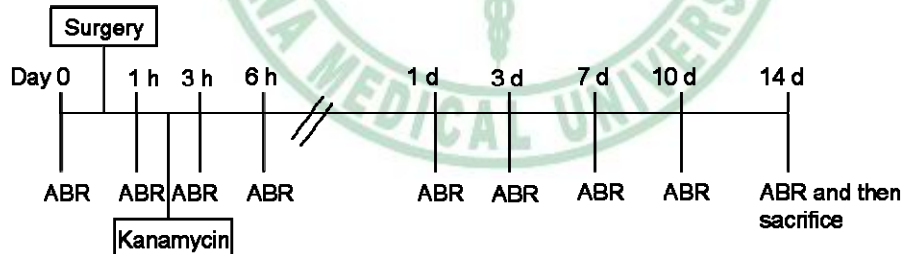


Figure 5.1 The experimental schema for this study. The details of the grouping and surgical procedures are described in the text. NS: normal saline; KM: kanamycin; 3-NP: 3-nitropropionic acid; ABR: auditory brainstem response.

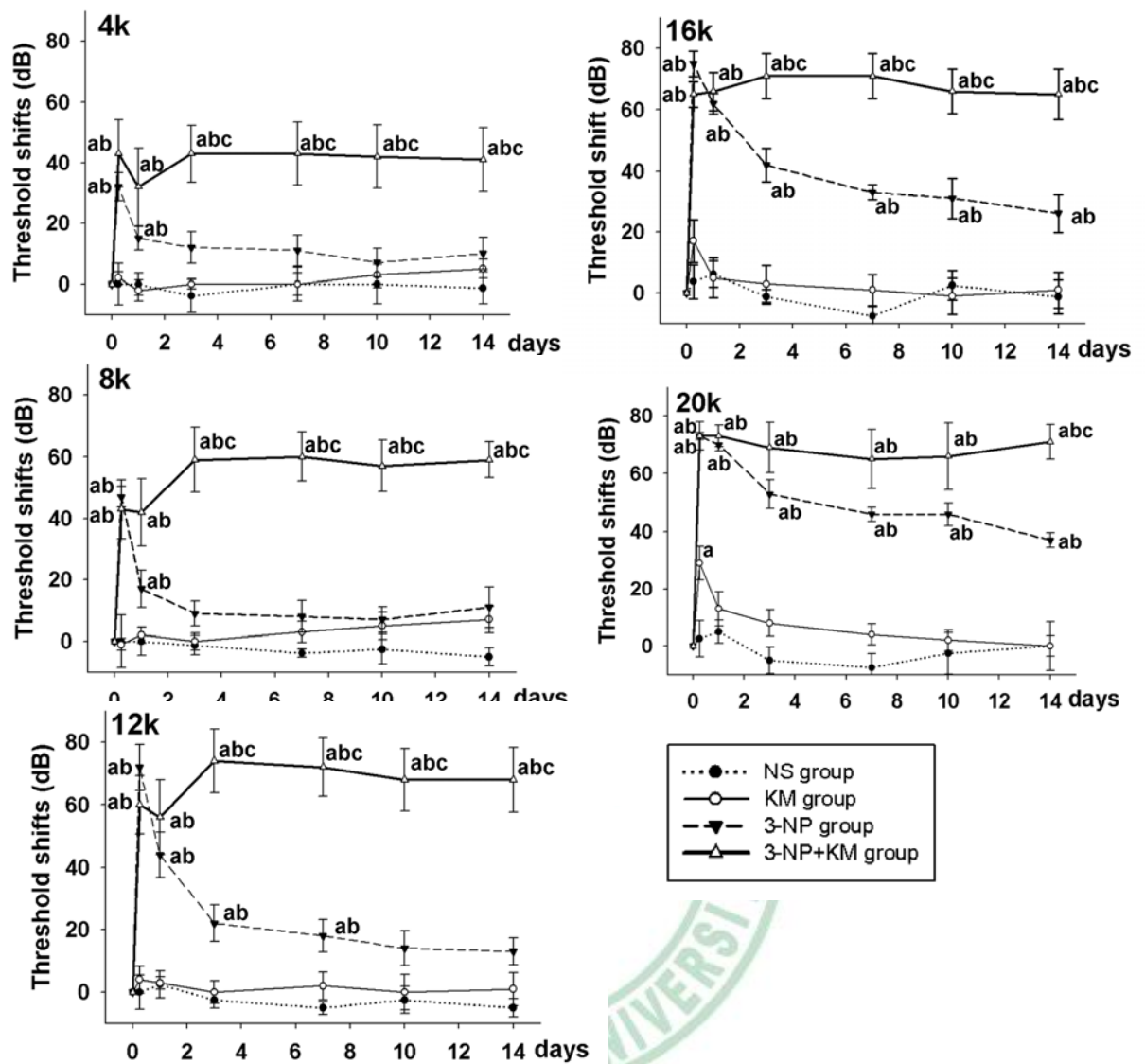


Figure 5.2 The ABR threshold shifts in each group at each frequency tested. Filled circle, open circle, filled triangle and open triangle indicate Group A: normal saline (NS) group; Group B: kamanycin (KM) group; Group C: 3-nitropropionic acid (3-NP) group; and Group D: 3-NP+KM group, respectively. ^aSignificantly different from the value in the NS group; ^bsignificantly different from the value in the KM group; ^csignificantly differently from the value in the 3-NP group. Data are presented as the mean±standard error (S.E.).

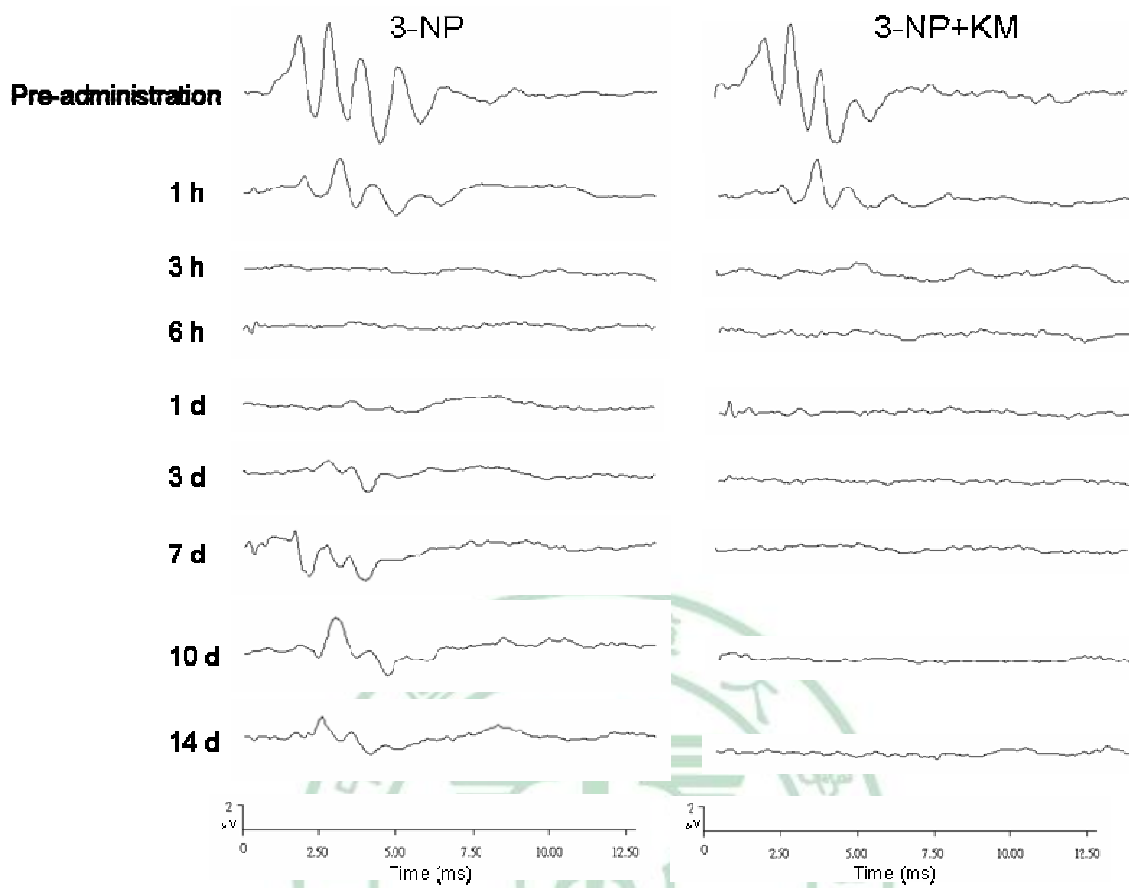


Figure 5.3 Representative serial ABR tracings in 3-NP and 3-NP+KM group with tone burst stimuli at 20 kHz (80.1dB SPL). Time after administration is indicated at the left of the tracings. The amplitudes of ABR waveform declined 1 hour after administration of 3-NP and no identifiable waveform was noted 3 hours after administration. The ABR waveform reappeared 3 days after administration in the 3-NP group. The ABR waveform persisted unidentifiable 2 weeks after administration in the 3NP+KM group.

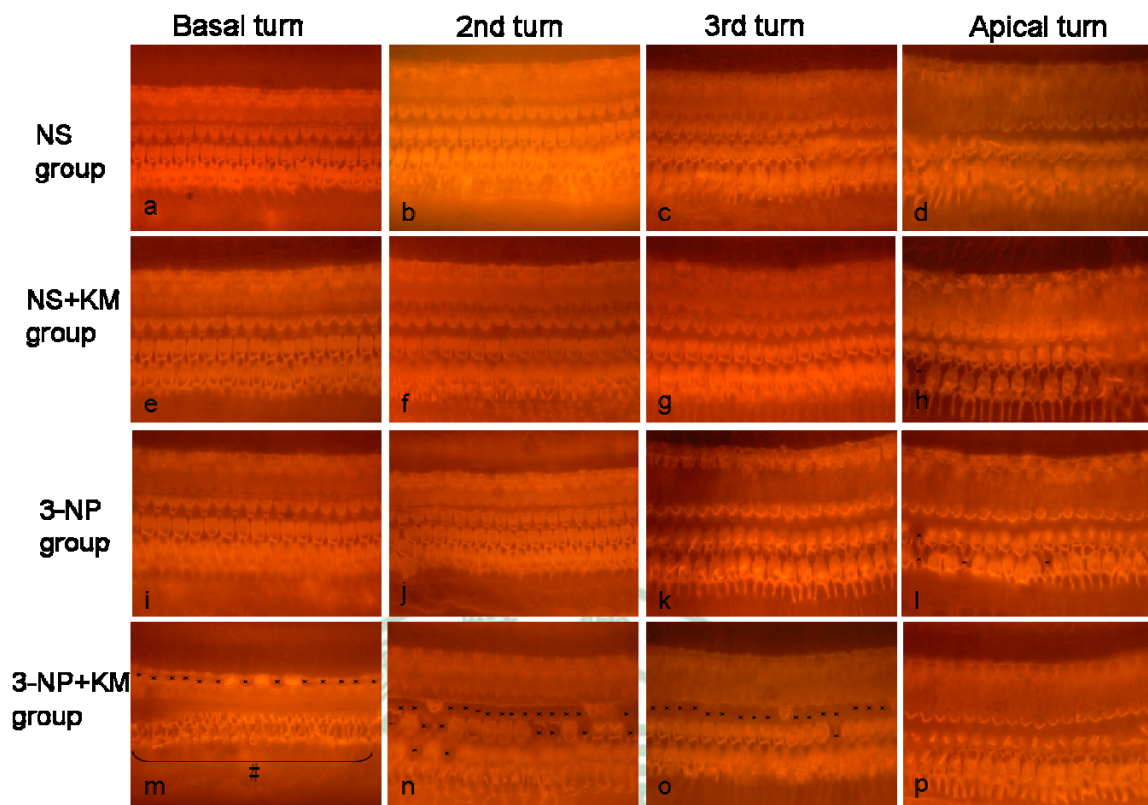


Figure 5.4 Hair cells labeling with rhodamine conjugated phalloidin in each group. In the NS group, KM group and 3-NP group, an orderly row of IHC with organized three rows of OHC was demonstrated from the basal turn to the apical turn (a-l). In the basal turn of the 3-NP+KM group, a severely disrupted pattern of cytoarchitecture occurred in the outer hair cells with somewhat loss of IHC (m). The overall cytoarchitecture remained organized after second turn in the 3-NP+KM group but significant loss of OHCs with preservation of IHCs was demonstrated (n). Somewhat degeneration of OHCs in third turn was found in some cochleae of the 3-NP+KM group (o). Asterisks mark sites of individual hair cell loss. # indicates the region with severely distorted architecture of the three rows of outer hair cells.

Table 1 Percentage of hair cell loss from IHC to OHC and from basal turn to apical turn in each group. Data are presented as the mean±S.D.. Asterisks indicate a significant inter-group difference between the 3NP+KM group and the other group (unpaired t-test, $p<0.05$).

	turn	% of IHC loss	% of OHC1 loss	% of OHC2 loss	% of OHC3 loss
NS	Basal turn	0.10±0.20	4.87±9.02	2.73±3.87	1.87±1.55
	2nd turn	0.15±0.17	0.61±0.34	0.87±0.58	0.52±0.27
	3rd turn	0.10±0.19	1.02±0.34	0.71±0.34	4.30±2.97
	Apical turn	0.13±1.55	1.59±1.34	1.86±1.00	13.14±6.47
NS+KM	Basal turn	0.12±0.13	0.78±0.46	0.62±0.50	1.11±1.16
	2nd turn	0.11±0.15	0.82±0.90	1.11±0.87	1.09±0.48
	3rd turn	0.28±0.18	1.34±1.60	0.29±0.33	1.92±1.13
	Apical turn	0.16±0.22	1.20±1.88	1.62±1.51	13.97±6.86
3-NP	Basal turn	0.20±0.17	1.04±0.73	1.71±1.72	3.47±3.32
	2nd turn	0.32±0.25	0.50±0.29	1.12±0.86	1.30±0.94
	3rd turn	0.12±0.16	0.68±0.46	0.56±0.44	4.00±4.18
	Apical turn	0.31±0.33	0.95±1.17	2.43±3.28	15.80±12.07
3-NP+KM	Basal turn	27.71±33.16	*98.22±2.36	*95.12±7.53	*92.64±10.14
	2nd turn	2.85±5.46	*65.08±38.20	*51.26±28.73	*34.47±20.26
	3rd turn	0.32±0.44	21.57±34.14	2.22±2.92	2.65±1.56
	Apical turn	0.22±0.20	2.04±1.88	1.79±0.98	7.61±5.08

Chapter 6 Transient ischemia/hypoxia may enhance aminoglycoside ototoxicity

ABSTRACT

Background: Aminoglycoside ototoxicity is one of the most important preventable causes of drug-induced hearing loss at present. The toxicity is dose-related but some patients may develop hearing loss even under safe dosage. Many clinical situations such as noise, sepsis, hypovolemia or shock may contribute to the development of aminoglycoside ototoxicity. One of the common basic phenomena in these clinical situations is hypoperfusion or ischemia. However, few studies yet to investigate the direct interaction of ischemia and aminoglycoside ototoxicity.

Aim of this study: This study was undergone to assess the gentamicin effects on the ischemia-reperfusion cochlear damage to a better understanding the events of ototoxic cochlear changes during acute transient cochlear ischemia.

Materials & Methods: Adult guinea pigs were used for the *in vivo* study. Transient cochlear ischemia was induced via ventral approach by clamping the labyrinthine artery. Gentamicin was given immediately after the surgery. Hearing test was performed by auditory brainstem responses. Chronic recording of auditory changes was made until 4 weeks after the treatment. Morphological examination was examination by hair cell counting with rhodamine-phalloidin staining and cochlear section with hematoxylin/eosin staining. Fluorescence gentamicin was prepared to evaluate the gentamicin uptake after ischemia. HEI-OC1 cells were used for *in vitro* investigation of the cellular changes during the interaction of hypoxia and gentamicin administration.

Results: Transient cochlear ischemia of 30 min may cause a transient and reversible hearing threshold shifts in the guinea pigs. However, persistent auditory threshold shifts were observed when the gentamicin was co-administrated after ischemia. Auditory changes were associated more with the high-frequency range (reflecting lower cochlear turn) than with the low-frequency range (reflecting upper cochlear turns). The distribution pattern of hair cell damage was also more severe in the basal cochlear turns than the

upper ones. In addition to hair cell damage, spiral ganglion neurons were another regions most affected at the co-administration of gentamicin and ischemia. Increased uptake of gentamicin was depicted after transient ischemia. Apoptosis contributes to the cell death during the interaction of ischemia and gentamicin ototoxicity. Generation of reactive oxygen species, loss of mitochondrial membrane potential, calcium release and caspase-dependent apoptotic cell death were shown during the interaction of hypoxia/ischemia and gentamicin ototoxicity *in vitro*.

Conclusion: The ototoxicity of gentamicin may be potentiated by transient cochlear ischemia. Cochlear hair cells and spiral ganglion neurons are the two major regions mostly affected. Apoptosis contributes to the cell death during the interaction of ischemia and gentamicin ototoxicity via a caspase-dependent apoptotic cell death pathway. These results may improve our understanding of the interacting mechanism and potential preventive strategy for the development of aminoglycoside ototoxicity.

6.1 Background

Aminoglycoside is an effective antibiotic against gram-negative infection and is widely used in clinical infectious diseases. The application of the aminoglycoside has been shifted to less toxic antibiotics in industrialized countries because of its tissue-specific toxicity to the inner ear (ototoxicity) and kidney (nephrotoxicity). However, in developing countries, the aminoglycoside still remains as the frontline antibiotics because of their efficacy and low cost. Even the World Health Organization still recommends the aminoglycoside as an essential component of the combined regimens to treat the increasing prevalence of multidrug-resistance tuberculosis (Gupta et al., 2001). Therefore, aminoglycosides may be one of the most commonly used antibiotics worldly.

The toxicity of aminoglycoside is well-known to be dose-related, which occur when the dosage is sufficient to be toxic (Brummett and Morrison, 1990). When the dosage of aminoglycoside could cause a reversible nephrotoxicity, similar dosage would induce irreversible damage to the inner ear (Dulon et al., 1988). In a PubMed (1966-2003), Embase (1982-2003) and Conchrane Controlled Trials Registry (2003) search of the

published literature, the pooled ototoxicity rates of systemic aminoglycoside were about 2.0~2.3% (Contopoulos-Ioannidis et al., 2004). Since the worldwide use of aminoglycoside, aminoglycoside ototoxicity is one of the most common causes of acquired hearing loss and constitutes as one of the major preventable causes of drug-induced hearing loss at present (Forge & Schacht, 2000).

Although the aminoglycoside ototoxicity is correlated to the cumulative dose and mode of drug administration, a portion of patients still develop cochlear dysfunction even under therapeutic dosage (Bernard, 1981). The supposed therapeutically safe dose of aminoglycoside does not guarantee the safety from aminoglycoside ototoxicity. In addition to the dose-related toxic effects, the susceptibility of aminoglycoside ototoxicity has been imputed to genetic idiosyncrasy, especially mitochondrial gene mutations (Ensink et al., 1998; Guan et al., 2000). It is estimated that 10 to 20 percent of patients with aminoglycoside-induced ototoxicity carry mitochondrial gene mutations (Fischel-Ghodsian, 1999b). One of the most common mitochondrial gene mutations associated with the vulnerability to aminoglycoside ototoxicity is the A1555G in the mitochondrial MT-RNR1 gene that encodes the human *12S rRNA* ribosomal subunit (Qian and Guan, 2009). The A1555G mutation was demonstrated to cause increased binding of aminoglycosides to the *12S rRNA* ribosomal subunit (Qian & Guan, 2009), which results in the disruption of mitochondrial protein synthesis in the cell, for example a decrease in cytochrome c oxidase activity and mitochondrial protein synthesis (Kouzaki et al., 2007; Santorelli et al., 1999). All proteins synthesized in the mitochondria are involved in oxidative phosphorylation and the disruption thereof will ultimately lead to death of the cell. The inefficient energy production caused by the mitochondrial mutations may impair the cochlear processing, which requires considerable energy consumption (Santorelli et al., 1999). Such mitochondrial dysfunction from the A1555G mutation may extend beyond the inner ear to other energy-consuming tissues such as skeletal muscles (Kouzaki et al., 2007) or myocardium (Santorelli et al., 1999). However, a recent study shows that most patients carrying the mutations in the *12S rRNA* gene do not show evidence of hearing loss at the exposure of aminoglycoside (Johnson et al.,

2010). The predisposing factors contributing to the development of aminoglycoside need to be clarified more detailed.

Previous studies on the common predisposing factors for aminoglycoside ototoxicity include the drug-drug interaction (Bates et al., 2002; Tran Ba Huy et al., 1983), underlying medical conditions (Guthrie, 2008) and stress (Li and Steyger, 2009). Some drugs such as loop diuretics (Bates et al., 2002; Tran Ba Huy et al., 1983) are known to aggravate the aminoglycoside ototoxicity when used in combination. Renal dysfunction may decrease the clearance of aminoglycoside and thus predispose the ototoxic effect (Turnidge, 2003). Comorbid conditions such as perinatal asphyxia, hypovolemia, shock or sepsis, were also supposed to contribute to the augmentation of aminoglycoside ototoxicity (Aust, 2001; Chayasirisobhon et al., 1996; Salamy et al., 1989). Although multiple factors may confound these clinical situations, significant decrease of blood pressure is the common phenomenon observed in hypovolemia, shock or sepsis. Cochlear blood flow was observed to be stopped when acute reduction of blood pressure was induced in animals (Axelsson et al., 1990). In human, simply hypotension (Pirodda et al., 1997) or reduction in blood pressure in a previous hypertensive patient (Chao, 2004) may result in acute cochlear dysfunction manifested as sudden sensorineural hearing loss, which is supposed to be caused by cochlear ischemia. The role of cochlear ischemia in the sensitivity of aminoglycoside ototoxicity needs to be clarified.

The cochlea is a highly metabolic organ and it is vulnerable to hypoxia. Disturbance of cochlear microcirculation leading to local hypoxia/ischemia has been thought to be the fundamental mechanism contributing to some common otologic disorders, e.g. age related (Bohme, 1987; Seidman et al., 2002) or noise-induced (Henderson et al., 2006; Thorne and Nuttall, 1987) hearing losses. In these ischemia-related hearing losses, it is well known that increased aminoglycoside ototoxicity was shown in noise trauma (Li & Steyger, 2009; Bhattacharyya and Dayal, 1984; Boettcher et al., 1987; Kovacic and Somanathan, 2008). Age related hearing loss has also been proved to increase the susceptibility to aminoglycoside ototoxicity (Wu et al., 2001). We have established a transient cochlear ischemia model in guinea pigs (Lin et al., 2010). Using this model, we

investigated what the aminoglycoside ototoxicity will go on in the hypoxia/ischemia status. Then, we studied gentamicin-induced cell apoptosis in conditions of different hypoxic condition using HEI-OC1 (House Ear Institute-organ of Corti 1) cells lines *in vitro*. These results may provide us more understanding the development of aminoglycoside ototoxicity when interaction with hypoxia/ischemia, such as patients in critical conditions or intensive care unit treated with aminoglycoside.

6.2 Materials and methods

6.2.1 Animals, medications, reagents and antibodies

Albino guinea pigs were purchased from the Laboratory Animal Center in the National Taiwan University (Taipei, Taiwan). Zoletil which contained Tiletamine (125mg) and Zolazepam (125mg) per vial was purchase from VIRBAC S.A. (Carros, France). Xylazine (2%) was purchased from Bayer (Leverkusen, Germany). Atropine sulfate (1mg/ml/vial) was purchase from Taiwan Biotech Co. (Taoyuan, Taiwan). Xylocaine (1%) was purchase from AstraZeneca (Monts, France). Chloramphenicol Sodium Succinate was purchased from China Chemical & Pharmaceutical Co. (Hsinchu, Taiwan). Rhodamine-coupled phalloidin was purchase from Molecular Probes Inc. (Eugene, OR, USA). Anti-mouse and anti-rabbit IgG-conjugated horseradish peroxidase, rabbit polyclonal antibodies specific for Bcl-2, Bax, Bak, caspase 3, and caspase 9 were purchased from Santa Cruz Biotechnology (Santa Cruz, CA, USA). Rabbit polyclonal antibody specific for Caspase 3, caspase 9, PARP, calpain (calcium-dependent thiol proteases)-1, and calpain-2 were purchased from Cell Signaling (Danvers, MA, USA). Desferrioxamine (DFX), dihydrorhodamine 123 (DHR 123), JC-1, FURA-PE3 and inhibitors of caspase-3/9 were purchased from Calbiochem (EMD Biosciences, Inc. CA). Caspase-3/9 luciferase assay kit was purchased from Promega (Madison, MA, USA). Gentamicin and all other chemicals were purchased from Sigma-Aldrich (St. Louis, MO, USA).

6.2.2 *In vivo* study

Adult albino guinea pigs were used for this study. Guinea pigs have been proved to be a reliable animal model for hearing loss, in which a robust pathological response to aminoglycoside induced cochlear damage could be elicited.(Forge & Schacht, 2000) In addition, the historic role of guinea pigs in cochlear research is based on the easy surgical access to its cochlea, and well characterized cochlear anatomy and physiology. The ages of the animals were about 2~4 months old with body weight at about 350~550gm. The use and care of animals reported in the present study was approved by the Institutional Animal Care and Use Committee of the China Medical University (permission number: 97-60-N).

Animals were anesthetized by intramuscular injection of a mixture of Zoletil (30 mg/kg) and xylazine (10 mg/kg), which allowed for non-ventilator dependent oxygenation. A maintenance dose, 50% of the initial dose, was injected intramuscularly every 60 min thereafter. After sedation, atropine (0.05 mg/kg) and chloramphenicol (400 mg/kg) were given intramuscularly. For surgical accessibility and convenience, only the left ear was treated, but to avoid acoustical crossover from the cochlea of the right ear during auditory brainstem response (ABR) measurements, the latter was surgically destroyed.

6.2.2.1 Surgical procedures

After an animal had been anesthetized, the cervical hair was shaved. It was placed in the prone position, and 1% xylocaine was injected into the posterior auricular area of the right ear. The skin and subcutaneous myofascial plane of the ear were dissected to expose the mastoid bulla, which was then opened so that the cochlea could be directly destroyed by needle penetration and disruption.

The ventral approach to the labyrinthine branch of AICA has been described in details before (Perlman et al., 1959; Kimura & Perlman, 1958). The procedures were summarized as below. Electrodes were inserted subcutaneously into the left mastoid (anode), right mastoid (cathode), and the back (ground), and an earphone was inserted into the left ear canal to monitor the ABR perioperatively. The animal was then placed in

the supine position. The skin over the ventral neck was disinfected with 75% alcohol and draped with aseptic dressings. A submental incision about 2 to 3 centimeters in length was made medially to the mandibular edge. The submandibular gland was separated to expose the digastric muscle and the paracondylar process. Separation of the digastric muscle from the fractured paracondylar process exposed the tympanic bulla. The anterior wall of the tympanic bulla was opened using a rongeur so that the basal cochlear turns were visible. Drilling started at the petrous bone, continued medially to the basal turn and anteriorly to the inferior petrosal sinus. The dura and the inferior petrosal sinus were protected during drilling by placing a thin Silastic sheet over them. A fenestration about 1.5×3.0 mm was made at the base of the skull, so that the labyrinthine artery was visible under the dura. The dura was excised, and the area opened so that the labyrinthine artery was fully exposed. The labyrinthine artery was closed with V1 microclamps] (#00396-01, S&T Microsurgical Instruments, USA), and cochlear function was thereafter monitored by click ABR at a 120-dB sound pressure level (SPL) at least every 3 min. Compared with the pre-operative apparent ABR waveform, persistent absence of the ABR waveform indicated that the microclamps had successfully occluded the labyrinthine artery.

6.2.2.2 Hearing test

Tone burst ABR pre-operative and serial post-operative hearing tests were performed in a sound attenuated room. The pure tone bursts were generated with the amplitude specified by a real-time programmable attenuator (Intelligent Hearing Systems, IHC Smart EP version 3.97, Miami, Fla., USA) with ER2 insert earphone, with stimulus frequency at 1k, 2k, 4k, 8k, and 16k Hz (0.2ms rise/fall time and 1ms flat segment) with maximal output level 125, 123, 111, 117, and 98 dB SPL. The click/tone bursts were produced by IHS high frequency transducer in a closed acoustic system through the sound delivery system. Responses for 1024 sweeps were averaged at each intensity level around the threshold in 5 dB SPL steps. Threshold was defined as the lowest intensity at which a clear waveform was visible upon inspection of an evoked trace. At least two sequences of recordings were made at the threshold intensity to verify the reproducibility of the ABR

responses. Each ABR threshold was compared with the pre-operative threshold, which served as the baseline measurement.

For the sham operation (sham-op) and the treatment groups (described below), serial ABR measurements were performed pre-operatively, immediately after the operation (PODi), 1 and 3 days after the operation (POD1d, 3d,) and 1, 2, 3, and 4 weeks after the operation (POD1w, 2w, 3w, 4w).

6.2.2.3 Surface preparation of cochlea and hair cell counting

At the end of the study, the animals were deeply anesthetized and then sacrificed by decapitation. The left cochleae were fixed with 4% paraformaldehyde in 0.1 M phosphate-buffered saline (PBS) by perilymphatic perfusion and then immersed in 4% paraformaldehyde in 0.1 M PBS for 1 day. Surface preparation of cochlea was performed as previously described (Kohonen and Tarkkanen, 1966). The bony modiolus with the organ of Corti was carefully detached at the base of the cochlea following removal of the bony capsule, lateral wall, and tectorial membrane. After permeabilization with 0.3% Triton X-100 in PBS for 10 min, the tissues were incubated at room temperature with rhodamine-coupled phalloidin (Molecular Probes, Eugene, OR, USA) diluted 1:200 with PBS for 30 min. After the tissues were rinsed with PBS, strips of the organ of Corti were divided into the four turns, which were mounted on glass slides and examined with a fluorescence microscope (Model Leitz DM RBE; Leica, Wetzlar, Germany) to count the number of hair cells (HCs) present at each cochlear turn, thereby determining the extent of HC loss. For each group of animals, the mean losses of inner HCs (IHCs) and at each row of outer HCs (OHCs) in each group were calculated.

6.2.2.4 Histopathological examination

Cochlear sectioning along the paramodiolar axis was done followed by hematoxylin/eosin staining. After fixation as described above, the cochleae were decalcified by immersion in 10% ethylenediamine tetra-acetic acid (EDTA) (in 0.1M PBS, pH 7.4) for 4 weeks, with gentle stirring at 4°C. The cochleae were then dehydrated,

embedded in paraffin, and serially sectioned (4 μm thick) parallel to the modiolar axis. The sections were plated for hematoxylin/eosin staining and examined under a high-power light microscope.

6.2.2.5 Grouping

The animals were divided into the following groups. A1: Control (n = 6). No surgery. A2: Gentamicin (GM) group (n=6). The animals received single dose of gentamicin (125 mg/kg) by intramuscular (i.m.) injection. B1: Sham operation (n = 6): The animals received surgery as described above until the step at which the labyrinthine artery was exposed. Although the overlying dura was excised, the labyrinthine artery was fully exposed only momentarily, and then the wound was closed. B2: Sham-op/GM group (n=6): The animals received single dose of i.m. gentamicin (125 mg/kg) after sham surgery. C1: 30-min ischemia group (n=6). The animals received surgery as described above until the step at which the labyrinthine artery was exposed. The labyrinthine artery was then temporarily occluded with microclamps for 30 min (6 animals per subgroup). Then the microclamps was released, and the wounds were closed. During the time that the arteries were occluded, the effects that clamping had on hearing were monitored by serial click ABR at 120-dB SPL. C2: 30min-ischemia/GM group (n=6). The animals received single dose of i.m. gentamicin (125 mg/kg) after induction of transient cochlear ischemia for 30 minutes, described as above.

In each group of 6 sacrificed animals, 4 cochleae were prepared for cochlear surface preparation and HC counting. The cochleae of the other two animals were sectioned along paramodiolar axis and stained with hematoxylin/eosin.

6.2.3 Tracking gentamicin uptake using fluorescence gentamicin

The fluorescence-conjugated gentamicin made by conjugation of Texas Red (TR) esters and gentamicin (GM) was used to track the distribution of gentamicin in the

cochlea, according to previous studies(Wang and Steyger, 2009). In brief, 2.2 ml of gentamicin sulfate (Sigma, St. Louis, MO, USA; 50mg/ml in 100 mM K₂CO₃ at pH 9.0) and 0.6 ml of succinimidyl esters of Texas Red (Molecular Probes, OR, USA; 2 mg/ml in dimethyl formamide) were mixed and agitated at 4°C overnight to produce a gentamicin-Texas Red conjugate (GMTR). A high molar ratio (about 150:1) of GM to TR was used to prevent over-labeling GM molecule with more than one TR molecule and ensure the polycationic nature of conjugated GMTR. The left ear of the animal underwent transient cochlear ischemia of 30 minutes as described above and the right ear served as control. Immediately after the surgery, GM/GMTR (125 mg/kg or 250 mg/kg) was injected subcutaneously. The animals were sacrificed 30, 90 or 180 minutes later. The cochleae were harvested and fixed with 4% paraformaldehyde in 0.1 M PBS by perilymphatic perfusion and immersed in the same fixative for one day. The organ of Corti was dissected, mounted on glass slides and examined by fluorescence microscopy. For image analysis, the images of the cochlear strips from the middle cochlear turn in each experimental group were identified and regions of interest (inner hair cells and rows of outer hair cells) were manually segmented for pixel fluorescence intensity determination using the image analyzer (Image Pro Plus VI, Media Cybernetics, Maryland, USA). The relative mean fluorescence intensity was ratioed against the reference (the intensity of 1st row of outer hair cells 30 min after 125mg/kg GM/GTTR injection in the control cochlea) and plotted.

6.2.4 *In situ* detection of nuclear DNA fragmentation *in vivo*

We used the terminal deoxynucleotidyl transferase (TdT)-mediated deoxyuridine triphosphate (dUTP)-biotin nick end labeling (TUNEL) method to detect DNA fragmentation after the combination of gentamicin and cochlear ischemia. The animals, which received single dose of i.m. gentamicin (125 mg/kg) after induction of transient cochlear ischemia for 30 minutes, were sacrificed 1d, 3d and 7d after the operation.(n=2, in each time point) The otic bullae, removed after decapitation under deep anesthesia,

were fixed with 4% paraformaldehyde in 0.1 M phosphate-buffered saline (PBS) by perilymphatic perfusion and then immersed in 4% paraformaldehyde in 0.1 M PBS for 1 day. The organ of Corti was then dissected. The specimens were stained with a modified TUNEL method using an in situ cell death kit-fluorescein (Roche Diagnostics GmbH, USA). The kit contains terminal deoxynucleotidyl transferase, which catalyses the polymerization of fluorescein dUTP to free 3'-OH DNA ends in a template-independent manner. According to the manufacturer's instructions, the tissues were pre-treated with permeabilization solution (0.1% Triton X-100 in 0.1% sodium citrate) for 2 min on ice (4°C), and then incubated for 60 min at 37°C with the TUNEL reaction mixture. After washing in PBS, sections were photographed in a laser scanning confocal microscope (Zeiss LSM510). TUNEL-positive cells were identified directly by fluorescence of incorporated dUTP.

6.2.5 *In vitro* study

In order to clarify the possible cellular and molecular mechanisms after the interaction of hypoxia and gentamicin, we used the HEI-OC1 inner ear cell lines from conditionally immortalized auditory cell lines from transgenic mice (Kalinec et al., 2003). The HEI-OC1 cells, which express characteristic cell markers of organ of Corti sensory cells, have been proved to be a useful *in vitro* system to study the cellular and molecular mechanisms of drug-induced cochlear cell deaths (Kalinec et al., 2003).

6.2.5.1 Cell culture

The cochlear cells, HEI-OC1 cells, which were cultured in DMEM (Invitrogen, Carlsbad, CA, USA) supplemented with 10% de-complement FBS (HyClone, Logan, UT, USA). The cells used in this study were maintained at 33 °C under 5 % CO₂ in air.

6.2.5.2 Hypoxia of cultured HEI-OC1 cells

HEI-OC1 cells were seeded on culture dish (1×10^6 cells/dish) at 33 °C in 95% air and 5% CO₂ before exposure to hypoxia. For the generation of hypoxic condition, cells were

cultured in 95% N₂ and 5% CO₂ (Anaerobic System PROOX model 110; BioSpherix) condition and incubated at 33 °C within the chamber for 24 h. Cells incubated in hypoxia condition for 0-24 h did not affect cell viability by MTT assay (data not shown).

6.2.5.3 MTT assay

Cell viability was determined by 3-(4, 5-dimethylthiazol-2-yl)-2,5-diphenyltetrazolium bromide (MTT) assay, as described previously (Lai et al., 2008). Briefly, after treatment with gentamicin for the indicated time intervals, cultured cells were washed with PBS. MTT (0.5 mg/ml) was then added to each well and the mixture was incubated at 37°C for 4 h. Culture medium was then replaced with an equal volume of DMSO to dissolve formazan crystals. After the mixture was shaken at room temperature for 10 min, absorbance of each well was determined at 570 nm using a microplate reader (Bio-Tek, Winooski, VT, USA).

6.2.5.4 Quantification of apoptosis by flow cytometry

Apoptosis was assessed using Annexin V, a protein that binds to phosphatidylserine (PS) residues which exposed on the cell surface of apoptotic cells. Cells were treated with vehicle or gentamicin and cultured in hypoxia for the indicated time intervals. After treatment, cells were washed twice with PBS, and resuspended in staining buffer containing 1 µg/ml PI and 0.025 µg/ml Annexin V-FITC. Double-labeling was performed at room temperature for 10 min in the dark before the flow cytometric analysis. Cells were immediately analyzed using FACScan and the Cellquest program (Becton Dickinson; Lincoln Park, NJ, USA) (Liu et al., 2010).

Quantitative assessment of apoptotic cells was also assessed by cell cycle. Cells were collected by centrifugation and adjusted to 3×10^6 cells/ml. Pre-chilled ethanol was added to 0.5 ml of the cells and incubated at 4°C for 30 min. Ethanol was then removed by centrifugation and DNA of the cells was stained with propidium iodide (PI) [100 µg/ml PI, 0.1% Triton-X, 1 mM EDTA in PBS] in the presence of an equal volume of DNase-free RNase (200 µg/ml) and analyzed immediately by a FACScan and the

Cellquest program (Becton Dickinson).

Quantitative assessment of apoptotic cells was also detected by using TUNEL technique (in situ Cell Death Detection Kit; Roche Applied Science, Mannheim, Germany) according to manufacturer's instructions. Briefly, cells were incubated with gentamicin in hypoxia for the indicated time intervals. The cells were trypsinized, fixed with 4% paraformaldehyde, and permeabilized with 0.1% Triton-X-100 in 0.1% sodium citrate. After being washed, the cells were incubated with the reaction mixture for 60 min at 37 °C in the dark. The stained cells were then analyzed using a FACScan and the Cellquest program (Becton Dickinson).

6.2.5.5 Determination of the mitochondrial membrane potential

The mitochondrial membrane potential ($\Delta\Psi_m$) was assessed using a fluorometric probe JC-1 (Calbiochem, CA, USA), with a positive charge of a mitochondrial-specific fluorophore, indicated by a fluorescence emission shift from green (525 nm) to red (610 nm). Briefly, cells were plated in 6-well culture dishes. After reaching confluence, cells were treated with vehicle or gentamicin. After incubation, cells were stained with JC-1 (5 $\mu\text{g/ml}$) for 15 min at 37°C. Samples were analyzed by FACScan using an argon laser (488 nm). Mitochondrial depolarization is specifically indicated by a decrease in the red to green fluorescence intensity ratio and analyzed by a FACScan and the Cellquest program (Becton Dickinson).

6.2.5.6 Measurements of ROS

To detect the level of ROS production, cells were loaded with 10 μM dihydrorhodamine 123 (DHR 123) for 15 min, as described previously (Kim et al., 2008). The fluorescence intensities were obtained by recording the FITC fluorescence. Cells were collected and analyzed by a FACScan and the Cellquest program (Becton Dickinson).

6.2.5.7 Detection of Ca²⁺ concentrations

Approximately 5×10^5 cells/well of HEI-OC1 cells in 12-well plates were incubated with gentamicin in hypoxia for the indicated time intervals to detect changes in Ca²⁺ levels. Cells were harvested and washed twice, and re-suspension in FURA-PE3/AM (3 μ M) at 37 °C for 30 min and analyzed by a FACScan and the Cellquest program (Becton Dickinson) (Liu et al., 2010).

6.2.5.8 Western blot analysis

The cellular lysates were prepared as described previously (Chen et al., 2008). Proteins were resolved on SDS-PAGE and transferred to Immobilon polyvinylidene difluoride (PVDF) membranes (Millipore, Billerica, MA, USA). The blots were blocked with 5% skim milk for 1 h at room temperature and then probed with antibodies against Bcl-2, Bcl-xl, Bax, Bak, caspase 3, caspase 9, PARP, calpain-1 and calpain-2 (1:1000) for 1 h at room temperature. After three washes, the blots were subsequently incubated with a donkey anti-rabbit peroxidase conjugated secondary antibody (1:1000) for 1 h at room temperature. The blots were visualized by enhanced chemiluminescence using Kodak X-OMAT LS film (Eastman Kodak, Rochester, NY, USA).

6.2.5.9 Determination of caspase activity

The assay is based on the ability of the active enzyme to cleave the chromophore from the enzyme substrate LEHD-pNA (for caspase 9) and Ac-DEVD-pNA (for caspase 3) (Promega; Madison, WI, USA). The cell lysates were prepared and incubated with specific anti-caspase 9 and caspase 3 antibodies. Immunocomplexes were incubated with peptide substrate in assay buffer (100 mM NaCl, 50 mM 4-(2-hydroxyethyl)-1-piperazine-ethanesulphonic acid (HEPES), 10mM dithiothreitol, 1mM EDTA, 10% glycerol, 0.1% 3-[(3-cholamidopropyl)dimethylammonio]-1-propanesulfonate (CHAPS), pH 7.4 for 2 h at 37 °C. The release of *p*-nitroaniline was monitored at 405 nm. Results are represented as the percent change of the activity compared to the untreated control.

6.2.6 Statistics analysis

The auditory threshold shifts and percentages of hair cell loss between the control and the other groups were analyzed with a non-parametrical Mann-Whitney *U*-test. Statistical analysis between two *in vitro* samples was performed with a Student's *t*-test. Statistical comparisons of more than two groups were performed with a one-way analysis of variance (ANOVA) test. The statistical software was SPSS program (version 12.0 for Windows, SPSS Inc., Chicago, Illinois, USA). In all cases, $p < 0.05$ was considered significant.

6.3 Results

6.3.1 Transient ischemia increases the gentamicin-induced ABR threshold shifts

The ABR threshold shifts for all six groups of animals are present in Fig. 6.1 for ABR stimuli at 1, 2, 4, 8 and 16 kHz. No significant ABR threshold changes were noted in the control, gentamicin alone (GM), sham-op and sham-op/GM group at all frequencies examined. The ABR thresholds increased immediately after 30 min ischemia, but such ABR threshold elevation soon returned to nearly baseline level in three days. When single dose of gentamicin at 125 mg/kg was given immediately after 30-min ischemia, persistent ABR threshold elevations were shown without significant recovery.

After 4 weeks, the ABR threshold elevations for the GM, sham-op, sham-op/GM and 30-min ischemia groups were not significantly different from the control group at all frequencies tested. The ABR threshold shifts at 4 weeks after combination of gentamicin and 30 min ischemia were about 60 dB (1k Hz: 44.2 ± 5.3 , 2k Hz: 46.7 ± 6.6 , 4k Hz: 67.5 ± 5.0 , 8k Hz: 68.3 ± 6.8 , 16 kHz: 70.8 ± 5.1 , in dB, mean \pm standard error), and significantly different from the control group. The ABR threshold shifts 4 weeks after combination of 30-min ischemia and gentamicin showed more severe threshold shifts in higher frequencies (4-16 kHz) than in lower frequencies (1-2 kHz).(Fig. 6.2)

6.3.2 Increased hair cell loss after interaction of gentamicin and ischemia

Most IHCs were preserved in all experimental groups, except for the basal ($42.1 \pm 20.8\%$ loss) and third ($42.8 \pm 16.2\%$ loss) turns in the 30-min ischemia/GM group, which was significantly different from the other groups. Remarkable OHC loss was observed in the 30-min ischemia/GM group, mainly in the basal and second turn, where $> 80\%$ loss was observed. (Fig. 6.3 and 6.4) There were no significant differences in HC loss in the control, GM, sham-op and sham-op/GM group.

6.3.3 Histological analysis after combination of gentamicin and transient ischemia

Two animals in each group were used for histological examination. No significant morphological changes were observed in the animals without changes in hearing level. In the animals that received gentamicin after 30-min ischemia, obvious morphologic changes were observed, especially in the basal cochlear turns. Distortion of organ of Corti with collapsed Corti's tunnel was seen with loss of spiral ganglion neurons (Fig. 6.5 E, F). However, the morphology of stria vascularis seemed not to change much in the lower and upper turns (Fig. 6.5 A, D). In the upper turns, the organ of Corti and distribution of spiral ganglion neurons retain their architectures (Fig. 6.5 B,C).

6.3.4 Enhanced gentamicin uptake after transient cochlear ischemia

For the animals receiving 125 mg/kg GM/GTTR injection, faint GMTR fluorescence was depicted in the OHCs 30 minutes after the application of GM/GTTR (Fig. 6.6 A, D). The IHCs displayed GMTR fluorescence 90 minutes later in the 30-min ischemic cochlea (Fig. 6.6 E), but were negligibly visible in the control cochlea (Fig. 6.6 B). The GMTR fluorescence was also found in the cytoplasm of sporadic OHCs 90 minutes after GM/GMTR injection, which was more prominent in the 30-min ischemic cochlea (Fig. 6.6 B, E). Apparent cytoplasmic GMTR fluorescence labeling in hair cells was visible

180 minutes later, in which it was more intensely labeled in the 30-min ischemic cochlea (Fig. 6.6 C, F). The GMTR fluorescence was brighter in the ischemic cochleae than that in the control ones, especially 180 minutes after GMTR injection (Fig. 6.6 G).

More distinct GMTR fluorescence was depicted in the cochleae with higher dosage of GM/GMTR (250mg/kg) than in those with lower dosage (125mg/kg) (Fig. 6.7). Similarly, the ischemic cochlea displayed more GMTR fluorescence than the control cochlea.

6.3.5 TUNEL stain *in vivo*

Fig. 6.8 shows representative TUNEL staining of hair cells in the basal turns 1, 3, and 7 days after co-administration of gentamicin immediately after 30-min ischemia. OHCs were observed to be labeled with TUNEL-fluorescence 1 day after co-treatment and IHCs were 3 days. TUNEL-stained positive cells were not observed 7 days later. The positive control procedure for the TUNEL method labeled all nuclei, and the negative control procedure labeled no nuclei in the specimens.

6.3.6 Gentamicin-induced cell apoptosis in HEI-OC1 cells

To investigate the potential cell death form of gentamicin in cochlear cells under a hypoxia environment (0.5% O₂), we first examined the effect of gentamicin on cell survival in mouse cochlear cells (HEI-OC1). Treatment of HEI-OC1 cells with gentamicin-induced cell death in a concentration-dependent manner using an MTT assay (Fig. 6.9A). Significant decreasing of cell viability was ranging from 4-40 μM. When cells were treated with gentamicin at a concentration of 20 μM, the cell viability showed decreasing in a time-dependent manner as determined by MTT assay (Fig. 6.9B). We next investigated whether gentamicin induces cell death through an apoptotic mechanism. Annexin V–PI double-labeling was used for the detection of PS externalization, a marker for early phase of apoptosis. Compared with vehicle-treated HEI-OC1 cells, a high proportion of Annexin V⁺ labeling was detected in HEI-OC1 cells treated with gentamicin in hypoxia (Fig. 6.10A). In addition, gentamicin-induced apoptosis in HEI-OC1 cells in a

concentration-dependent manner as determined by Annexin V–PI staining (Fig. 6.10B–E). Next, we investigated the effect of gentamicin-induced apoptosis using a TUNEL assay. Compared with vehicle-treated cells, those treated with gentamicin showed significant cell apoptosis (Fig. 6.11). These data suggest gentamicin increases cell apoptosis under hypoxia condition in cultured cochlear cells.

6.3.7 Gentamicin caused mitochondrial dysfunction in HEI-OC1 cells

To determine whether gentamicin-induced apoptosis is mediated through mitochondrial dysfunction, we determined the mitochondrial membrane potential (MMP) with a probe, JC-1, using flow cytometry analysis. As shown in Fig. 5.10A, treatment of cells with gentamicin at a concentration of 20 μM for 0-24 h induced the loss of the mitochondrial membrane potential in a time-dependent manner. Furthermore, we examined whether ROS accumulation was involved in gentamicin-induced cell death. DHR-based flow cytometry analysis revealed that intracellular O_2^- level increased in HEI-OC1 cells following treatment with gentamicin under hypoxia condition (Fig. 6.12B). To further investigate whether gentamicin-induced HEI-OC1 cell apoptosis by triggering the mitochondrial apoptotic pathway, we measured the change in expression of Bcl-2 family proteins. Treatment of HEI-OC1 cells with gentamicin under hypoxia condition induced an increase in Bax and Bak protein levels (Fig. 6.12C). In addition, gentamicin reduced the expression of Bcl-2, which led to an increase in the proapoptotic/antiapoptotic Bcl-2 ratio (Fig. 6.10C). These data suggest that mitochondrial dysfunction is involved in the cell apoptosis caused by the interaction of hypoxia and gentamicin in HEI-OC1 cells.

6.3.8 Gentamicin caused ER stress, Ca^{2+} release and calpain activity

We further assessed the effect of gentamicin on the mobilization of Ca^{2+} in HEI-OC1 cells. When cells were treated with gentamicin and cultured in hypoxia, Ca^{2+}

levels significantly increased compared with the vehicle-treated control (Fig. 6.13A). The data also demonstrated that gentamicin promoted a Ca^{2+} flux in a time-dependent manner (Fig. 6.13A). We further examined whether the activity of calpain (calcium-dependent thiol proteases) would be induced by gentamicin in HEI-OC1 cells under hypoxia condition. As shown in Fig. 6.13, gentamicin increased calpain-1 and calpain-2 expression in a time-dependent manner. Therefore, these results indicate that Ca^{2+} release and calpain activity are involved in the cell death during the interaction of gentamicin and hypoxia in HEI-OC1 cells. We next examined the effects of gentamicin on the expression of caspase-9 and caspase-3 in HEI-OC1 cells. Our data showed that gentamicin increased the activation of caspase-9 and caspase-3 in a concentration-dependent manner in HEI-OC1 cells using western blot analysis (Fig. 6.11C), as well as ELISA assay (Fig. 6.13D). On the other hand, gentamicin also decreased PARP activity (Fig. 6.11C). In addition, treatment of cells with caspase-3 and caspase-9 inhibitors reduced gentamicin-induced apoptosis of cells (Fig. 6.13E). Therefore, these results indicate that gentamicin-induced cell apoptosis during hypoxia status is mediated through mitochondrial dysfunction, endoplasmic reticulum (ER) stress, and caspase cascade (Fig. 6.14).

6.4 Comments and conclusion

This study showed a transient hearing loss (Fig. 6.1) without obvious HC loss (Fig. 6.3) at 4 weeks after transient cochlear ischemia of 30 minutes, reflecting a revival potential of cochlea to transient ischemia in guinea pigs may be more than 30 min. (Perlman et al., 1959) The administration of gentamicin in 125 mg/kg alone could not produce prolonged significant ABR threshold shifts or HC loss, which is consistent to previous study (Jin et al., 2001). However, the administration of gentamicin after transient cochlear ischemia elicited significant ABR threshold shifts at all frequencies examined (Figures 6.1, 6.2). The hearing deterioration was considered to be permanent, because no recovery in ABR threshold was observed by 4 weeks after treatment, and

there was significant loss of OHCs and some portions of IHCs, which cannot be regenerated in mammals.

Our results also showed that ABR threshold shifts were associated more with the high-frequency range (4-16 kHz) than with the low-frequency range (1-2 kHz) (Fig. 6.2). These observations were confirmed by morphological examination of the cochlear surface preparation and the numbers of HCs that were stained with phalloidin.(Fig. 6.3) The basal turn HCs, which represent higher frequency, seemed to be more susceptible to damage than were the upper turn HCs, which represent lower frequency.(Fig. 6.3, 6.4) Hair cells are the primary targets during aminoglycoside ototoxicity. Flattening of Corti's tunnel was observed 6 months after administration of toxic dose of aminoglycoside (Leake & Hradek, 1988). In this study, dysmorphic organ of Corti in the basal turn was observed 4 weeks after the interaction of gentamicin and ischemia (Fig. 6.5E). These observations had also consistent with previous investigations on cochlear ischemia(Perlman et al., 1959; Maetani et al., 2003).This may signify that the ischemia may attenuate and fasten the gentamicin ototoxicity.

The ototoxicity of aminoglycosides to cochlear hair cells also progresses in a base-to-apex gradient(Forge & Schacht, 2000). The uptake of gentamicin by hair cells in the basal turns is greater than that in the apical turns (Hayashida et al., 1985). The basal portion of the cochlea has a greater rate of oxygen consumption than does the upper apical portion (Mizukoshi & Daly, 1967). Conversely, the energy reserve of the organ of Corti, especially glycogen, follows an inverse base-to-apex distribution—more glycogen is found in the apical turns than in the basal turns (Thalman et al., 1972). A base-to-apex gradient of differential intrinsic susceptibility to free radicals has also been reported(Sha et al., 2001). Free radicals and reactive oxygen species are common products of ischemia-reperfusion injuries. The HCs in the basal turns are more vulnerable to free-radical damage than are those in the apical turns (Sha et al., 2001). These observations could explain why the apical turn tolerates the damage from co-administered gentamicin-ischemia better than the basal turn does.

In addition to the intrinsic base-to-apical differential susceptibility to ischemia, this

study also showed that guinea pig OHCs were more vulnerable to combined gentamicin-ischemia than were the IHCs. OHCs have also been shown to be more vulnerable to GM ototoxicity than IHCs (Jiang et al., 2006; McDowell, 1982; Suzuki et al., 2000). It is still unclear that why IHCs could tolerate the AG ototoxicity better than OHCs. However, similar result was also observed in mice as the observation of the OHC loss by GM ototoxicity precedes IHC loss (Forge & Schacht, 2000). After 4 weeks, minimal OHC loss occurred when ischemia lasted 30 min, but significant OHC loss nearly in each cochlear turn was apparent after combined gentamicin-ischemia treatment (Fig. 6.3, 6.4). In guinea pigs, OHCs may be more vulnerable to ischemia-reperfusion injury than are IHCs (Perlman et al., 1959; Tabuchi et al., 2002). In addition to ischemic damage, OHCs in guinea pigs are more vulnerable to other kinds of cochlear injuries, such as aminoglycoside ototoxicity (Suzuki et al., 2008). With the longer periods of ischemia, both IHCs and OHCs may be affected.

We also found that SGNs were damaged 4 weeks after combined gentamicin-ischemia treatment, especially in the lower cochlear turns (basal and second turns) where the hair cells were mostly damaged (Fig. 6.5F). In addition to the synergic toxic effects of ischemia and gentamicin ototoxicity to the spiral ganglion neurons, this may be caused by the secondary loss to the hair cell, especially IHC loss (Bae et al., 2008). The chronic cochlear changes after aminoglycoside ototoxicity also include the degeneration of spiral ganglion neurons (Leake & Hradek, 1988). The loss of organ of Corti has been demonstrated to cause a slow but progressive loss of spiral ganglion neurons with variable time courses of different cochlear insults (Leake & Hradek, 1988; Webster and Webster, 1981). External insults such as noise trauma, aminoglycoside ototoxicity, or cochlear ischemia could induce excessive glutamate release from IHCs into synaptic clefts. A large glutamate concentration causes SGN cell death (Steinbach & Lutz, 2007). In this study, hair cell loss was not apparent unless the animals were treated by combination of gentamicin and 30-min ischemia. The IHC loss was most significant in the lower cochlear turns (Fig. 6.3). In the upper cochlear turns (apical and third turns), mild to moderate significant OHC loss was found, whereas IHCs remained relatively

unaffected (Fig. 6.3). Additionally, SGN loss was apparent in the lower turns in the animals received combined ischemia-gentamicin treatment (Fig. 6.5F), while the morphology of the SGNs remained relatively intact in the upper cochlear turns (Fig. 6.5C). The loss of the SGNs seemed to parallel the loss of IHCs. To summarize the cochlear changes after interaction of ischemia and aminoglycoside, the cochlear damage moves from the basal turn towards the apex, occurs first in outer hair cells and then in inner hair cells, and then shifts to the more central neural structures such as spiral ganglion neurons. Such differential and orderly pattern of cochlear damage is similar to previous study of ototoxicity by prolonged high dose of aminoglycoside (Kalkandelen et al., 2002).

There are several reasons to explain why ischemia contributes to the development of aminoglycoside ototoxicity. The aminoglycoside ototoxicity depends on the aminoglycoside concentration in the cochlear fluid rather than the serum concentration (Hayashida et al., 1985). The development of aminoglycoside ototoxicity is related to the diffusion of aminoglycoside into the inner ear and its subsequent binding to cochlear tissues, followed by slowly releasing into inner ear fluid (Tran Ba Huy et al., 1983). The entry of aminoglycoside into cochlear cells includes the attachment of the cationic aminoglycoside molecule to the negatively charged cell membrane and entering the cochlear cells via endocytosis *in vivo* (Hashino and Shero, 1995) or by permeating through non-selective cation channels such as the mechanosensitive transduction channels at the stereocilia tips (Marcotti et al., 2005; Myrdal et al., 2005; Wang & Steyger, 2009). A blood-labyrinthine barrier (BLB) which is a regulatable barrier for aminoglycoside entry exists at the interface between the perilymphatic and endolymphatic space (Dai and Steyger, 2008). The toxicity of aminoglycoside may therefore depend on the integrity of the BLB in the individual at the time of treatment. When gentamicin is administered alone, gentamicin would not disrupt endothelial cell junction which constitutes the BLB (Laurell et al., 2000). The immature or defective BLB has been shown to increase the aminoglycoside ototoxicity such as in newborn (Bernard, 1981). Ischemic damage have been well known to alter the integrity and permeability of

blood-brain barrier (Spatz, 2010), which is morphologically similar to the BLB (Jahnke, 1980). The permeability of BLB was ever shown to be increased when cochlea microcirculatory disorders occurred (Zhang and Wang, 2000). Oxidative stress such as reactive nitrogen stress which is the by-product of ischemia/reperfusion injury was also shown to be involved in the disruption of blood-labyrinthine barrier (Kastenbauer et al., 2001). Using fluorescent gentamicin tracking technique, our study also demonstrated increased uptake of gentamicin after transient cochlear ischemia (Fig. 6.6, 6.7). Therefore, ischemia may disrupt or damage the BLB, at which it is possible that higher drug concentrations may reach the inner ear and result in cochlear damage.

The predisposition of AG ototoxicity by ischemia/reperfusion injury may also be explained on a cellular level. Currently, aminoglycoside is believed to exert its ototoxicity by increasing a variety of free-radical species, including both reactive oxygen species (ROS) and reactive nitrogen species, through an iron-dependent pathway (Forge & Schacht, 2000; Priuska and Schacht, 1995). The formation of free radicals by AGs is initiated by the iron-aminoglycoside complex which actively reduces the molecular oxygen to superoxide by an electron donor and formation of other free radicals ensue (Forge & Schacht, 2000; Lesniak et al., 2005). Such iron-aminoglycoside complex is believed to mediate the free-radical induced cell damage and initiate the apoptotic cascades. Ischemia-reperfusion injury of cochlea has been also shown to elicit the release of free iron and massive production of nitric oxide (NO) by nitric oxide synthase (Tabuchi et al., 2001). The free iron may further chelate with the aminoglycoside, which induces a cascade of ROS formation. The excessive NO production also has been shown to induce cochlear hair cell death (Yamane et al., 2004). Such high level of ROS, coupled with the disruption in the BLB may result in auditory dysfunction or even irreversible hearing loss.

Multiple death pathways, including necrotic and apoptotic pathways, contribute to the cochlear hair cell death after AG ototoxicity (Jiang et al., 2006). In acute administration of the aminoglycoside, apoptosis may be the predominant form of cell death and caspase cascades were shown to be the downstream pathways (Forge and Li, 2000; Pirvola et al.,

2000; Matsui et al., 2002; Ylikoski et al., 2002). When chronic administration of aminoglycosides, both necrotic and apoptotic morphology were observed in the cochlear hair cells and caspase-independent apoptosis was shown in the chronic model of aminoglycoside ototoxicity instead of traditional caspase dependent apoptosis(Jiang et al., 2006). In this study, the acute interaction of hypoxia and gentamicin was investigated, which revealed an apoptotic cellular death through a caspase-dependent pathway (Fig. 6.13, 6.14).

The caspase-dependent apoptotic pathway is mediated by activation of caspase through either intrinsic or extrinsic pathways (Rybak and Kelly, 2003). Previous study shows that gentamicin does not cause apoptosis through the extrinsic apoptotic pathway via the Fas receptor (Bodmer et al., 2003). However, many evidences support that mitochondrial dependent intrinsic apoptotic pathway plays an important role in the aminoglycoside-induced cell apoptosis. Many genetic and biochemical evidences also support that the mitochondrial dysfunction plays an important role in the susceptibility of aminoglycoside ototoxicity (Guan, 2004b). Gentamicin has been depicted to elicit the release of iron from mitochondria, and to enhance the generation of hydroxyl radicals(Walker et al., 1999). In our previous study, a direct demonstration of increased susceptibility of AG toxicity in acute mitochondrial dysfunction was exhibited(Lin et al., 2008). In this study, when ischemia was interacted with gentamicin *in vitro*, loss of mitochondrial membrane potential (Fig. 6.11A) was observed in the early stage of hypoxia, followed by elevation of oxidative stress (Fig. 6.11B). The caspase cascades are then activated by the initiator caspase 9 and the executioner caspase 3, which results in the processing of apoptotic cell death.

In addition to the mitochondrial dependent apoptotic pathway, calcium influx (Fig. 6.13A) and increased expression of calpain (Fig. 6.13B) was also observed in the early stage of ischemia interacting with gentamicin *in vitro*. Previous studies has demonstrated that gentamicin may cause a dose-dependent increase in intracellular calcium in chicken hair cells(Hirose et al., 1999). The cellular influx caused by gentamicin-induced hair cell damage may further activate calpain and result in the apoptotic cascades (Ding et al.,

2002).

The interaction between hypoxia/ischemia and aminoglycoside ototoxicity may occur in at least three different scenarios: (1) simultaneous application of aminoglycoside and occurrence of hypoxia/ischemia; (2) sub-damaging doses of aminoglycoside enhancing hypoxia/ischemia; and (3) prior hypoxia/ischemia augment subsequent aminoglycoside toxicity. The hypoxia/ischemia-then-drug paradigm in this study displayed apparent synergism. This implies that ischemia could increase the susceptibility to aminoglycoside ototoxicity. This paradigm is more relevant to ordinary clinical situations that the aminoglycoside usually is given when the patient is infected or in hypoperfusion status like sepsis, hypovolemia or impending shock.

Outlook. For translation into clinical practice—possible preventing synergistic toxicity induced by hypoxia/ischemia and aminoglycosides. Preventing synergistic toxicity induced by ischemia and aminoglycosides is likely to involve a combination of aminoglycoside uptake inhibitors (once identified) working at the BLB to reduce cochlear uptake of aminoglycosides, combined with a one or several anti-oxidants known to ameliorate either aminoglycoside or noise-induced hearing loss. More immediately, it may be more important to remove the sources that contribute to cochlear ischemia, such as shock status or hypovolemia. It may be difficult in clinical practice and may meet many conflicts during the scenario that we have to make a decision to choose the best therapeutic strategy for the patient in suffering or under risk. This study could provide us another insight to better understand the complicated interaction between ischemia and aminoglycoside, and the cytotoxic mechanisms they may induce within the cochlea that potentiate ischemia or AG ototoxicity into cytotoxic phenomenon.

Conclusion

Increased susceptibility of hypoxia/ischemia to gentamicin ototoxicity was demonstrated in this study. Apoptosis contributes to the cell death during the interaction of ischemia and gentamicin ototoxicity. Cochlear hair cells and spiral ganglion neurons are the two major regions affected during this interaction. Generation of reactive oxygen

species, loss of mitochondrial membrane potential, calcium release and caspase-dependent apoptotic cell death were shown during the interaction of hypoxia/ischemia and gentamicin ototoxicity *in vitro*. These results may improve our understanding of the interacting mechanism and potential preventive strategy for the development of aminoglycoside ototoxicity.



6.5 Figures

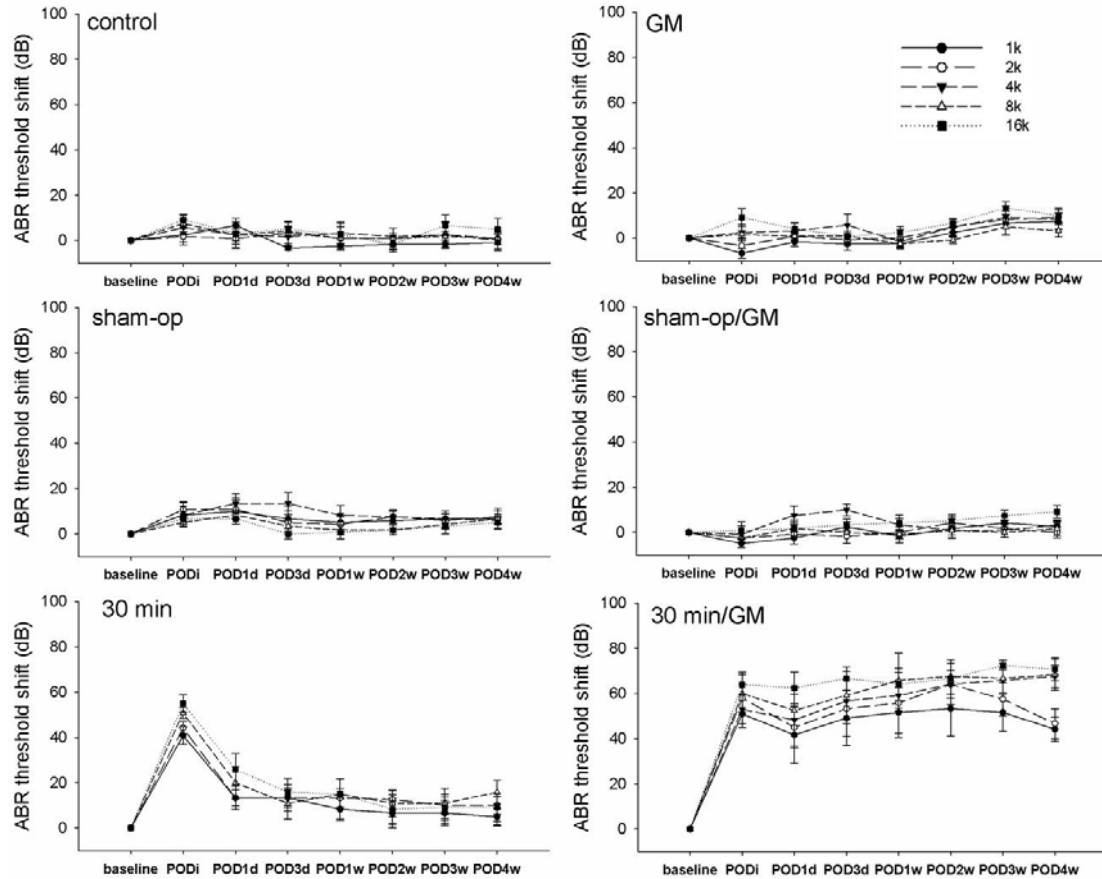


Figure 6.1 Serial ABR threshold shifts from the baseline in different treatment groups after different duration of follow-up. The ABR was recorded by different tone burst stimulation (1k Hz, filled circle; 2k Hz, empty circle; 4k Hz, filled triangle; 8k Hz, empty triangle; 16k Hz, filled square) No significant ABR threshold shifts were noted in the control, gentamicin alone (GM), sham-op and sham-op/GM groups. Transient ABR threshold shifts were depicted in the 30-min ischemia group. Persistent ABR threshold elevations were shown in the 30-min/gentamicin group. Y-axis indicates the ABR threshold shifts in decibel (dB) by different auditory stimuli. X-axis indicates the timing for serial ABR measurement, from baseline, PODi, POD1d, 3d, 1w, 2w, 3w, and 4w. The abbreviations PODi, POD1d, 3d, 1w, 2w, 3w, and 4w are defined in Materials and Methods. The value with error bar in each point indicates mean \pm standard error.

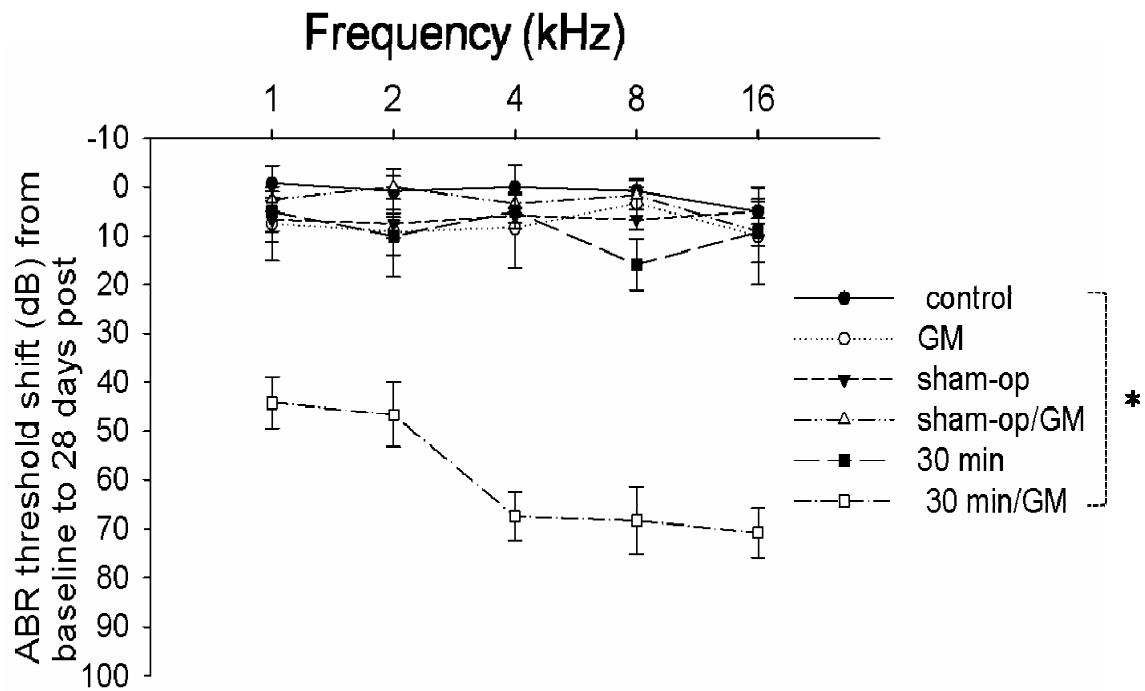


Figure 6.2 ABR threshold shifts from baseline to 28 days in different treatment groups. Compared with the control group, no significant ABR threshold shifts were noted in the gentamicin alone (GM), sham-op, sham-op/GM or 30-min ischemia groups, but significant ABR threshold shifts were depicted in the 30-min ischemia/GM group. (*, $p < 0.001$) The value with error bar in each point indicates mean \pm standard error.

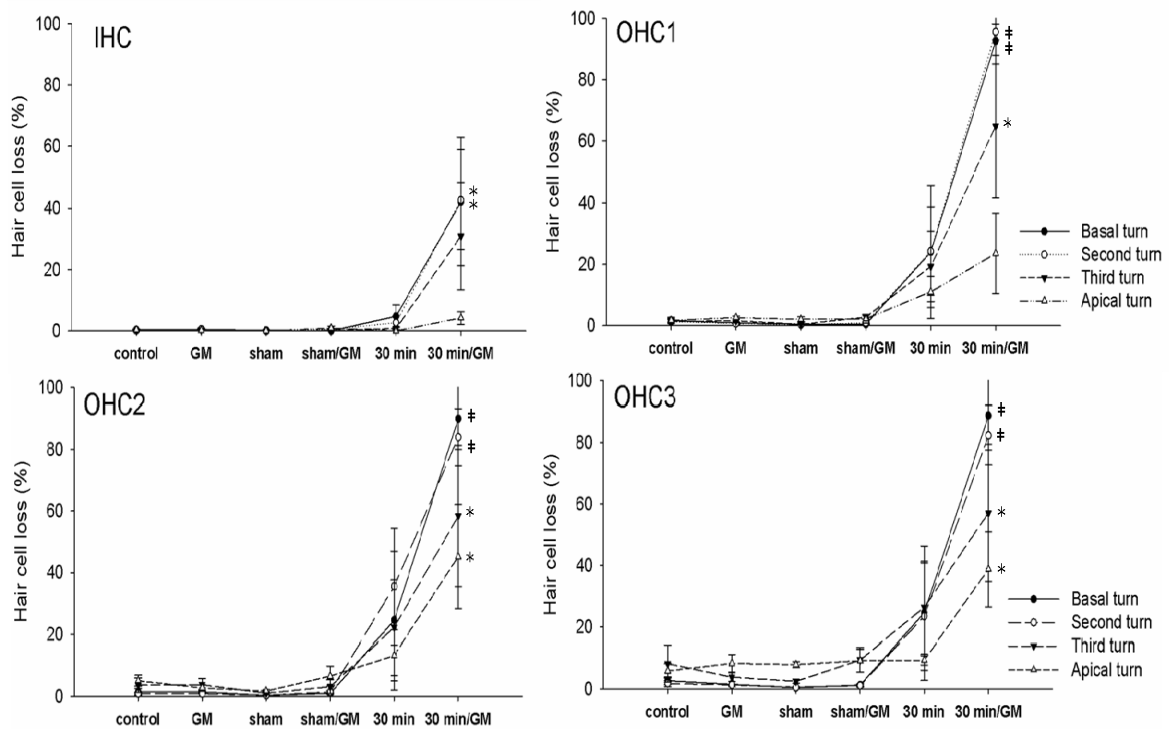


Figure 6.3 Hair cell losses in different groups at different cochlear turns (basal turn, filled circle; second turn, empty circle; third turn, filled triangle; apical turn, empty triangle). Compared with the control group, significant hair cell loss was depicted when the administration of gentamicin was given after transient cochlear ischemia, especially in the basal turn. X-axis indicates different treatment groups, from control, GM, sham-op, sham-op/GM, 30-min ischemia, and 30min-ischemia/GM. The value with error bar in each point indicates mean \pm standard error. (*, $p < 0.05$; ‡, $p < 0.001$).

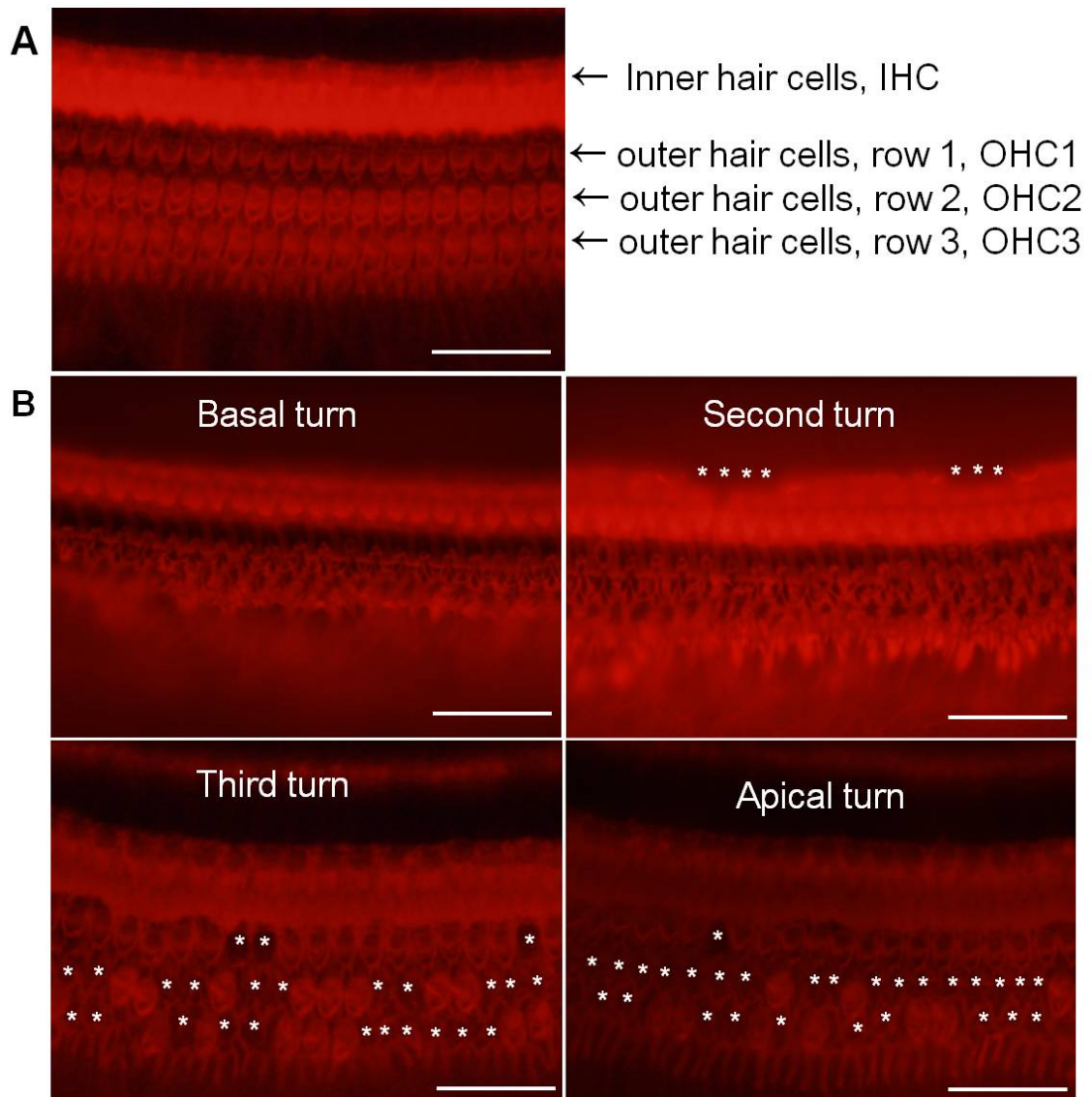


Figure 6.4 Hair cell (HC) labeling with rhodamine-conjugated phalloidin in animals treated with gentamicin after 30-min ischemia. Compared with the normal hair cell architecture (A), differential hair cell losses were depicted (B). Complete loss of Inner HCs (IHC) and the three rows of outer HCs (OHC1, OHC2, OHC3) were depicted in the basal turn. Partial loss of IHCs and complete loss of OHCs could be identified in the second turn. Fairly normal morphology of IHC in third and apical turn was present. Some outer hair cell loss was found in the second turn and apical turn by labeling defect. Most OHC loss are lost in the outer rows (second and third rows). Asterisks indicate IHC loss in the third turn and OHC loss in the second and apical turns. Bar=20 μ m.

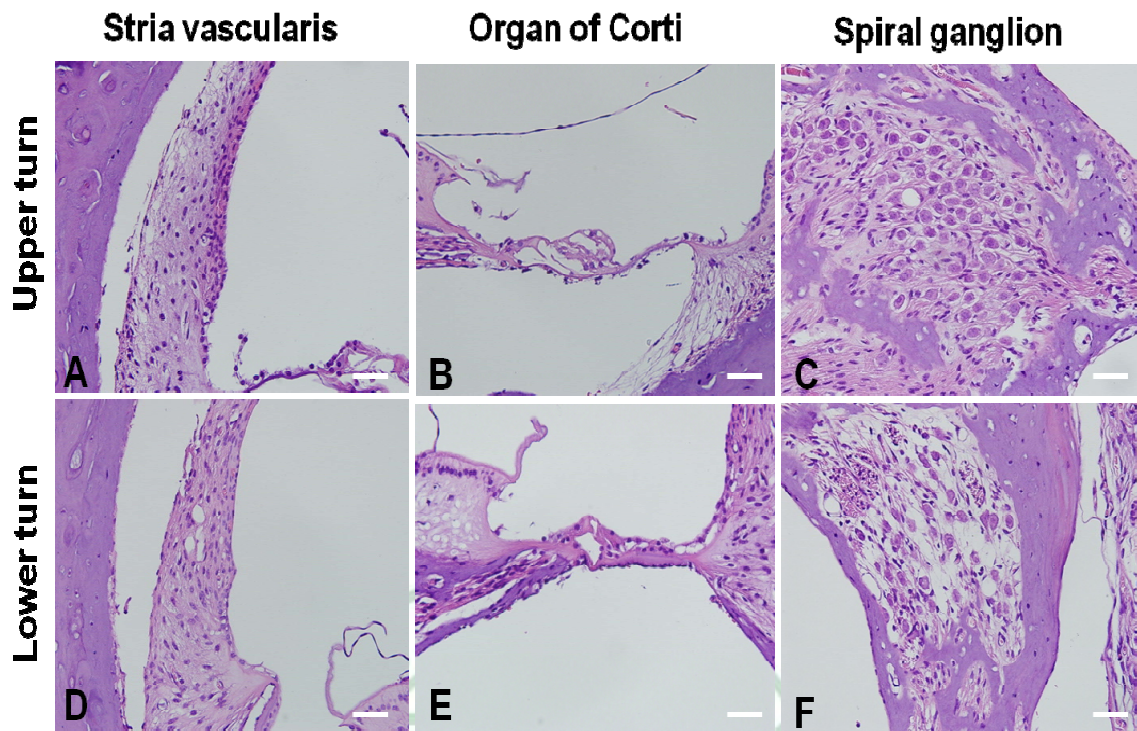


Figure 6.5 The sections in upper turn (A-C) and lower turn (D-F) of the cochlea from the animals that received gentamicin after 30 minutes ischemia. The histopathology of the stria vascularis (A,D), organ of Corti (B,E) and spiral ganglion (C,F) was depicted. Loss of spiral ganglion cells and dysmorphic arrangement in the organ of Corti was noted in the lower turns of cochlea, compared with those in the upper turns. Bar=20 μ m.

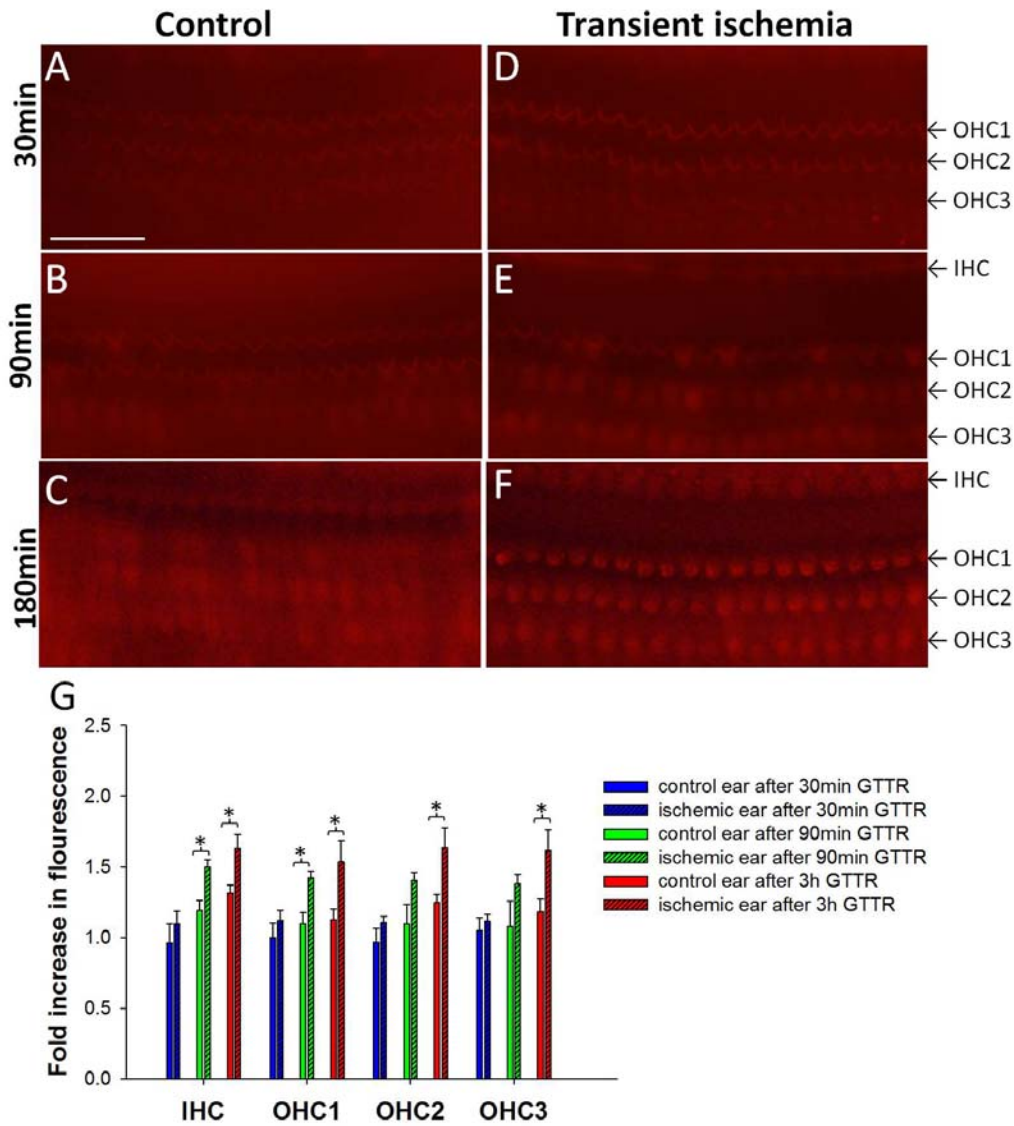


Figure 6.6 Sequential GMTR fluorescence in the middle cochlear turn examined at 30, 90 and 180 min after 125 mg/kg GM/GMTR injection in the control (A-C) and 30-min ischemic cochlea (D-F). GMTR fluorescence in outer hair cells was depicted 30 minutes after injection of GMTR in both groups (A, D). 90 minutes after application of GMTR, gentamicin fluorescence was still negligibly labeled at the inner hair cell of the control (B) but visible in those of the 30-min ischemic cochlea. Diffusion of GMTR fluorescence into hair cell cytoplasm could be found, especially in the ischemic cochlea (E). After 180 minutes, diffused GMTR fluorescence was labeled in the outer hair cells cytoplasm and some soma of inner hair cells (C, F), in which more intense GMTR fluorescence was labeled in 30-min ischemic cochlea (F). (G) Comparison of the sequential hair cells fluorescence differences between control and ischemic cochleae (n=4 in each group). The GMTR fluorescence is more intense in the outer hair cells. In addition, the hair cells in the ischemic cochleae exhibit more fluorescent intensity that those in the control cochleae at least 90 min after GMTR injection. Y-axis indicates the relative fluorescence intensity ratioed against that of the 1st row of OHCs 30 min after 125mg/kg GM/GMTR injection in the control cochlea. X-axis indicates the different hair cell types. The value with error bar in each point indicates mean \pm standard error. (*, $p < 0.05$) GM: gentamicin; GMTR: conjugate of gentamicin and Texas-Red esters. Bar=20 μ m.

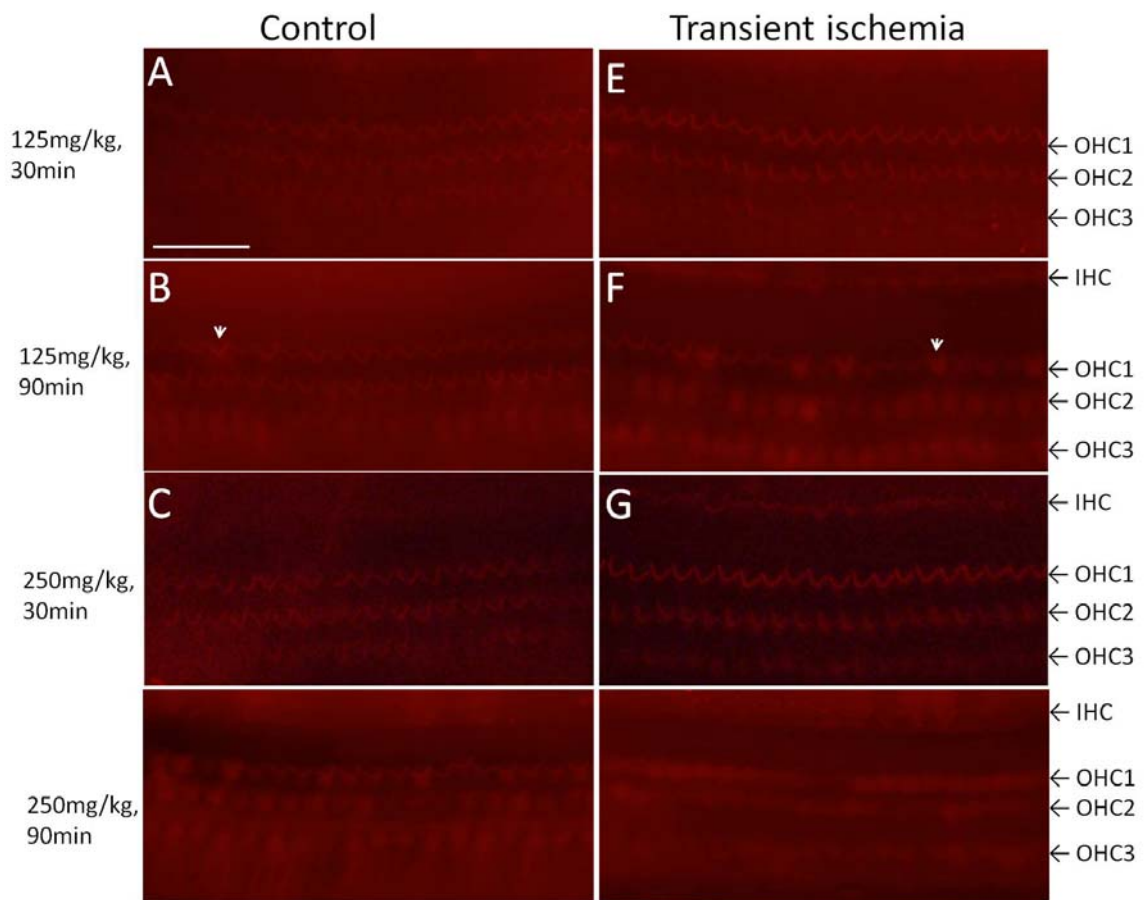


Figure 6.7 Expression of GMTR fluorescence from middle cochlear turns examined at 30 min (A, C, E, G) and 90 min (B, D, F, H) after 125 mg/kg (A, B, E, F) or 250 mg/kg (C, D, G, H) GM/GMTR injection in the control (A-D) and 30-min ischemic cochlea (E-H). GMTR fluorescence in inner hair cells was depicted in 30 min ischemia after prolonged exposure (F) or high GM/GMTR dosage (C, D, G, H). More distinctly labeled GMTR fluorescence in outer hair cell cytoplasm as well as in the soma of some inner hair cells were observed in 30-min ischemic cochlea. GM: gentamicin; GMTR: conjugate of gentamicin and Texas-Red esters. Bar=20 μ m.

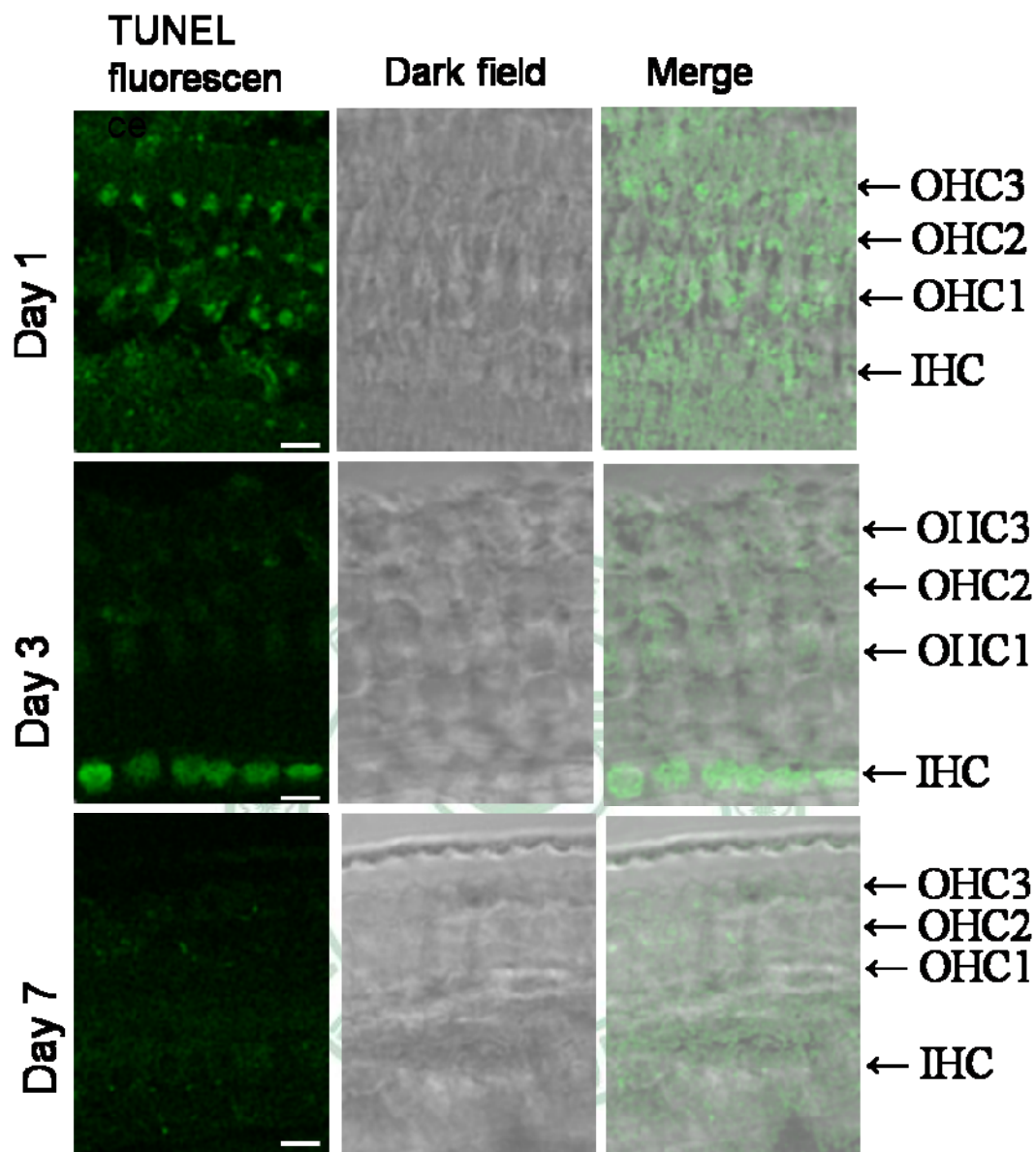


Figure 6.8 Hair cell (HC) staining with TUNEL fluorescence seen 1, 3 and 7 days in animals treated with gentamicin after 30-min ischemia. OHC labeling by TUNEL fluorescence was observed 1 day after combination of gentamin and 30-min ischemia. 3 days later, IHC labeling with TUNEL fluorescence was observed. Bar = 10 μ m.

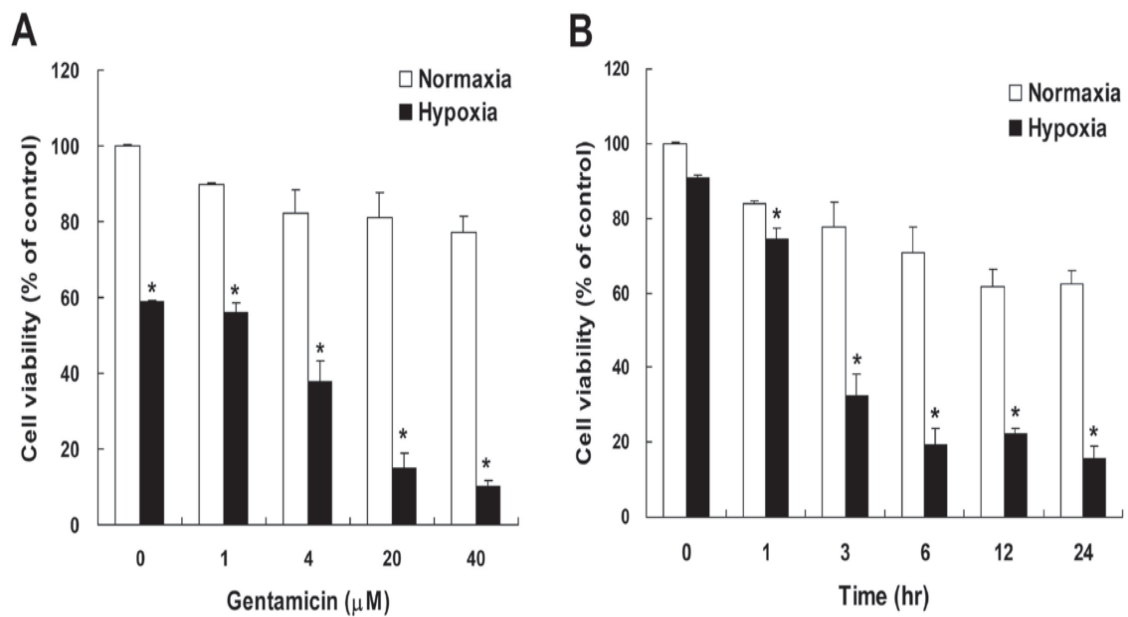


Figure 6.9 Gentamicin-induced cell death of cultured cochlear cells. (A) HEI-OC1 cells were incubated with various concentrations of gentamicin for 24 h under hypoxia condition, and cell viability was examined by MTT assay (n=6). (B) HEI-OC1 cells were incubated with gentamicin (20 μM) for different time intervals under hypoxia condition, and the cell viability was examined by MTT assay (n=6). Results are represented as the mean \pm S.D. *, $p < 0.05$ as compared with control group.

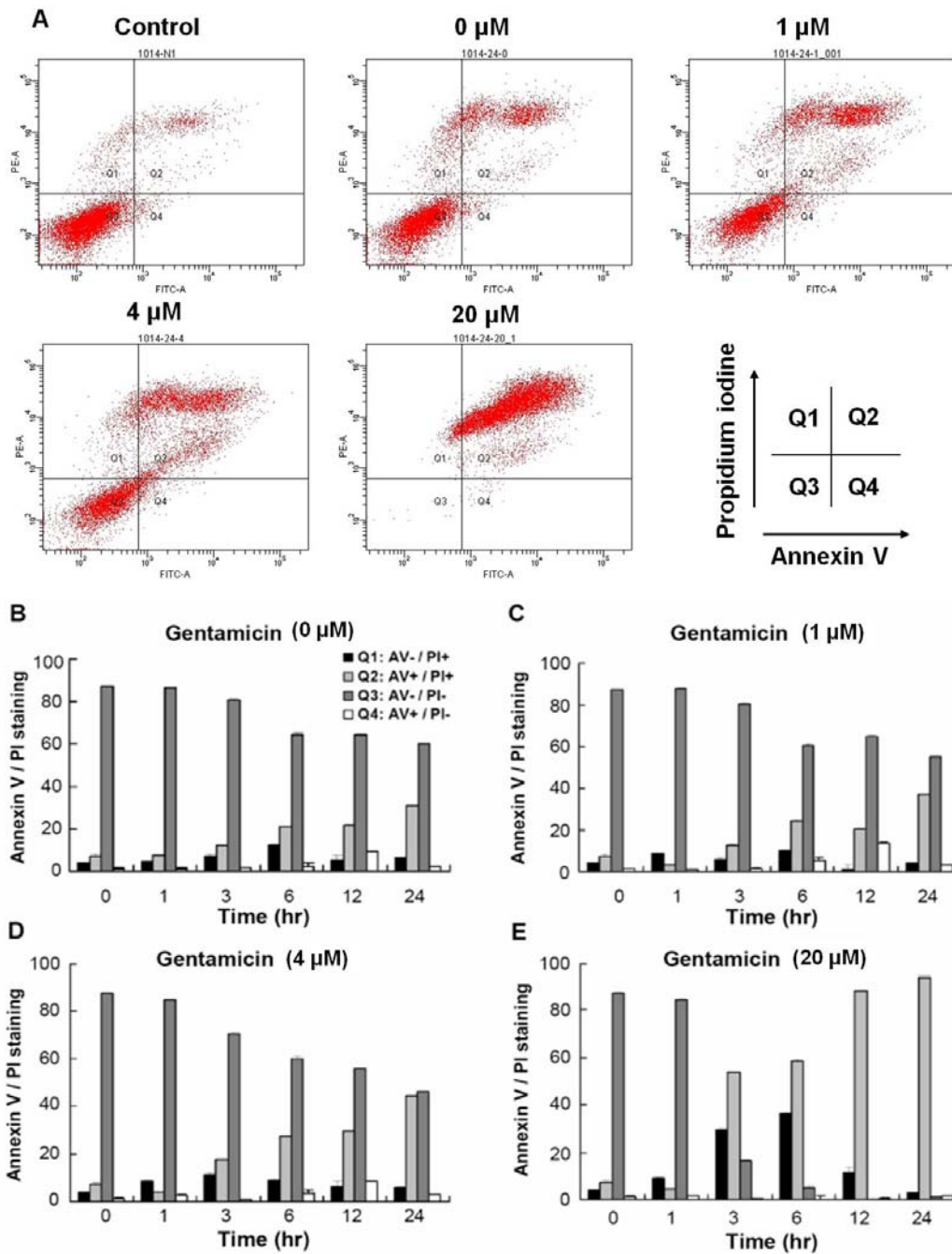


Figure 6.10 Gentamicin-induced apoptosis of cultured cochlear cells. (A) HEI-OC1 cells were treated with vehicle or various concentrations of gentamicin for 24 h under hypoxia condition, the percentage of apoptotic cells was assessed by flow cytometric analysis of Annexin V-PI staining ($n=3$). (B-E) Relative levels of apoptotic cells were calculated. Results are expressed as the mean \pm S.D.

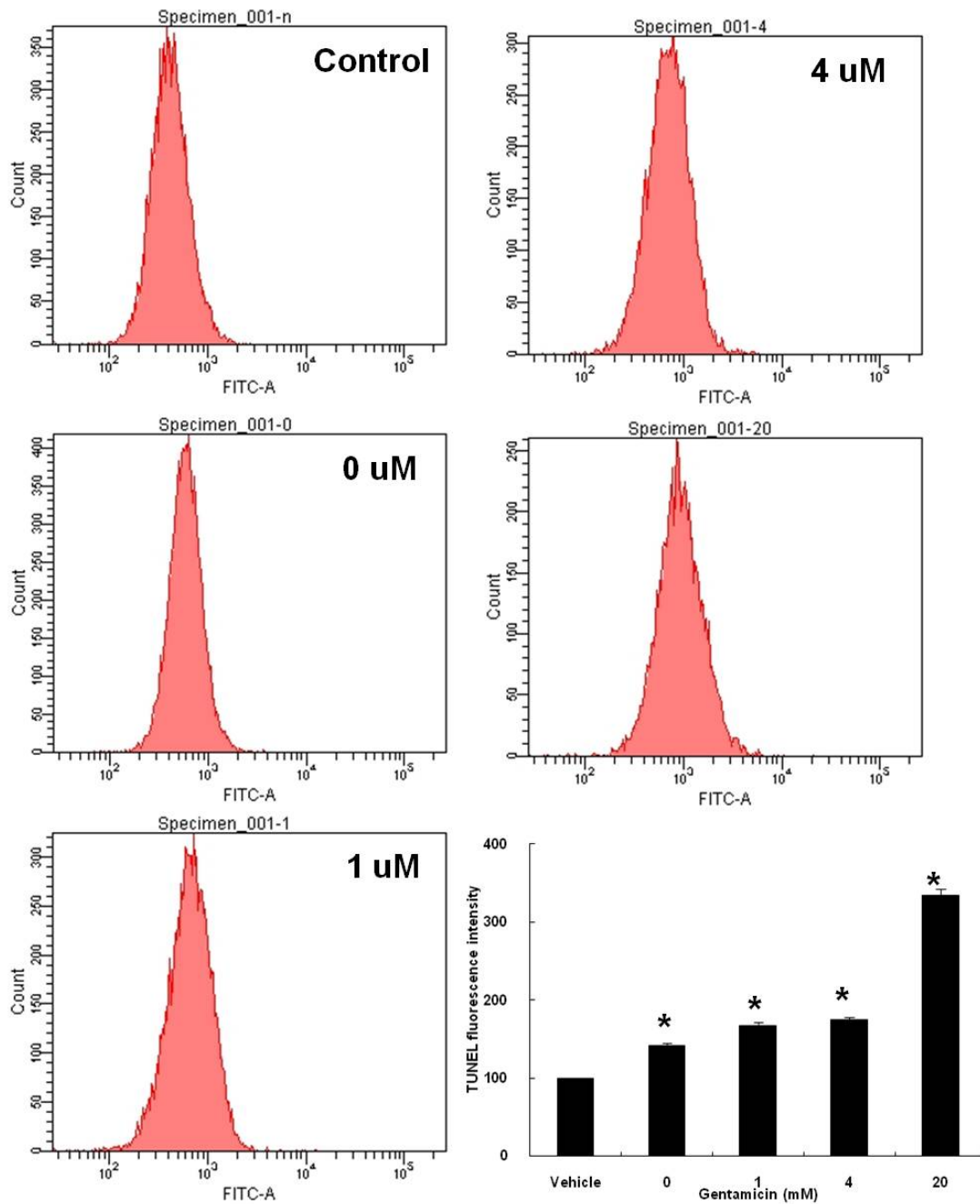


Figure 6.11 Gentamicin increased TUNEL positive cells of cultured cochlear cells. HEI-OC1 cells were treated with vehicle or various concentrations of gentamicin under hypoxia condition for 24 h, the TUNEL positive cells were examined by flow cytometric analysis (n=3). The relative fluorescence levels were measured and represented in the right-bottom. Results are expressed as the mean \pm S.D.

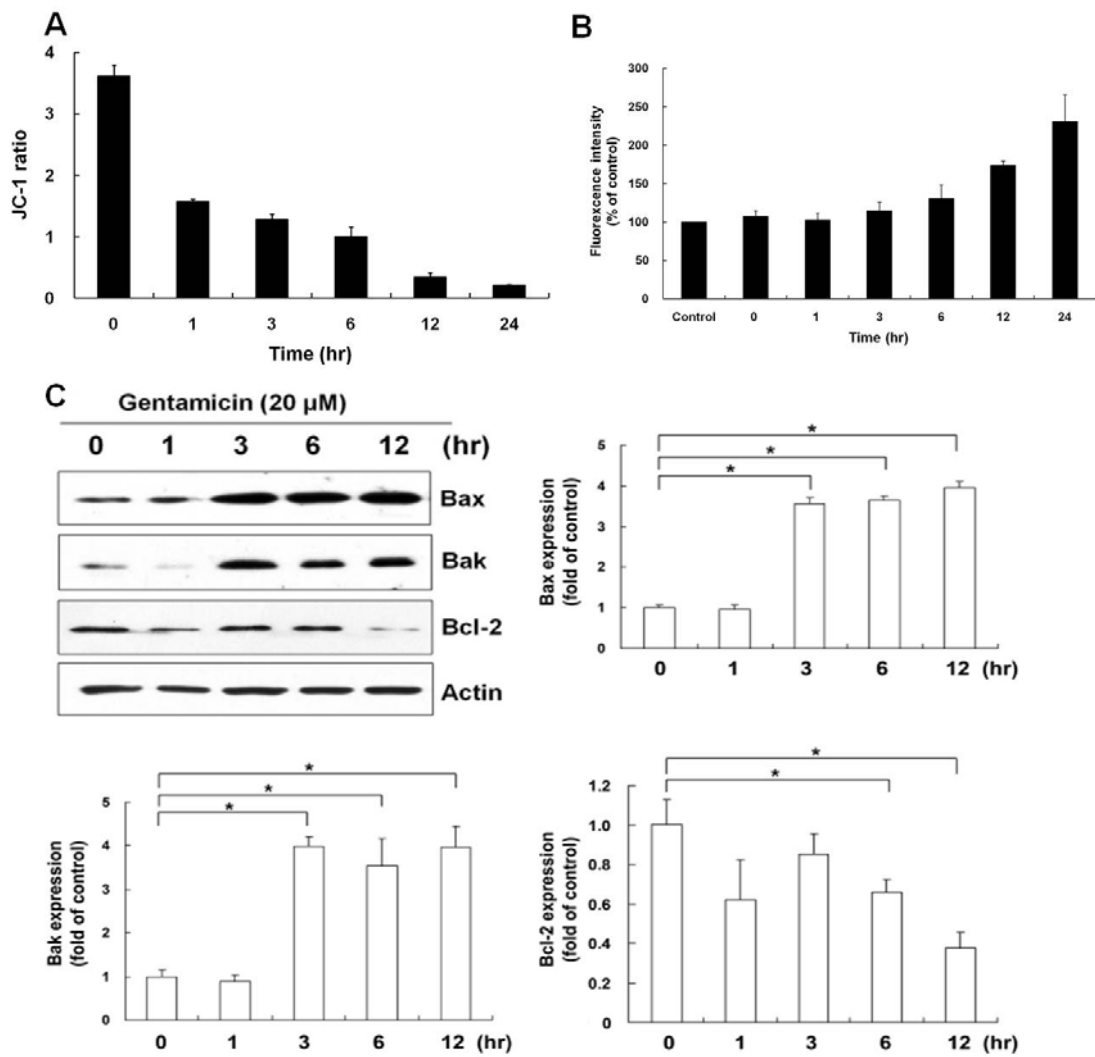


Figure 6.12 Gentamicin induced mitochondrial dysfunction in cultured cochlear cells. HEI-OC1 cells were treated with gentamicin (20 μ M) for different time intervals under hypoxia condition, (A) mitochondrial membrane potential and (B) the level of ROS production were examined by flow cytometry analysis (n=3). (C) HEI-OC1 cells were incubated with gentamicin (20 μ M) for different time intervals under hypoxia condition, the Bax, Bak and Bcl-2 expressions were examined by western blot analysis. Results are represented as the mean \pm S.D. *, $p < 0.05$ compared with control group.

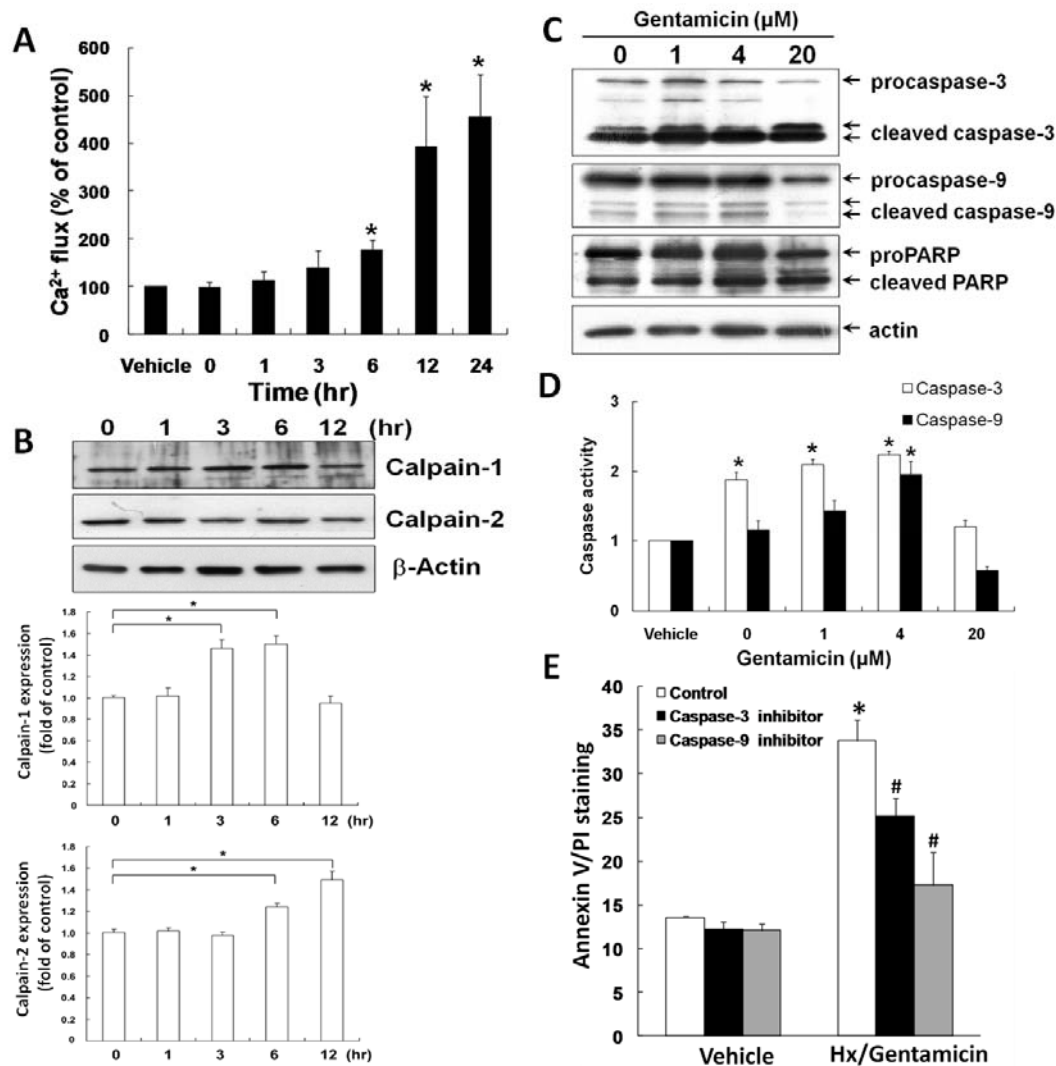


Figure 6.13 Ca²⁺ release and calpain activity are involved in gentamicin-induced apoptosis of cultured cochlear cells. HEI-OC1 cells were incubated with gentamicin (20 μM) in hypoxia for different time intervals under hypoxia condition, (A) Ca²⁺ flux was examined by flow cytometry (n=3), (B) calpain-1 and calpain-2, (C) caspase-3, -9, and PARP expressions were examined by western blot analysis. (D) HEI-OC1 cells were incubated with gentamicin (20 μM) for different time intervals under hypoxia condition, caspase-3 and caspase-9 activities were examined by caspase ELISA kit (n=3). HEI-OC1 cells were pretreated for 30 min with inhibitors of caspase-3 and -9 followed by stimulation with gentamicin (20 μM) under hypoxia condition for 24 h, the percentage of apoptotic cells were then analyzed with flow cytometry analysis of Annexin V-PI staining (n=3). Results are represented as the mean ± S.D. *, *p*<0.05 compared with control group.

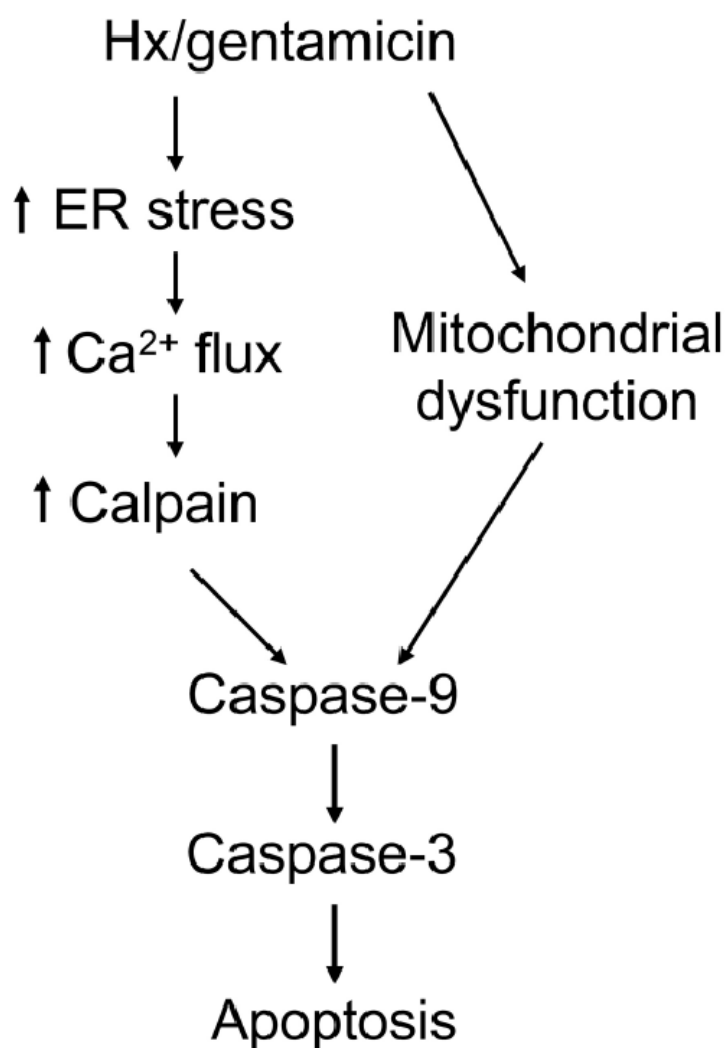


Figure 6.14 Schematic diagram of the pathways involved in gentamicin-induced cell apoptosis in cultured cochlear cells cultured in hypoxia condition. Proposed models showing how hypoxia-gentamicin interaction affects various biochemical processes and events in cochlear cells, resulting in apoptotic cell death, are illustrated in this schematic diagram.

Chapter 7 Further clinical implications and conclusion

Hearing loss is one of the most common neurosensorial dysfunctions in human beings. It has been estimated that more than 70 million people suffer from severe hearing disturbances worldwide (Tekin et al., 2001). The incidence of hearing loss increases significantly after 60 years of age. The cochlea plays a key role in converting the mechanical sound energy into electrical potential and sensory inputs. Normal hearing relies on the integrity of cochlear function which is dependent upon the maintenance of a delicate homeostatic environment. The cochlea comprises essentially two components, the organ of Corti and the stria vascularis. The organ of Corti is an organ of high metabolic activity. The processes of high-energy consumption are involved in the activation of ion pump in the stria vascularis to the maintenance of electrochemical gradient between perilymph and endolymph and tuning of the basilar membrane by the outer hair cells (Brass & Kemp, 1993).

The cochlea is an end-artery organ and mainly supplied by the labyrinthine artery, which is a branch of anterior inferior cerebellar artery (Nakashima et al., 2003). Therefore, the cochlea is sensitive to disturbance of blood flow. Perturbations in the inner ear microcirculation have been considered to be one of the factors implicated in the pathophysiology of various kinds of sensorineural hearing loss (Nakashima et al., 2003). Clinical and experimental studies have shown that hearing disorders, including presbycusis (Riva et al., 2005; Riva et al., 2007), noise-induced hearing loss (Lamm & Arnold, 1996; Scheibe et al., 1990), sudden deafness (Yamasoba et al., 1993; Kim et al., 1999), endolymphatic drops (Larsen et al., 1988; Yazawa et al., 1998; Yamamoto et al., 1991) are related to alterations in the blood flow of inner ear.

Most sensorineural deafness is characterized by a loss of hair cells and of spiral ganglion neurons (Lin et al., 2010). Because of the lack of treatment of neurosensory deafness capable of restoring auditory function or altering the course of a progressive

hearing loss, hearing aids are the only satisfactory means available for the hearing impairment at present. The experimental strategies to approach the treatment of neurosensory deafness may include: (1) **OTOPROTECTION**, which is designed to prevent a further degradation of auditory function; (2) **OTOREPAIR**, which is aimed to fix the injured cochlear cells; and (3) **OTOREGENERATION**, which is defined as the replacement of lost hair cells in the deafened ear by way of proliferation and transdifferentiation or and their reconnection by primary auditory neurons to the central auditory pathway (Tabuchi et al., 2010).

Giving the complexity of cell death pathway in cochlear neuropathy, an intervention in the early stages of ischemia (such as the generation of ROS) may be a promising approach to the prevention of ischemia-related hearing loss in clinical setting. Several strategies have been shown to be effective to “PREVENT” the ischemia-reperfusion injury of cochlea such as steroid (Tabuchi et al., 2003; Tabuchi et al., 2006; Otake et al., 2009), nitric oxide synthetase inhibitors (Ruan et al., 2001; Tabuchi et al., 1999; Iadecola et al., 1997; Morizane et al., 2005), glutamate antagonist (Tabuchi et al., 2010), or even stem cells (Yoshida et al., 2007). However, few of these therapies have been shown effective to “TREAT” the ischemia-related hearing loss. Currently, there are very few effective neurotherapeutic interventions for ischemia-related hearing loss. This inadequate effect may be due to the complicated pathological changes encountered with the ischemia-reperfusion in inner ears, which include oxidative damages, mitochondrial dysfunction, necrosis and apoptosis. The actual underlying molecular mechanisms of ischemic cochlear damage have not been fully elucidated, mainly because of the difficulties with the available animal models. Such chronic animal experiments are often unsuccessful because the anatomical access to the labyrinthine artery is extremely difficult. In addition, the longterm post-operative animal care after the intensive surgery is time consuming and requires much experience and patience.

In the past three years, we devoted ourselves to investigate the peculiar inner ear anatomy and blood supply of the cochleae in guinea pigs. We have successfully

developed a reversible animal model of selective cochlear ischemia by temporarily occluding the labyrinthine artery with vascular microclamps. Using this technique, we are able to obtain a long-term observation of cochlear changes after different duration of cochlear ischemia (Lin et al., 2010). Combined with our *in vivo* model, we also have successfully applied an *in vitro* method (Kalinec et al., 2003) to study the interactions of ischemia-reperfusion injuries of cochlear hair cells by virtue of HEI-OC1 cochlear hair cell line (accepted by Laboratory Investigation, 2011). The *in vitro* method is feasible to study the molecular changes and the *in vivo* animal model is more relevant to clinical situation. For translation into clinical practice—our preliminary studies have established reliable *in vivo* and *in vitro* models to elucidate the underlying molecular mechanisms in cochlear ischemia-reperfusion. Our serial studies could also provide another insight into better understanding the complicated interaction between ischemia and other ototoxic events, and their cytotoxic mechanisms. Of utmost importance, these models for reversible cochlear ischemia, which were developed in this thesis, will be a useful platform to identify some novel neurotherapeutic strategies for ischemia-related hearing losses.

In addition, we also have developed novel animal model to investigate the cochlear changes in hyperbaric oxygen status (Lin et al., 2011). Based on these experiences, the effectiveness of some candidate therapeutic strategies for cochlear ischemic neuropathy both *in vitro* and *in vivo* may be tried. The ultimate goal is to verify current therapies for ischemia-related cochlear neuropathies and to identify some novel agents that may be effective for the ischemia-related hearing loss through the comprehensive investigation by the *in vitro* model and our newly developed chronic animal model of cochlear ischemia. The further clarification of these changes in cochlear ischemia will increase our understanding of the complexity of ischemia-related hearing loss and may offer additional therapeutic possibilities for the common hearing disorders related to ischemia such as noise induced hearing loss, sudden deafness or presbycusis.

References

- Alston,T.A., Mela,L., and Bright,H.J. 3-Nitropropionate, the toxic substance of *Indigofera*, is a suicide inactivator of succinate dehydrogenase. *Proc.Natl.Acad.Sci.U.S.A* 1977; 74:3767-3771.
- Andreeva,N., Nyamaa,A., Haupt,H. and others. Recombinant human erythropoietin prevents ischemia-induced apoptosis and necrosis in explant cultures of the rat organ of Corti. *Neurosci.Lett.* 2006; 396:86-90.
- Asai,Y., Umemura,K., and Nakashima,M. Reversibility of compound action potential during the acute phase after transitory local ischemia. *Annals of Otolaryngology and Laryngology* 1996; 105:472-475.
- Aslan,I., Oysu,C., Veyseller,B. and others. Does the addition of hyperbaric oxygen therapy to the conventional treatment modalities influence the outcome of sudden deafness? *Otolaryngol.Head Neck Surg.* 2002; 126:121-126.
- Atochin,D.N., Demchenko,I.T., Astern,J. and others. Contributions of endothelial and neuronal nitric oxide synthases to cerebrovascular responses to hyperoxia. *J.Cereb.Blood Flow Metab* 2003; 23:1219-1226.
- Aust,G. Vestibulotoxicity and ototoxicity of gentamicin in newborns at risk. *Int Tinnitus J.* 2001; 7:27-29.
- Axelsson,A., Nuttall,A.L., and Miller,J.M. Observations of cochlear microcirculation using intravital microscopy. *Acta Otolaryngol.(Stockh)* 1990; 109:263-270.
- Bae,W.Y., Kim,L.S., Hur,D.Y. and others. Secondary apoptosis of spiral ganglion cells induced by aminoglycoside: Fas-Fas ligand signaling pathway. *Laryngoscope* 2008; 118:1659-1668.
- Bates,D.E., Beaumont,S.J., and Baylis,B.W. Ototoxicity induced by gentamicin and furosemide. *Ann.Pharmacother.* 2002; 36:446-451.
- Bernard,P.A. Freedom from ototoxicity in aminoglycoside treated neonates: a mistaken notion. *Laryngoscope* 1981; 91:1985-1994.
- Beuerlein,M., Nelson,R.N., and Welling,D.B. Inner and middle ear hyperbaric oxygen-induced barotrauma. *Laryngoscope* 1997; 107:1350-1356.
- Bhattacharyya,T.K. and Dayal,V.S. Ototoxicity and noise-drug interaction. *J.Otolaryngol* 1984; 13:361-366.
- Bodmer,D., Brors,D., Pak,K. and others. Gentamicin-induced hair cell death is not dependent on the apoptosis receptor Fas. *Laryngoscope* 2003; 113:452-455.
- Boettcher,F.A., Henderson,D., Gratton,M.A. and others. Synergistic interactions of noise and other ototraumatic agents. *Ear Hear.* 1987; 8:192-212.
- Bohme,G. Hearing disorders in peripheral arterial vascular diseases. A contribution on

hearing loss in the aged. *Laryngol.Rhinol.Otol.(Stuttg)* 1987; 66:638-642.

Brass,D. and Kemp,D.T. Analyses of Mossbauer Mechanical Measurements Indicate That the Cochlea Is Mechanically Active. *Journal of the Acoustical Society of America* 1993; 93:1502-1515.

Brechtelsbauer,P.B., Nuttall,A.L., and Miller,J.M. Basal nitric oxide production in regulation of cochlear blood flow. *Hear.Res.* 1994; 77:38-42.

Brummett,R.E. and Morrison,R.B. The incidence of aminoglycoside antibiotic-induced hearing loss. *Arch.Otolaryngol Head Neck Surg.* 1990; 116:406-410.

Bubici,C., Papa,S., Pham,C.G. and others. The NF-kappaB-mediated control of ROS and JNK signaling. *Histol.Histopathol.* 2006; 21:69-80.

Bykhovskaya,Y., Mengesha,E., Wang,D. and others. Human mitochondrial transcription factor B1 as a modifier gene for hearing loss associated with the mitochondrial A1555G mutation. *Mol.Genet.Metab* 2004; 82:27-32.

Byl,F.M., Jr. Sudden hearing loss: eight years' experience and suggested prognostic table. *Laryngoscope* 1984; 94:647-661.

Cabigas,B.P., Su,J.D., Hutchins,W. and others. Hyperoxic and hyperbaric-induced cardioprotection: Role of nitric oxide synthase 3. *Cardiovascular Research* 2006; 72:143-151.

Cakir,B.O., Ercan,I., Civelek,S. and others. Negative effect of immediate hyperbaric oxygen therapy in acute acoustic trauma. *Otol.Neurotol.* 2006; 27:478-483.

Casano,R.A., Johnson,D.F., Bykhovskaya,Y. and others. Inherited susceptibility to aminoglycoside ototoxicity: genetic heterogeneity and clinical implications. *Am.J.Otolaryngol.* 1999; 20:151-156.

Chao,T.K. Sudden sensorineural hearing loss after rapid reduction of blood pressure in malignant hypertension. *Ann.Otol.Rhinol.Laryngol.* 2004; 113:73-75.

Chayasirisobhon,S., Yu,L., Griggs,L. and others. Recording of brainstem evoked potentials and their association with gentamicin in neonates. *Pediatr.Neurol* 1996; 14:277-280.

Chen,J.T., Fong,Y.C., Li,T.M. and others. DDTD, an isoflavone derivative, induces cell apoptosis through the reactive oxygen species/apoptosis signal-regulating kinase 1 pathway in human osteosarcoma cells. *Eur.J.Pharmacol.* 2008; 597:19-26.

Coles,C.J., Edmondson,D.E., and Singer,T.P. Inactivation of succinate dehydrogenase by 3-nitropropionate. *J.Biol.Chem.* 1979; 254:5161-5167.

Contopoulos-Ioannidis,D.G., Giotis,N.D., Baliatsa,D.V. and others. Extended-interval aminoglycoside administration for children: a meta-analysis. *Pediatrics* 2004; 114:e111-e118.

Dai,C.F. and Steyger,P.S. A systemic gentamicin pathway across the stria vascularis. *Hear.Res.* 2008; 235:114-124.

Demchenko,I.T., Atochin,D.N., Boso,A.E. and others. Oxygen seizure latency and peroxynitrite formation in mice lacking neuronal or endothelial nitric oxide synthases. *Neurosci.Lett.* 2003; 344:53-56.

Department of Household Registration, Ministry Of Interior Republic Of China. Population by Sex and 5 Year Age Group for Counties and Cities. <http://www.ris.gov.tw/version96/stpeqr.html> . 2010.

Ref Type: Online Source

Ding,D., Stracher,A., and Salvi,R.J. Leupeptin protects cochlear and vestibular hair cells from gentamicin ototoxicity. *Hear.Res.* 2002; 164:115-126.

Dulon,D., Aurousseau,C., Erre,J.P. and others. Relationship between the nephrotoxicity and ototoxicity induced by gentamicin in the guinea pig. *Acta Otolaryngol.(Stockh)* 1988; 106:219-225.

Ensink,R.J., Camp,G.V., and Cremers,C.W. Mitochondrial inherited hearing loss. *Clin.Otolaryngol Allied Sci.* 1998; 23:3-8.

Estivill,X., Govea,N., Barcelo,E. and others. Familial progressive sensorineural deafness is mainly due to the mtDNA A1555G mutation and is enhanced by treatment of aminoglycosides. *Am.J.Hum.Genet.* 1998; 62:27-35.

Fessenden,J.D. and Schacht,J. Localization of soluble guanylate cyclase activity in the guinea pig cochlea suggests involvement in regulation of blood flow and supporting cell physiology. *J.Histochem.Cytochem.* 1997; 45:1401-1408.

Fischel-Ghodsian,N. Genetic factors in aminoglycoside toxicity. *Ann.N.Y.Acad.Sci.* 1999a; 884:99-109.

Fischel-Ghodsian,N. Mitochondrial deafness mutations reviewed. *Hum.Mutat.* 1999b; 13:261-270.

Fischel-Ghodsian,N. Mitochondrial deafness. *Ear Hear.* 2003; 24:303-313.

Forge,A. and Li,L. Apoptotic death of hair cells in mammalian vestibular sensory epithelia. *Hear.Res.* 2000; 139:97-115.

Forge,A. and Schacht,J. Aminoglycoside antibiotics. *Audiology and Neuro-Otology* 2000; 5:3-22.

Franz,P., Hauser-Kronberger,C., Bock,P. and others. Localization of nitric oxide synthase I and III in the cochlea. *Acta Otolaryngol.(Stockh)* 1996; 116:726-731.

Fujimura,T., Suzuki,H., Shiomori,T. and others. Hyperbaric oxygen and steroid therapy for idiopathic sudden sensorineural hearing loss. *Eur.Arch.Otorhinolaryngol.* 2007; 264:861-866.

Fujita,K., Hakuba,N., Hata,R. and others. Ginsenoside Rb1 protects against damage to the spiral ganglion cells after cochlear ischemia. *Neurosci.Lett.* 2007; 415:113-117.

Gosepath,K., Gath,I., Maurer,J. and others. Characterization of nitric oxide synthase isoforms expressed in different structures of the guinea pig cochlea. *Brain Res* 1997;

747:26-33.

Guan,M.X. Molecular pathogenetic mechanism of maternally inherited deafness. *Ann.N.Y.Acad.Sci.* 2004a; 1011:259-271.

Guan,M.X., Fischel-Ghodsian,N., and Attardi,G. Biochemical evidence for nuclear gene involvement in phenotype of non-syndromic deafness associated with mitochondrial 12S rRNA mutation. *Hum.Mol.Genet.* 1996; 5:963-971.

Guan,M.X., Fischel-Ghodsian,N., and Attardi,G. A biochemical basis for the inherited susceptibility to aminoglycoside ototoxicity. *Hum.Mol.Genet.* 2000; 9:1787-1793.

Guan,M.X. Molecular pathogenetic mechanism of maternally inherited deafness. *Ann.N.Y.Acad.Sci.* 2004b; 1011:259-271.

Guan,M.X., Yan,Q., Li,X. and others. Mutation in TRMU related to transfer RNA modification modulates the phenotypic expression of the deafness-associated mitochondrial 12S ribosomal RNA mutations. *Am.J.Hum.Genet.* 2006; 79:291-302.

Gupta,R., Kim,J.Y., Espinal,M.A. and others. Public health. Responding to market failures in tuberculosis control. *Science* 2001; 293:1049-1051.

Guthrie,O.W. Aminoglycoside induced ototoxicity. *Toxicology* 2008; 249:91-96.

Hakuba,N., Hata,R., Morizane,I. and others. Neural stem cells suppress the hearing threshold shift caused by cochlear ischemia. *Neuroreport* 2005; 16:1545-1549.

Hakuba,N., Matsubara,A., Hyodo,J. and others. AMPA/kainate-type glutamate receptor antagonist reduces progressive inner hair cell loss after transient cochlear ischemia. *Brain Res* 2003a; 979:194-202.

Hakuba,N., Watabe,K., Hyodo,J. and others. Adenovirus-mediated overexpression of a gene prevents hearing loss and progressive inner hair cell loss after transient cochlear ischemia in gerbils. *Gene Ther.* 2003b; 10:426-433.

Hashino,E. and Shero,M. Endocytosis of aminoglycoside antibiotics in sensory hair cells. *Brain Res* 1995; 704:135-140.

Hata,R., Matsumoto,M., Hatakeyama,T. and others. Differential Vulnerability in the Hindbrain Neurons and Local Cerebral Blood-Flow During Bilateral Vertebral Occlusion in Gerbils. *Neuroscience* 1993; 56:423-439.

Hayashida,T., Nomura,Y., Iwamori,M. and others. Distribution of gentamicin by immunofluorescence in the guinea pig inner ear. *Arch.Otorhinolaryngol.* 1985; 242:257-264.

Heinrich,U.R., Selivanova,O., Brieger,J. and others. Endothelial nitric oxide synthase upregulation in the cochlea of the guinea pig after intratympanic gentamicin injection. *Eur.Arch.Otorhinolaryngol.* 2006; 263:62-68.

Helms,A.K., Whelan,H.T., and Torbey,M.T. Hyperbaric oxygen therapy of cerebral ischemia. *Cerebrovascular Diseases* 2005; 20:417-426.

Henderson,D., Bielefeld,E.C., Harris,K.C. and others. The role of oxidative stress in

noise-induced hearing loss. *Ear Hear.* 2006; 27:1-19.

Higashi,K. Unique inheritance of streptomycin-induced deafness. *Clin.Genet.* 1989; 35:433-436.

Hirose,K., Westrum,L.E., Stone,J.S. and others. Dynamic studies of ototoxicity in mature avian auditory epithelium. *Ann.N.Y.Acad.Sci.* 1999; 884:389-409.

Hong,S.H., Park,S.K., Cho,Y.S. and others. Gentamicin induced nitric oxide-related oxidative damages on vestibular afferents in the guinea pig. *Hear.Res.* 2006; 211:46-53.

Hoya,N., Okamoto,Y., Kamiya,K. and others. A novel animal model of acute cochlear mitochondrial dysfunction. *Neuroreport* 2004; 15:1597-1600.

Hu,D.N., Qui,W.Q., Wu,B.T. and others. Genetic aspects of antibiotic induced deafness: mitochondrial inheritance. *J.Med.Genet.* 1991a; 28:79-83.

Hu,Z.Y., Shi,X.F., Liang,Z.F. and others. The protective effect of hyperbaric oxygen on hearing during chronic noise exposure. *Aviat.Space Environ.Med* 1991b; 62:403-406.

Hutchin,T., Haworth,I., Higashi,K. and others. A molecular basis for human hypersensitivity to aminoglycoside antibiotics. *Nucleic Acids Res.* 1993; 21:4174-4179.

Iadecola,C., Zhang,F.Y., Casey,R. and others. Delayed reduction of ischemic brain injury and neurological deficits in mice lacking the inducible nitric oxide synthase gene. *J.Neurosci.* 1997; 17:9157-9164.

Jahnke,K. The blood-perilymph barrier. *Arch.Otorhinolaryngol.* 1980; 228:29-34.

Jiang,H., Sha,S.H., Forge,A. and others. Caspase-independent pathways of hair cell death induced by kanamycin in vivo. *Cell Death and Differentiation* 2006; 13:20-30.

Jiang,H., Sha,S.H., and Schacht,J. NF-kappaB pathway protects cochlear hair cells from aminoglycoside-induced ototoxicity. *J.Neurosci.Res.* 2005; 79:644-651.

Jin,X., Jin,X., and Sheng,X. Methylcobalamin as antagonist to transient ototoxic action of gentamicin. *Acta Otolaryngol.(Stockh)* 2001; 121:351-354.

Johnson,R.F., Cohen,A.P., Guo,Y. and others. Genetic mutations and aminoglycoside-induced ototoxicity in neonates. *Otolaryngol.Head Neck Surg.* 2010; 142:704-707.

Kalinec,G.M., Webster,P., Lim,D.J. and others. A cochlear cell line as an in vitro system for drug ototoxicity screening. *Audiol.Neurootol.* 2003; 8:177-189.

Kalkandelen,S., Selimoglu,E., Erdogan,F. and others. Comparative cochlear toxicities of streptomycin, gentamicin, amikacin and netilmicin in guinea-pigs. *J.Int.Med.Res.* 2002; 30:406-412.

Kastenbauer,S., Klein,M., Koedel,U. and others. Reactive nitrogen species contribute to blood-labyrinth barrier disruption in suppurative labyrinthitis complicating experimental pneumococcal meningitis in the rat. *Brain Res* 2001; 904:208-217.

Kim,D.Y., Won,S.J., and Gwag,B.J. Analysis of mitochondrial free radical generation in animal models of neuronal disease. *Free Radic.Biol.Med.* 2002; 33:715-723.

Kim,G.W., Gasche,Y., Grzeschik,S. and others. Neurodegeneration in striatum induced by the mitochondrial toxin 3-nitropropionic acid: role of matrix metalloproteinase-9 in early blood-brain barrier disruption? *J.Neurosci.* 2003; 23:8733-8742.

Kim,J.S., Lopez,I., DiPatre,P.L. and others. Internal auditory artery infarction - Clinicopathologic correlation. *Neurology* 1999; 52:40-44.

Kim,S.J., Jeong,H.J., Myung,N.Y. and others. The protective mechanism of antioxidants in cadmium-induced ototoxicity in vitro and in vivo. *Environ.Health Perspect.* 2008; 116:854-862.

Kimura,R. and Perlman,H.B. Arterial obstruction of the labyrinth. I. Cochlear changes. *Ann.Otol.Rhinol.Laryngol.* 1958; 67:5-24.

Klingmann,C., Praetorius,M., Baumann,I. and others. Barotrauma and decompression illness of the inner ear: 46 cases during treatment and follow-up. *Otol.Neurol.* 2007; 28:447-454.

Kohonen,A. and Tarkkanen,J.V. Dihydrostreptomycin and kanamycin ototoxicity. An experimental study by surface preparation technique. *Laryngoscope* 1966; 76:1671-1680.

Kouzaki,H., Suzuki,M., and Shimizu,T. Immunohistochemical and ultrastructural abnormalities in muscle from a patient with sensorineural hearing loss related to a 1555 A-to-G mitochondrial mutation. *J.Clin.Neurosci.* 2007; 14:603-607.

Kovacic,P. and Somanathan,R. Ototoxicity and noise trauma: electron transfer, reactive oxygen species, cell signaling, electrical effects, and protection by antioxidants: practical medical aspects. *Med.Hypotheses* 2008; 70:914-923.

Kuokkanen,J., Virkkala,J., Zhai,S. and others. Effect of hyperbaric oxygen treatment on permanent threshold shift in acoustic trauma among rats. *Acta Otolaryngol.Suppl (Stockh)* 1997; 529:80-82.

Kusakari,J., Kambayashi,J., Kobayashi,T. and others. The effect of transient anoxia upon the cochlear potentials. *Auris Nasus Larynx* 1981; 8:55-64.

Lai,C.H., Fang,S.H., Rao,Y.K. and others. Inhibition of Helicobacter pylori-induced inflammation in human gastric epithelial AGS cells by Phyllanthus urinaria extracts. *J.Ethnopharmacol.* 2008; 118:522-526.

Lamm,K. and Arnold,W. Noise-induced cochlear hypoxia is intensity dependent, correlates with hearing loss and precedes reduction of cochlear blood flow. *Audiol Neurootol* 1996; 1:148-160.

Lamm,K., Lamm,C., and Arnold,W. Effect of isobaric oxygen versus hyperbaric oxygen on the normal and noise-damaged hypoxic and ischemic guinea pig inner ear. *Adv.Otorhinolaryngol.* 1998; 54:59-85.

Larsen,H.C., Albers,F., Jansson,B. and others. Cochlear Blood-Flow in Endolymphatic Hydrops. *Acta Otolaryngol.(Stockh)* 1988; 106:404-408.

Laurell,G., Viberg,A., Teixeira,M. and others. Blood-perilymph barrier and ototoxicity:

an in vivo study in the rat. *Acta Otolaryngol.(Stockh)* 2000; 120:796-803.

Leake,P.A. and Hradek,G.T. Cochlear pathology of long term neomycin induced deafness in cats. *Hear.Res.* 1988; 33:11-33.

Legatt,A.D. Mechanisms of intraoperative brainstem auditory evoked potential changes. *J.Clin.Neurophysiol.* 2002; 19:396-408.

Lesniak,W., Pecoraro,V.L., and Schacht,J. Ternary complexes of gentamicin with iron and lipid catalyze formation of reactive oxygen species. *Chem.Res Toxicol.* 2005; 18:357-364.

Levendag,P.C., Kuijpers,W., Eggermont,J.J. and others. The inner ear and hyperbaric conditions. An electrophysiological and morphological study. *Acta Otolaryngol Suppl* 1981; 382:1-110.

Li,H. and Steyger,P.S. Synergistic ototoxicity due to noise exposure and aminoglycoside antibiotics. *Noise Health* 2009; 11:26-32.

Lin,C.D., Wei,I.H., Lai,C.H. and others. Hyperbaric oxygen upregulates cochlear constitutive nitric oxide synthase. *Bmc Neuroscience* 2011; 12.

Lin,C.D., Wei,I.H., Tsai,M.H. and others. Changes in guinea pig cochlea after transient cochlear ischemia. *Neuroreport* 2010; 21:968-975.

Lin,C.D., Oshima,T., Oda,K. and others. Ototoxic interaction of kanamycin and 3-nitropropionic acid. *Acta Otolaryngol.(Stockh)* 2008; 128:1280-1285.

Lin,H.C., Shu,M.T., Chang,K.C. and others. A universal newborn hearing screening program in Taiwan. *International Journal of Pediatric Otorhinolaryngology* 2002; 63:209-218.

Lindberg,P.E., Parell,G.J., Gajewski,B.J. and others. Hyperbaric compression in the guinea pig with perilymph fistula. *Otolaryngology-Head and Neck Surgery* 2003; 129:259-264.

Lindh,C., Wennersten,A., Arnberg,F. and others. Differences in cell death between high and low energy brain injury in adult rats. *Acta Neurochir.(Wien.)* 2008; 150:1269-1275.

Lindsay,J.R. and Hinojosa,R. Histopathologic features of the inner ear associated with Kearns-Sayre syndrome. *Arch.Otolaryngol.* 1976; 102:747-752.

Liu,J.F., Yang,W.H., Fong,Y.C. and others. BFPP, a phloroglucinol derivative, induces cell apoptosis in human chondrosarcoma cells through endoplasmic reticulum stress. *Biochem.Pharmacol.* 2010; 79:1410-1417.

Liu,W.W., Li,J.S., Sun,X.J. and others. Repetitive hyperbaric oxygen exposures enhance sensitivity to convulsion by upregulation of eNOS and nNOS. *Brain Res* 2008; 1201:128-134.

Maetani,T., Hyodo,J., Takeda,S. and others. Prednisolone prevents transient ischemia-induced cochlear damage in gerbils. *Acta Otolaryngol.(Stockh)* 2009; 129:24-27.

Maetani,T., Hakuba,N., Taniguchi,M. and others. Free radical scavenger protects against inner hair cell loss after cochlear ischemia. *Neuroreport* 2003; 14:1881-1884.

Marcotti,W., van Netten,S.M., and Kros,C.J. The aminoglycoside antibiotic dihydrostreptomycin rapidly enters mouse outer hair cells through the mechano-electrical transducer channels. *J.Physiol (Lond)* 2005; 567:505-521.

Matsui,J.I., Ogilvie,J.M., and Warchol,M.E. Inhibition of caspases prevents ototoxic and ongoing hair cell death. *J.Neurosci.* 2002; 22:1218-1227.

Matsunaga,T., Kumanomido,H., Shiroma,M. and others. Deafness due to A1555G mitochondrial mutation without use of aminoglycoside. *Laryngoscope* 2004; 114:1085-1091.

Mazurek,B., Haupt,H., Georgiewa,P. and others. A model of peripherally developing hearing loss and tinnitus based on the role of hypoxia and ischemia. *Med.Hypotheses* 2006; 67:892-899.

Mazurek,B., Stover,T., Haupt,H. and others. Pathogenesis and treatment of presbycusis. *Hno* 2008; 56:429-+.

McDowell,B. Patterns of cochlear degeneration following gentamicin administration in both old and young guinea pigs. *Br.J.Audiol.* 1982; 16:123-129.

Mendel,L.L., Knafelc,M.E., and Cudahy,E.A. Hearing function in a hyperbaric environment. *Undersea & Hyperbaric Medicine* 2000; 27:91-105.

Meyers,R.M. Ototoxic effects of gentamicin. *Arch.Otolaryngol.* 1970; 92:160-162.

Miller,H.E. Cochlear Potentials at 11 Atmospheres. *Laryngoscope* 1971; 81:979-988.

Mizukoshi,O. and Daly,J.F. Oxygen consumption in normal and kanamycin damaged cochleae. *Acta Otolaryngol.* 1967; 64:45-54.

Mom,T., Avan,P., Romand,R. and others. Monitoring of functional changes after transient ischemia in gerbil cochlea. *Brain Res* 1997; 751:20-30.

Morawski,K., Telischi,F.F., and Niemczyk,K. A model of real time monitoring of the cochlear function during an induced local ischemia. *Hear.Res.* 2006; 212:117-127.

Morizane,I., Hakuba,N., Hyodo,J. and others. Ischemic damage increases nitric oxide production via inducible nitric oxide synthase in the cochlea. *Neurosci.Lett.* 2005; 391:62-67.

Murata,K., Takeda,T., and Iwai,H. Cochlear Microphonics in Oxygen at High-Pressure. *Arch.Otorhinolaryngol.* 1974; 208:77-88.

Myrdal,S.E., Johnson,K.C., and Steyger,P.S. Cytoplasmic and intra-nuclear binding of gentamicin does not require endocytosis. *Hear.Res.* 2005; 204:156-169.

Nagahara,K., Fisch,U., and Yagi,N. Perilymph oxygenation in sudden and progressive sensorineural hearing loss. *Acta Otolaryngol.(Stockh)* 1983; 96:57-68.

Nakashima,T., Fukuta,S., and Yanagita,N. Hyperbaric oxygen therapy for sudden deafness. *Adv.Otorhinolaryngol.* 1998; 54:100-109.

Nakashima,T., Naganawa,S., Sone,M. and others. Disorders of cochlear blood flow. *Brain Research Reviews* 2003; 43:17-28.

Nishino,H., Kumazaki,M., Fukuda,A. and others. Acute 3-nitropropionic acid intoxication induces striatal astrocytic cell death and dysfunction of the blood-brain barrier: involvement of dopamine toxicity. *Neurosci.Res.* 1997; 27:343-355.

Okamoto,Y., Hoya,N., Kamiya,K. and others. Permanent threshold shift caused by acute cochlear mitochondrial dysfunction is primarily mediated by degeneration of the lateral wall of the cochlea. *Audiol.Neurotol.* 2005; 10:220-233.

Olszewski,J., Chudzik,W., Milonski,J. and others. Qualitative and quantitative studies in electron microscopy on influence of experimental ischemia of the vertebral arteries on the outer hair cells function in guinea pigs. *Acta Otorhinolaryngol.Belg.* 2003; 57:151-154.

Otake,H., Yamamoto,H., Teranishi,M. and others. Cochlear blood flow during occlusion and reperfusion of the anterior inferior cerebellar artery - effect of topical application of dexamethasone to the round window. *Acta Otolaryngol.(Stockh)* 2009; 129:127-131.

Perlman,H.B., Kimura,R., and Fernandez,C. Experiments on temporary obstruction of the internal auditory artery. *Laryngoscope* 1959; 69:591-613.

Picciotti,P.M., Agostino,S.E., Di,N.W. and others. Scanning electron microscopy of cochlea in new-born rats exposed to hyperbaric oxygen: preliminary report. *Acta Otorhinolaryngol.Ital.* 2005; 25:267-270.

Pirodda,A., Saggese,D., Giausa,G. and others. Can hypotension episodes cause cochlear damage in young subjects? *Med.Hypotheses* 1997; 48:195-196.

Pirvola,U., Xing-Qun,L., Virkkala,J. and others. Rescue of hearing, auditory hair cells, and neurons by CEP-1347/KT7515, an inhibitor of c-Jun N-terminal kinase activation. *J.Neurosci.* 2000; 20:43-50.

Prezant,T.R., Agopian,J.V., Bohlman,M.C. and others. Mitochondrial ribosomal RNA mutation associated with both antibiotic-induced and non-syndromic deafness. *Nat.Genet.* 1993; 4:289-294.

Priuska,E.M. and Schacht,J. Formation of free radicals by gentamicin and iron and evidence for an iron/gentamicin complex. *Biochem.Pharmacol.* 1995; 50:1749-1752.

Qian,Y. and Guan,M.X. Interaction of aminoglycosides with human mitochondrial 12S rRNA carrying the deafness-associated mutation. *Antimicrob.Agents Chemother.* 2009; 53:4612-4618.

Randolf,H.B., Haupt,H., and Scheibe,F. Cochlear blood flow following temporary occlusion of the cerebellar arteries. *Eur.Arch.Otorhinolaryngol.* 1990; 247:226-228.

Raphael,Y. and Altschuler,R.A. Reorganization of cytoskeletal and junctional proteins during cochlear hair cell degeneration. *Cell Motil.Cytoskeleton* 1991; 18:215-227.

Ren,T., Nuttall,A.L., and Miller,J.M. Contribution of the anterior inferior cerebellar artery to cochlear blood flow in guinea pig: a model-based analysis. *Hear.Res.* 1993;

71:91-97.

Ren,T.Y., Brown,N.J., Zhang,M.S. and others. A reversible ischemia model in gerbil cochlea. *Hear.Res.* 1995; 92:30-37.

Riva,C., Donadieu,E., Magnan,J. and others. Age-related hearing loss in CD/1 mice is associated to ROS formation and HIF target proteins up-regulation in the cochlea. *Experimental Gerontology* 2007; 42:327-336.

Riva,C., Longuet,M., Lucciano,M. and others. [Implication of mitochondrial apoptosis in neural degeneration of cochlea in a murine model for presbycusis]. *Rev Laryngol Otol Rhinol (Bord)* 2005; 126:67-74.

Ruan,R.S. Possible roles of nitric oxide in the physiology and pathophysiology of the mammalian cochlea. *Ann.N.Y.Acad.Sci.* 2002; 962:260-274.

Ruan,R.S., Leong,S.K., and Yeoh,K.H. Effects of nitric oxide on normal and ischemic cochlea of the guinea pig. *Experimental Neurology* 2001; 169:200-207.

Rusyniak,D.E., Kirk,M.A., May,J.D. and others. Hyperbaric oxygen therapy in acute ischemic stroke: results of the Hyperbaric Oxygen in Acute Ischemic Stroke Trial Pilot Study. *Stroke* 2003; 34:571-574.

Rybak,L.P. and Kelly,T. Ototoxicity: bioprotective mechanisms. *CURR.* 2003; 11:328-333.

Salamy,A., Eldredge,L., and Tooley,W.H. Neonatal status and hearing loss in high-risk infants. *J.Pediatr.* 1989; 114:847-852.

Salt,A.N. and Ma,Y. Quantification of solute entry into cochlear perilymph through the round window membrane. *Hear.Res.* 2001; 154:88-97.

Santorelli,F.M., Tanji,K., Manta,P. and others. Maternally inherited cardiomyopathy: an atypical presentation of the mtDNA 12S rRNA gene A1555G mutation. *Am.J.Hum.Genet.* 1999; 64:295-300.

Schatz,A., Bugie,E., and Waksman,S.A. Streptomycin, a substance exhibiting antibiotic activity against gram-positive and gram-negative bacteria. 1944. *Clin.Orthop.* 2005;3-6.

Scheibe,F., Haupt,H., and Grunert,H. Laser Doppler measurements of inner ear blood flow during experimental thrombosis of cochlear blood vessels in the guinea pig. *Eur.Arch.Otorhinolaryngol.* 1997; 254:86-90.

Scheibe,F., Haupt,H., Nuttall,A.L. and others. Laser Doppler Measurements of Cochlear Blood-Flow During Loud Sound Presentation. *Eur.Arch.Otorhinolaryngol.* 1990; 247:84-88.

Scheibe,F., Haupt,H., and Vlastos,G.A. Preventive magnesium supplement reduces ischemia-induced hearing loss and blood viscosity in the guinea pig. *Eur.Arch.Otorhinolaryngol.* 2000; 257:355-361.

Schrijver,I. Hereditary non-syndromic sensorineural hearing loss: transforming silence to sound. *J.Mol.Diagn.* 2004; 6:275-284.

Schweinfurth, J.M. and Cacace, A.T. Cochlear ischemia induced by circulating iron particles under magnetic control: An animal model for sudden hearing loss. *American Journal of Otology* 2000; 21:636-640.

Seidman, M.D., Ahmad, N., Joshi, D. and others. Age-related hearing loss and its association with reactive oxygen species and mitochondrial DNA damage. *Acta Otolaryngol.(Stockh)* 2004; 124:16-24.

Seidman, M.D. and Quirk, W.S. The Protective Effects of Tirilated Mesylate (U74006F) on Ischemic and Reperfusion-Induced Cochlear Damage. *Otolaryngology-Head and Neck Surgery* 1991; 105:511-516.

Seidman, M.D., Quirk, W.S., Nuttall, A.L. and others. The Protective Effects of Allopurinol and Superoxide Dismutase-Polyethylene Glycol on Ischemic and Reperfusion-Induced Cochlear Damage. *Otolaryngology-Head and Neck Surgery* 1991; 105:457-463.

Seidman, M.D., Ahmad, N., and Bai, U. Molecular mechanisms of age-related hearing loss. *Ageing Res.Rev.* 2002; 1:331-343.

Sha, S.H. and Schacht, J. Formation of reactive oxygen species following bioactivation of gentamicin. *Free Radic.Biol.Med.* 1999; 26:341-347.

Sha, S.H., Taylor, R., Forge, A. and others. Differential vulnerability of basal and apical hair cells is based on intrinsic susceptibility to free radicals. *Hear.Res.* 2001; 155:1-8.

Sheppard, W.M., Wanamaker, H.H., Pack, A. and others. Direct round window application of gentamicin with varying delivery vehicles: a comparison of ototoxicity. *Otolaryngol.Head Neck Surg.* 2004; 131:890-896.

Shi, X. and Nuttall, A.L. Upregulated iNOS and oxidative damage to the cochlear stria vascularis due to noise stress. *Brain Res* 2003; 967:1-10.

Shi, X. and Nuttall, A.L. The demonstration of nitric oxide in cochlear blood vessels in vivo and in vitro: the role of endothelial nitric oxide in venular permeability. *Hear.Res.* 2002; 172:73-80.

Short, S.O., Goodwin, P.C., Kaplan, J.N. and others. Measuring Cochlear Blood-Flow by Laser Doppler Spectroscopy. *Otolaryngology-Head and Neck Surgery* 1985; 93:786-793.

Spatz, M. Past and recent BBB studies with particular emphasis on changes in ischemic brain edema. *Acta Neurochir.Suppl* 2010; 106:21-27.

Steinbach, S. and Lutz, J. Glutamate induces apoptosis in cultured spiral ganglion explants. *Biochem.Biophys.Res Commun.* 2007; 357:14-19.

Suzuki, M., Ushio, M., and Yamasoba, T. Time course of apoptotic cell death in guinea pig cochlea following intratympanic gentamicin application. *Acta Otolaryngol.(Stockh)* 2008; 128:724-731.

Suzuki, M., Yagi, M., Brown, J.N. and others. Effect of transgenic GDNF expression on gentamicin-induced cochlear and vestibular toxicity. *Gene Ther.* 2000; 7:1046-1054.

Tabuchi,K., Ito,Z., Tsuji,S. and others. The contribution of phospholipase A2 to the cochlear dysfunction induced by transient ischemia. *Hear.Res.* 2000; 144:1-7.

Tabuchi,K., Ito,Z., Wada,T. and others. The effect of mannitol upon cochlear dysfunction induced by transient local anoxia. *Hear.Res.* 1998; 126:28-36.

Tabuchi,K., Kusakari,J., Ito,Z. and others. Effect of nitric oxide synthase inhibitor on cochlear dysfunction induced by transient local anoxia. *Acta Otolaryngol.(Stockh)* 1999; 119:179-184.

Tabuchi,K., Nishimura,B., Tanaka,S. and others. Ischemia-Reperfusion Injury of the Cochlea: Pharmacological Strategies for Cochlear Protection and Implications of Glutamate and Reactive Oxygen Species. *Current Neuropharmacology* 2010; 8:128-134.

Tabuchi,K., Oikawa,K., Uemaetomari,I. and others. Glucocorticoids and dehydroepiandrosterone sulfate ameliorate ischemia-induced injury of the cochlea. *Hear.Res.* 2003; 180:51-56.

Tabuchi,K., Okubo,H., Fujihira,K. and others. Protection of outer hair cells from reperfusion injury by an iron chelator and a nitric oxide synthase inhibitor in the guinea pig cochlea. *Neurosci.Lett.* 2001; 307:29-32.

Tabuchi,K., Oikawa,K., Murashita,H. and others. Protective effects of glucocorticoids on ischemia-reperfusion injury of outer hair cells. *Laryngoscope* 2006; 116:627-629.

Tabuchi,K., Tsuji,S., Fujihira,K. and others. Outer hair cells functionally and structurally deteriorate during reperfusion. *Hear.Res.* 2002; 173:153-163.

Takahashi,K., Merchant,S.N., Miyazawa,T. and others. Temporal bone histopathological and quantitative analysis of mitochondrial DNA in MELAS. *Laryngoscope* 2003; 113:1362-1368.

Takumida,M. and Anniko,M. Nitric oxide in guinea pig vestibular sensory cells following gentamicin exposure in vitro. *Acta Otolaryngol.(Stockh)* 2001; 121:346-350.

Takumida,M., Anniko,M., Ropa,P. and others. Lipopolysaccharide-induced expression of inducible nitric oxide synthase in the guinea pig organ of Corti. *Hear.Res.* 2000; 140:91-98.

Teed,R.W. Factors producing obstruction of the auditory tube in submarine personnel. *US Naval Med Bull* 1944; 42:293-306.

Tekin,M., Arnos,K.S., and Pandya,A. Advances in hereditary deafness. *Lancet* 2001; 358:1082-1090.

Thalman,R., Miyoshi,T., and Thalman,I. The influence of ischemia upon the energy reserves of inner ear tissues. *Laryngoscope* 1972; 82:2249-2272.

Thom,S.R. Oxidative stress is fundamental to hyperbaric oxygen therapy. *J.Appl.Physiol* 2009; 106:988-995.

Thorne,P.R. and Nuttall,A.L. Laser Doppler measurements of cochlear blood flow during loud sound exposure in the guinea pig. *Hear.Res.* 1987; 27:1-10.

Tran Ba Huy,P., Manuel,C., Meulemans,A. and others. Ethacrynic acid facilitates gentamicin entry into endolymph of the rat. *Hear.Res.* 1983; 11:191-202.

Tsai,M.H., Wei,I.H., Jiang-Shieh,Y.F. and others. Expression of protein gene product 9.5, tyrosine hydroxylase and serotonin in the pineal gland of rats with streptozotocin-induced diabetes. *Neurosci.Res.* 2008; 60:233-243.

Tsuji,S., Tabuchi,K., Hara,A. and others. Long-term observations on the reversibility of cochlear dysfunction after transient ischemia. *Hear.Res.* 2002; 166:72-81.

Turnidge,J. Pharmacodynamics and dosing of aminoglycosides. *Infect.Dis.Clin.North Am.* 2003; 17:503-528.

Usami,S., Abe,S., Akita,J. and others. Prevalence of mitochondrial gene mutations among hearing impaired patients. *J.Med.Genet.* 2000; 37:38-40.

Usami,S., Hjelle,O.P., and Ottersen,O.P. Differential cellular distribution of glutathione--an endogenous antioxidant--in the guinea pig inner ear. *Brain Res* 1996; 743:337-340.

Walker,P.D., Barri,Y., and Shah,S.V. Oxidant mechanisms in gentamicin nephrotoxicity. *Ren Fail.* 1999; 21:433-442.

Wang,Q. and Steyger,P.S. Trafficking of systemic fluorescent gentamicin into the cochlea and hair cells. *J.Assoc.Res Otolaryngol* 2009; 10:205-219.

Webster,M. and Webster,D.B. Spiral ganglion neuron loss following organ of Corti loss: a quantitative study. *Brain Res* 1981; 212:17-30.

Wei,I.H., Huang,C.C., Chang,H.M. and others. Neuronal NADPH-d/NOS expression in the nodose ganglion of severe hypoxic rats with or without mild hypoxic preconditioning. *J.Chem.Neuroanat.* 2005; 29:149-156.

Wilkins,S.A., Jr., Mattox,D.E., and Lyles,A. Evaluation of a "shotgun" regimen for sudden hearing loss. *Otolaryngol.Head Neck Surg.* 1987; 97:474-480.

Willems,P.J. Genetic causes of hearing loss. *N.Engl.J.Med.* 2000; 342:1101-1109.

Wu,W.J., Sha,S.H., McLaren,J.D. and others. Aminoglycoside ototoxicity in adult CBA, C57BL and BALB mice and the Sprague-Dawley rat. *Hear.Res.* 2001; 158:165-178.

Yamamoto,K., Kubo,T., and Matsunaga,T. Autoregulation of Inner-Ear Blood-Flow in Normal and Hydropic Guinea-Pigs. *Acta Otolaryngol.(Stockh)* 1991; 111:312-318.

Yamane,H., Takayama,M., Sunami,K. and others. Nitric oxide induces apoptosis of the hair cells of cochlea. *Acta Otolaryngol.Suppl (Stockh)* 2004;6-11.

Yamasoba,T., Goto,Y., Komaki,H. and others. Cochlear damage due to germanium-induced mitochondrial dysfunction in guinea pigs. *Neurosci.Lett.* 2006; 395:18-22.

Yamasoba,T., Kikuchi,S., Higo,R. and others. Sudden Sensorineural Hearing-Loss Associated with Slow Blood-Flow of the Vertebrobasilar System. *Annals of Otolology Rhinology and Laryngology* 1993; 102:873-877.

- Yamasoba,T., Tsukuda,K., Oka,Y. and others. Cochlear histopathology associated with mitochondrial transfer RNA(Leu(UUR)) gene mutation. *Neurology* 1999; 52:1705-1707.
- Yan,Q., Bykhovskaya,Y., Li,R. and others. Human TRMU encoding the mitochondrial 5-methylaminomethyl-2-thiouridylate-methyltransferase is a putative nuclear modifier gene for the phenotypic expression of the deafness-associated 12S rRNA mutations. *Biochem.Biophys.Res Commun.* 2006; 342:1130-1136.
- Yazawa,Y., Kitano,H., Suzuki,M. and others. Studies of cochlear blood flow in guinea pigs with endolymphatic hydrops. *Orl-Journal for Oto-Rhino-Laryngology and Its Related Specialties* 1998; 60:4-11.
- Ylikoski,J., Mrena,R., Makitie,A. and others. Hyperbaric oxygen therapy seems to enhance recovery from acute acoustic trauma. *Acta Otolaryngol.(Stockh)* 2008; 128:1110-1115.
- Ylikoski,J., Xing-Qun,L., Virkkala,J. and others. Blockade of c-Jun N-terminal kinase pathway attenuates gentamicin-induced cochlear and vestibular hair cell death. *Hear.Res.* 2002; 166:33-43.
- Yoshida,T., Hakuba,N., Morizane,I. and others. Hematopoietic stem cells prevent hair cell death after transient cochlear ischemia through paracrine effects. *Neuroscience* 2007; 145:923-930.
- Zdanski,C.J., Prazma,J., Petrusz,P. and others. Nitric oxide synthase is an active enzyme in the spiral ganglion cells of the rat cochlea. *Hear.Res.* 1994; 79:39-47.
- Zhang,X. and Wang,J. Effects of microcirculatory disorders of inner ear on blood-labyrinth barrier permeability in guinea pigs. *Chinese Journal of Otorhinolaryngology* 2000; 35:339-341.
- Zhao,H., Li,R., Wang,Q. and others. Maternally inherited aminoglycoside-induced and nonsyndromic deafness is associated with the novel C1494T mutation in the mitochondrial 12S rRNA gene in a large Chinese family. *Am.J.Hum.Genet.* 2004; 74:139-152.
- Zheng,X.Y. and Gong,J.H. Cochlear Degeneration in Guinea-Pigs After Repeated Hyperbaric Exposures. *Aviation Space and Environmental Medicine* 1992; 63:360-363.

Appendix

動物實驗申請表暨同意書



中國醫藥大學動物實驗管理小組審查同意書

Affidavit of Approval of Animal Use Protocol
China Medical University

動物實驗申請表暨同意書：96-95-N

計畫申請人：林嘉德 職稱：主治醫師
單位：中國醫藥大學附設醫院耳鼻喉部 飼養/應用地點：本校動物中心 / 附醫耳鼻喉部聽性腦幹反應檢查室與平衡檢查室
計畫名稱：role of oxidative stress in aminoglycoside ototoxicity

本計畫之「動物實驗計畫書」業經動物實驗管理小組 實質 形式
審查通過。本計畫預定飼養應用之動物如下：

動物種類	動物數量	飼養及應用期間
Hartley strain guinea pig	200 隻(總數)	96 年 7 月 1 日至 97 年 6 月 30 日

The animal use protocol listed below has been reviewed and approved by
the Institutional Animal Care and Use Committee (IACUC)

Protocol Title : role of oxidative stress in aminoglycoside ototoxicity
Protocol No : 96-95-N
Period of Protocol : Valid From : _____ To : _____ (mm/dd/yyyy)
Principle Investigator (PI) : 林嘉德 (Lin-De-Lin)

動物實驗管理小組召集人： _____ 日期

IACUC Chairman : Long B. Long Date : Dec 27, 2006

中國醫藥大學動物實驗管理小組審查同意書

Affidavit of Approval of Animal Use Protocol
China Medical University

動物實驗申請表暨同意書：97-60-√

計畫申請人：林嘉德 職稱：主治醫師
單位：中國醫藥大學附設醫院耳鼻喉部/臨床醫學研究所 飼養/應用
地點：本校動物中心 / 附醫耳鼻喉部聽性腦幹反應檢查室
計畫名稱：耳蝸缺血性病變時的分子機制及治療的蘊涵—體外試驗與動物體內
模式

本計劃之「動物實驗計畫書」業經動物實驗管理小組 實質 形式
審查通過。本計畫預定飼養應用之動物如下：

動物種類	動物數量	飼養及應用期間
Hartley strain guinea pig	150 隻(總數)	民國 97 年 8 月 1 日至 98 年 7 月 31 日
Hartley strain guinea pig	150 隻(總數)	民國 98 年 8 月 1 日至 99 年 7 月 31 日
Hartley strain guinea pig	150 隻(總數)	民國 99 年 8 月 1 日至 100 年 7 月 31 日

The animal use protocol listed below has been reviewed and approved by
the Institutional Animal Care and Use Committee (IACUC)

Protocol Title : The molecular mechanisms and therapeutic implications of cochlear
ischemia—the *in vitro* and *in vivo* animal model

Protocol No : 97-60-√

Period of Protocol : Valid From : 08/01/2008 To : 07/31/2011 (mm/dd/yyyy)

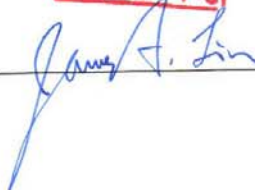
Principle Investigator (PI) : Chia-Der Lin

動物實驗管理小組召集人：



日期：96-12-25

IACUC Chairman :



Date: Dec 25, '07